UNIVERSITY OF CALIFORNIA,
IRVINE

Evaluating the Impacts of Centralized and Decentralized Electric Vehicle Smart Charging Algorithms on the Electric Grid

THESIS

submitted in partial satisfaction of the requirements
for the degree of

MASTER OF SCIENCE

in Mechanical and Aerospace Engineering

by

Aaron Jai-Wei Cheng

Thesis Committee:
Professor G. Scott Samuelsen, Chair
Professor Gregory N. Washington
Professor Vincent G. McDonell

2018

DEDICATION

To my family for their unconditional support and motivation.

TABLE OF CONTENTS

LIST OF FIGURES

LIST OF TABLES

NOMENCLATURE

AB32	Assembly Bill 32
AC	Alternating Current
AER	All Electric Range
AIRB	Anteater Instructional Research Building
APEP	Advanced Power and Energy Program
API	Application Programming Interface
APS	Anteater Parking Structure
BAU	Business as Usual
BEV	Battery Electric Vehicle
CA	California
CAISO	California Independent System Operator
CARB	California Air Resources Board
CEC	California Energy Commission
CO_2	Carbon Dioxide
CO_2e	Carbon Dioxide Equivalent
CPUC	California Public Utilities Commission
DC	Direct Current
DOE	Department of Energy
DSL	Digital Subscriber Line
ECPS	East Campus Parking Structure
EF	Emissions Factor
eGRID	Emissions and Generation Resource Integrated Dataset
EV	Electric Vehicle
EVSE	Electric Vehicle Supply Equipment
FCEV	Fuel Cell Electric Vehicle
GHG	Greenhouse Gas
GW	Gigawatt
HiGRID	Holistic Grid Resource Integration and Deployment
ICE	Internal Combustion Engine
ICT	Information and Communications Technology

IOU	Investor Owned Utility
kW	Kilowatt
kWh	Kilowatt-Hour
LF	Load Following
MATLAB	Matrix Laboratory
MMT	Million Metric Ton
MPS	Mesa Parking Structure
MSTB	Multipurpose Science Technology Building
MW	Megawatt
MWh	Megawatt-Hour
NEMA	National Electrical Manufacturers Association
NHTS	National Household Travel Survey
NO_x	Nitrogen Oxide
PEV	Plug-in Electric Vehicle
PG&E	Pacific Gas and Electric
PHEV	Plug-in Hybrid Electric Vehicle
PK	Peaker
PLC	Power Line Communication
SAE	Society of Automotive Engineers
SB32	Senate Bill 32
SCE	Southern California Edison
SCPS	Student Center Parking Structure
SOC	State of Charge
SSPS	Social Science Parking Structure
STD	Standard Deviation
TOU	Time of Use
UCI	University of California, Irvine
UI	User Interface
U.K.	United Kingdom
U.S.	United States
VMT	Vehicle Miles Traveled

ACKNOWLEDGMENTS

First, I would like to thank my advisor, Professor G. Scott Samuelsen for his guidance and leadership throughout the past two years. His support and mentorship has helped me grow and become a better researcher and individual.

I would also like to thank Brendan Shaffer and Dr. Brian Tarroja who are always there to provide their advice and input. Thank you to Edgar Ramos Muñoz, Theron Smith, and Professor Jabbari for their collaboration in the smart charging meetings. Thank you to Avram Grossman for his help in developing the API and thank you to HATCI for providing the Kia Souls. Thank you to John Stansberry and Jae Hwan Yi for their help in the vehicle testing. Thank you to my thesis committee, Professor Samuelsen, Professor Washington, and Professor McDonell for their help in refining this thesis.

Lastly, thank you to all of my friends and colleagues at the Advanced Power and Energy Program for making my graduate experience the best I could ever hope for.

ABSTRACT OF THE THESIS

Evaluating the Impacts of Centralized and Decentralized Electric Vehicle Smart Charging Algorithms on the Electric Grid

By

Aaron J. Cheng

Master of Science in Mechanical and Aerospace Engineering

University of California, Irvine, 2018

Professor G. Scott Samuelsen, Chair

Plug-in electric vehicles (PEVs) are considered one of the leading solutions in reducing greenhouse gas emissions since they remove carbon emissions from the tailpipe. However, as their penetration in the vehicle market increases, so will their impact on the electric grid. To minimize the impact that PEVs have on the electric grid, "smart" charging protocols are necessary to manage PEV charging. This study evaluates how two smart charging architectures, a centralized and decentralized architecture, impact both small and large-scale electric grids through real deployment of the algorithms as well as MATLAB simulations.

The "field-deployable" decentralized charging algorithm uses a telematics-based approach to create charging schedules for 10 PEVs deployed on the University of California, Irvine's (UCI) microgrid. The results reveal that a barrier associated with this approach is the need to retrieve the vehicles' status, referred to as "polling." Polling affects how the algorithm creates charging schedules. To determine the effect of polling, simulations are performed on different buildings on the UCI campus using National Household Travel Survey data to simulate vehicle travel patterns. The results show that, if polling occurs frequently (e.g., once every 10 minutes), the charging schedules are not significantly altered. To determine whether or not the decentralized algorithm

can provide the same emissions benefits as an ideal centralized algorithm on large-scale systems, both algorithms are simulated on the California electric grid for the year 2030. The results reveal that the decentralized algorithm provides the same emissions benefits as the centralized algorithm, but only if communication between the grid and vehicles is sufficiently frequent (e.g., 60 minutes or less).

1. INTRODUCTION

1.1 Overview

Since the 1900s, global carbon emissions have continued to rise, increasing by 90% from year 1970 levels by 2014, as shown in Figure 1 [1]. The United States (U.S.) is considered one of the largest producers of greenhouse gas (GHG) emissions, contributing to 14% of global GHG emissions [2]. In 2015, the transportation economic sector was the second largest producer of GHG emissions in the United States, and the largest in California (CA). Transportation accounted for 27% of total U.S. GHG emissions (Figure 2), with the primary source of GHG emissions coming from the burning of fossil fuels. Over 90% of transportation is fueled by petroleum [3] and in California, transportation accounted for 39% of GHG emissions (Figure 3) [4].

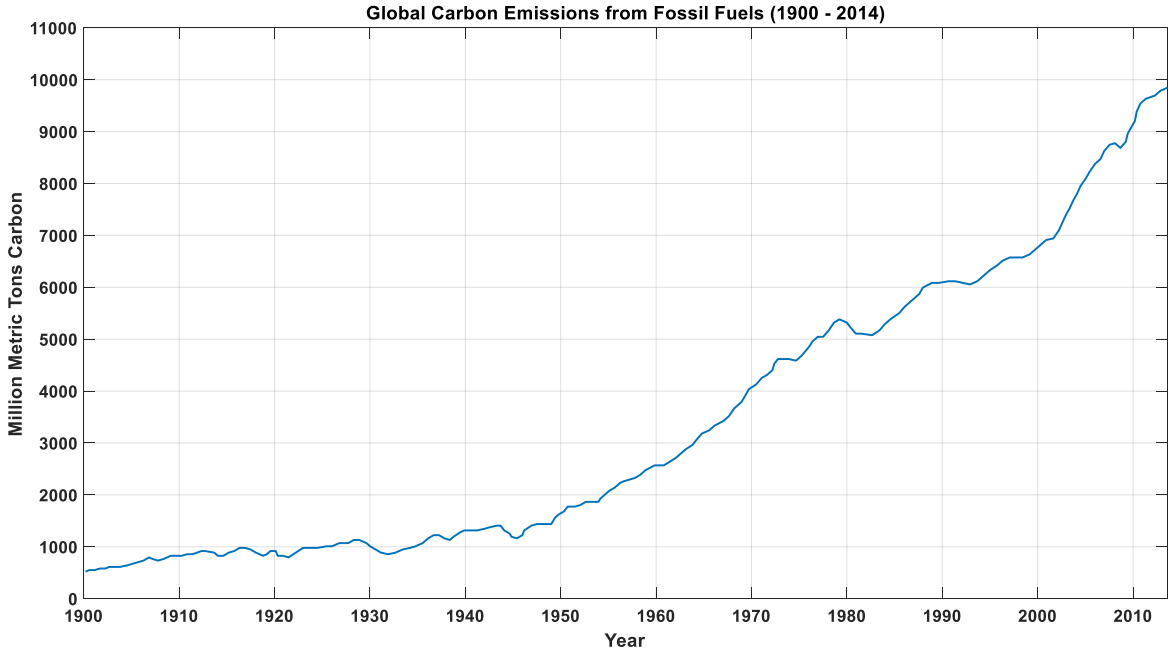

Figure 1. *Global Carbon Emissions from Fossil Fuels (Adapted from Ref. [1])*

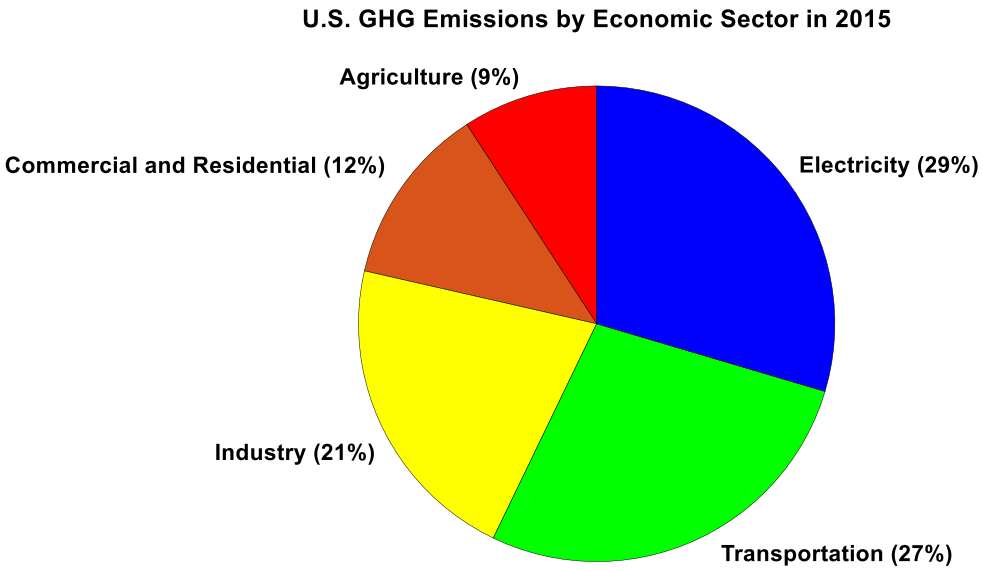

Figure 2. *U.S. GHG Emissions by Economic Sector in 2015 (Adapted from Ref. [3])*

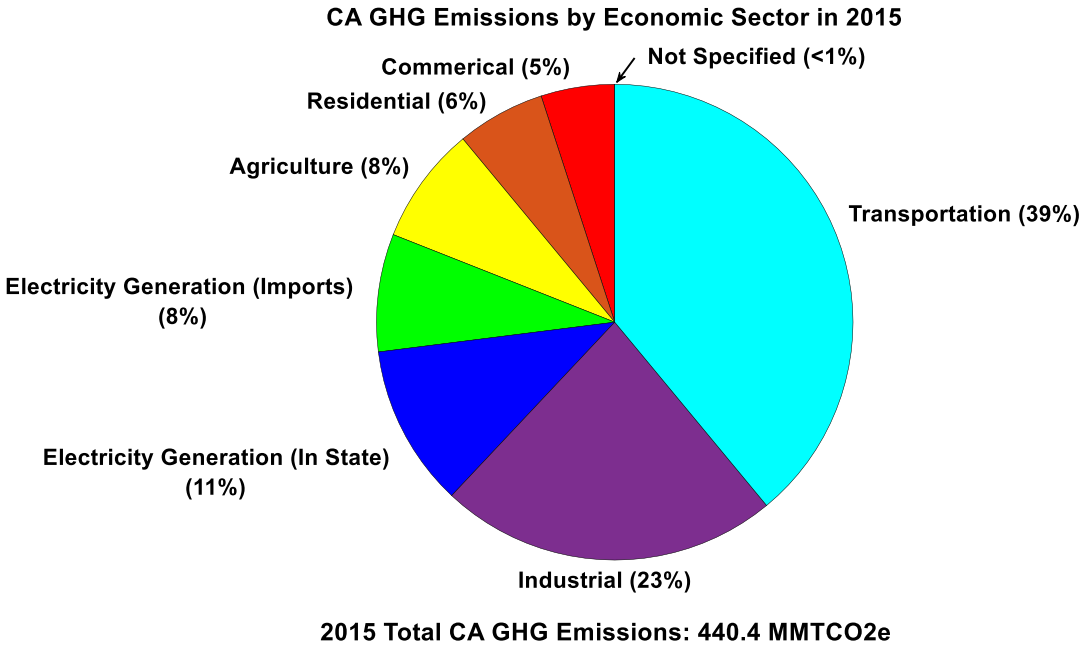

Figure 3. *CA GHG Emissions by Economic Sector in 2015 (Adapted from Ref. [4])*

As GHG emissions continue to increase yearly, California has become one of the leading states in the fight against climate change, issuing a series of bills in an attempt to reduce emissions. Assembly Bill 32 (AB32), the California Global Warming Solutions Act of 2006, mandates that California reduces its GHG emissions to 1990 levels by 2020 [5]. Senate Bill 32 (SB32), which was passed in 2015, expands on AB32 and requires that California reduces GHG emissions to 40% below 1990 levels by 2030, and 80% below 1990 levels by 2050, making this the most stringent standard set by any government in North America [6]. The transportation sector requires major changes in order to meet these goals. To reduce the dependence on fossil fuels in the transportation sector, alternative forms of transportation are necessary.

1.2 Goals

The goals of this thesis are to establish and evaluate a smart charging algorithm on a fleet of plug-in electric vehicles (PEVs) on a microgrid platform, and to project the impacts of PEV smart charging on the California electric grid.

1.3 Objectives

The following objectives are achieved to fulfill the goals:

1. Identify different smart charging algorithms to serve for analysis.
2. Modify the decentralized smart charging algorithm in order to deploy it on a fleet of PEVs.
3. Develop and simulate smart charging scenarios within a microgrid.
4. Integrate smart charging algorithms into the Holistic Grid Resource Integration and Deployment (HiGRID) model to determine California electric grid emissions.

2. BACKGROUND

2.1 Electric Vehicles

In order to reduce GHG emissions in the transportation sector, alternative forms of transportation such as electric vehicles (EVs) are necessary. Three types of EVs are battery electric vehicles (BEVs), fuel cell electric vehicles (FCEVs), and plug-in hybrid electric vehicles (PHEVs). Two of the three, BEVs and PHEVs, are plug-in electric vehicles (PEVs). The adoption of PEVs is a forefront solution in reducing GHG emissions since they offset vehicle tailpipe emissions [7].

2.1.1 History of Electric Vehicles

Electric vehicles have been in existence as early as the 1830s, with the first one debuting in the U.S. in 1890. By the early 20th century, EVs became one of the leading forms of transportation, with one-third of all vehicles being EVs. However, in 1908 when the Ford Model T became mass produced and widely available and gas became more affordable and available in the 1920s, the sale of EVs began to decline. By the 1930s, EVs had essentially disappeared. When the 1990 Clean Air Act, 1992 Energy Policy Act, and new emission regulations issued by the California Air Resources Board (CARB) passed, interest in EVs started to rise again [8].

2.1.2 Battery Electric Vehicles vs. Plug-in Hybrid Electric Vehicles

Battery electric vehicles and plug-in hybrid electric vehicles are the two major types of PEVs. BEVs solely rely on the electricity stored in the on-board battery as the source of power and use an electric drivetrain as their source of propulsion. Since they do not use gas, no tailpipe emissions exist. On the other hand, PHEVs have an internal-combustion engine (ICE) that work in conjunction with an on-board battery. The combination of the ICE and the on-board battery provides a longer range than the range of a BEV; however, since PHEVs have ICEs, this leads to tailpipe emissions. What the BEV and PHEV have in common is that they can both plug in to the

electric grid to charge. Since BEVs only rely on the on-board battery, their battery capacities are much larger than PHEV battery capacities [9]. Table 1 lists advantages and disadvantages of PEVs when compared to standard ICE vehicles.

Table 1. *PEV Advantages and Disadvantages (From Ref. [9])*

PEV Advantages and Disadvantages	
Advantages	**Disadvantages**
Low Operating Cost	Higher upfront costs
No tailpipe emissions (battery only operation)	Limited electric range
Convenient refueling at home	Need to install charging infrastructure
Reduction in petroleum consumption	High battery cost
Improvements in urban air quality	Long recharging time

2.1.3 PEV Classifications

PEVs can be classified into four different categories based off of their all electric range (AER): long-range BEVs, limited-range BEVs, range-extended PHEVs, and minimal PHEVs. Long-range BEVs are BEVs that have large batteries and can travel over 100 miles per charge. Limited-range BEVs are BEVs that can travel shorter distances, usually under 100 miles per charge. While they cannot travel as far, limited-range BEVs are more affordable than long-range BEVs. Range-extended PHEVs are PHEVs that operate using the battery only, and then switch to the ICE once the battery is fully depleted. Minimal PHEVs are similar to range-extended PHEVs, except that their AER is much smaller; however, their total range is larger. Table 2 lists examples of the four classes of PEVs and their corresponding range [9].

Table 2. *PEV Classes (From Ref. [9])*

PEV Classes		
PEV Class	**Vehicle Model**	**Range (Miles)**
Long-Range BEV	Tesla Model S	265 AER
Limited-Range BEV	Nissan Leaf	84 AER
Ranged-Extended PHEV	Chevrolet Volt	38 AER/380 total range
Minimal PHEV	Toyota Plug-in Prius	6-11 AER/540 total range

2.2 Charging Infrastructure

While gasoline stations are readily available, the same cannot be said for PEV charging stations. As stated in Table 1, one of the major disadvantages of PEVs is the need to install PEV charging infrastructure, or electric vehicle supply equipment (EVSE). To charge PEVs safely, consumers need access to EVSEs [9], [10]. EVSEs are designed to connect the vehicle and charger, and to determine any safety issues that could occur when charging [9]. Currently, three different charging levels exist: Alternating Current (AC) Level 1, AC Level 2, and Direct Current (DC) Level 3 Fast Charging. Each charging level has their own type of EVSE and charging rate.

2.2.1 AC Level 1 and 2 Charging

AC level 1 and 2 charging are the most common forms of PEV charging. Most drivers who drive BEVs and PHEVs use AC level 1 and 2 chargers to charge their vehicles overnight [11]. Most PEVs will come with an AC level 1 charger, which plugs into a standard 120-volt outlet [9], [10]. The end of the EVSE cable that plugs into the PEV is an SAE J1772 charging plug, and the end of the EVSE cable that plugs into the 120-volt outlet is a NEMA connector (e.g., NEMA 5-15 three-prong connector) [10]. AC level 1 charging provides 4 to 5 miles per hour charged, which allows for most PEV owners to meet their daily commute requirement [9], [11]. However, due to the charging rate, AC level 1 charging mainly suits BEVs with smaller battery sizes and PHEVs.

For owners with larger battery sizes, AC level 2 charging is frequently used; however, this requires additional equipment to be installed at the user's residence. Similar to AC level 1 chargers, AC level 2 chargers also use an EVSE cable that has the SAE J1772 charging plug [9]. However, AC level 2 chargers are plugged into 240-volt outlets, which are typically mounted on a garage wall. These are the same outlets that electric dryers and large air conditions use [9]. AC level 2

charging provides 10 to 20 miles of range per hour charged, providing a longer range and higher efficiency than AC level 1 charging [10].

2.2.2 DC Level 3 Fast Charging

DC level 3 charging is the most efficient charging level out of the three levels that are currently available on the market. DC level 3 charging provides 50 to 70 miles of range per 20 minutes charged [10]. While AC level 1 and level 2 chargers convert the AC electricity to DC electricity in the car, level 3 chargers convert the AC electricity to DC electricity in the EVSE. Currently, three different types of DC fast chargers exist on the market: the J1772 combination charger, the Charge de Move charger, and the Tesla supercharger [10]. However, level 3 chargers are too expensive to implement in residential areas. Therefore, vehicle manufacturers and the government are the main entities that have incentives to install level 3 chargers [9].

2.3 Microgrids

As defined by the U.S. government Department of Energy (DOE), microgrids are "a local energy grid with control capability, [meaning] it can disconnect from the traditional grid and operate autonomously" [12]. When microgrids are in grid-isolation mode, they need a source of power generation. For remote microgrids, diesel generators are a typical source of electricity since they are relatively cheap and simple to install. However, this leads to the burning of fossil fuels, resulting in GHG emissions [13]. One way to reduce fossil fuel consumption is to integrate different sources of renewable energy into the microgrid. Two of the fastest growing forms of renewable energy are solar and wind [14], which were also the two largest sources of renewable energy in California in 2014 [15]. Integrating renewable forms of power generation into microgrids has the potential to reduce GHG emissions. As vehicles become more and more electrified, PEVs

will likely be plugged-in at work “microgrids” or shopping center “microgrids”. As a result, vehicle charging is expected to be an anchor component of the modern microgrid.

2.4 Charging Strategies

As PEVs become more commonplace, the demand for PEV charging infrastructure will increase, which will lead to an increase in the electric demand [7]. It has previously been shown that home charging infrastructure ranks as the most important for PEV deployment, and work place charging infrastructure ranks as the second most important [9]. Typically, the overnight dwell period exceeds the time needed to charge PEVs; therefore, overnight charging has become a common time to charge PEVs. If most PEVs charge at the same time however, this has the potential to shift the overall demand curve [7]. As shown in the 2009 National Household Travel Survey (NHTS), the majority of vehicles arrive home from work around 5 PM [16]. In California, this is typically when renewable generation ramps down and the net load ramps up, as seen in the California “duck curve” (Figure 4). To avoid shifting the overall demand curve, charging schedules will need to be shifted to align as much as possible with renewable generation [7].

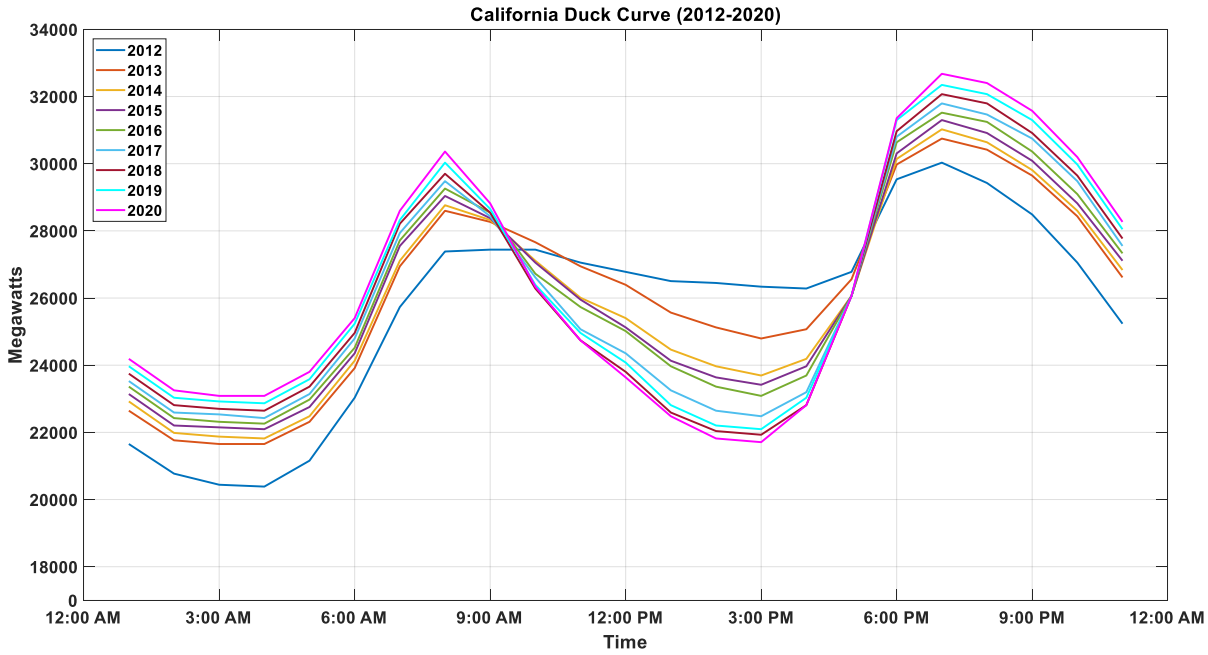

Figure 4. *California Duck Curve (Adapted from. Ref [17])*

One of the main challenges associated with PEVs is determining the optimal charging strategy. While PEVs can reduce tailpipe GHG emissions dramatically, they cause an increase in power plant produced GHG emissions since they need to plug in to the electric grid. Therefore, various charging algorithms have been examined and studied in an attempt to reduce GHG emissions.

2.4.1 Immediate Charging

One of the most common ways to charge PEVs is through the immediate charging strategy or "uncontrolled charging" strategy. Immediate charging is simply when the vehicle charges as soon as it is plugged in. While this is very convenient for the user, major issues such as the overload of transformers and lines, voltage deviations, peak power increases, and the increase of electricity CO_2 intensity can occur [18]. Figure 5 shows an example of uncontrolled charging.

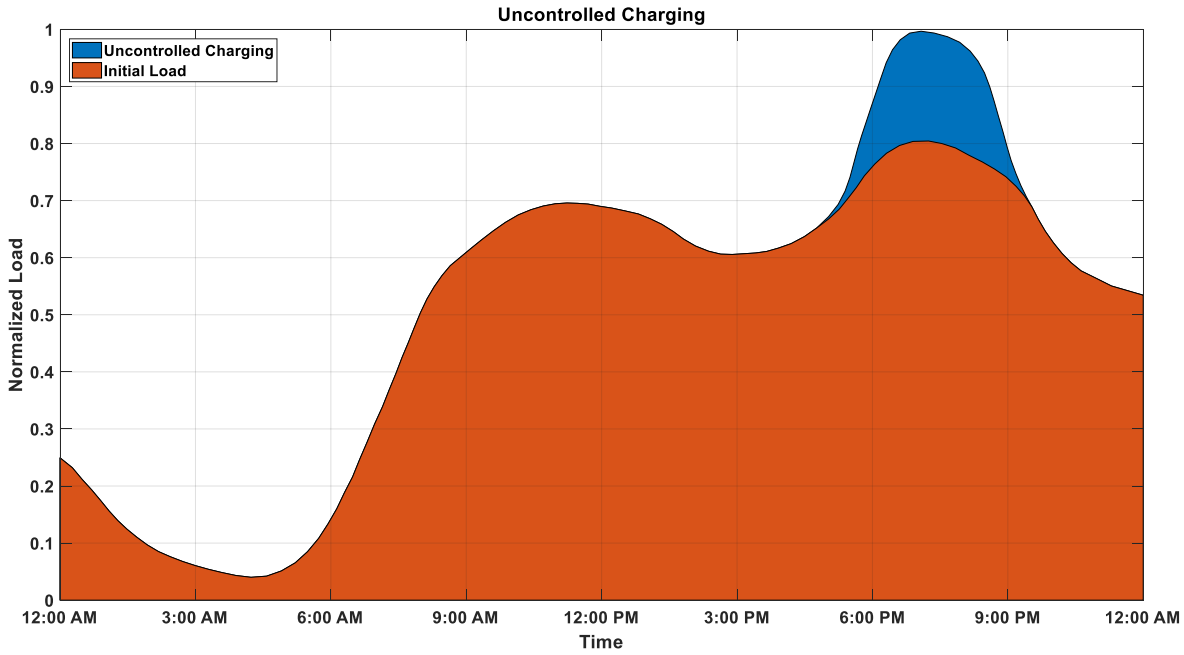

Figure 5. *Uncontrolled Charging Normalized to Peak Load (Adapted from Ref. [18])*

2.4.2 Off-Peak Charging

Another commonly used charging schedule is off-peak charging. Off-peak charging is the same as immediate charging where the vehicle charges as soon as it is plugged in. However, users charge their vehicles overnight rather than during the day, as shown in Figure 6. This has several advantages such as flattening the demand profile and integrating wind energy at off-peak hours; however, some major issues that occur from off-peak charging are the possible overload of transformers and lines, possible voltage deviations, and sudden power demand increases [18].

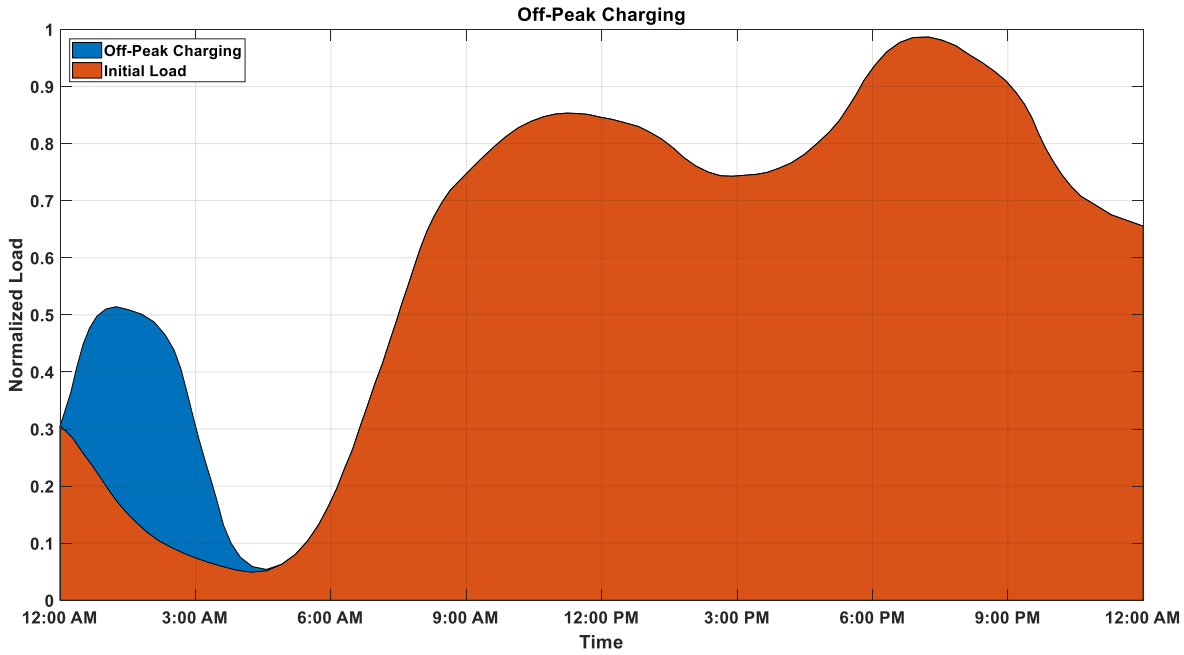

Figure 6. *Off-peak Charging Normalized to Peak Load (Adapted from Ref. [18])*

2.4.3 Smart Charging

With the current PEV penetration, immediate and off-peak charging are the most frequently used charging strategies. However, as PEV penetration increases, "smart" or controlled charging protocols will be necessary to manage PEV charging [7], [18]. The main goal of smart charging is to flatten the overall net load when the PEV charging profile is added so that the variation over a certain time period is minimized. By shifting the charging demand of PEVs to a time when the demand is the lowest, this can reduce the need to shut down and restart power plants, as shown in Figure 7. This is known as the "valley filling" approach [7]. While the valley filling approach is the most optimal charging strategy, it has many complexities associated with it. Valley filling has very complex implementation, it requires information and communications technology (ICT), and the willingness of the customer is required [18].

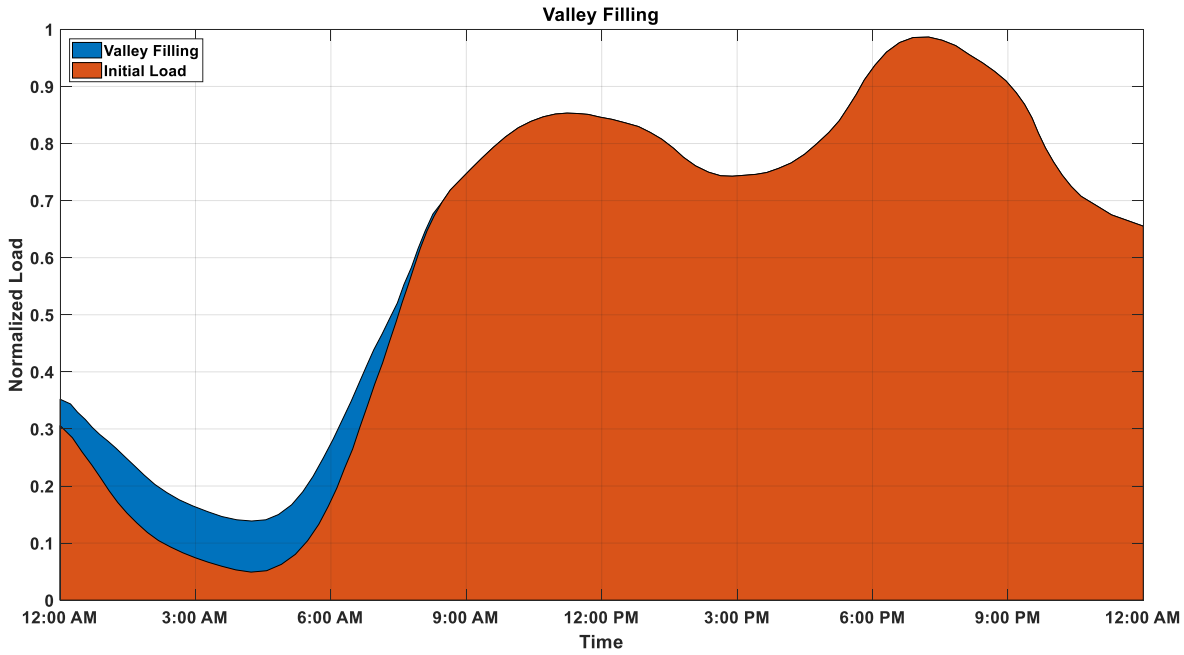

Figure 7. *Valley Filling Normalized to Peak Load (Adapted from. Ref [18])*

The smart charging strategy can be classified into two architectures: a centralized or global energy control strategy, and a decentralized or local energy control strategy [18], [19].

2.4.3.1 Centralized Control Architecture

In the centralized control architecture, a central aggregator controls the charging of all of the vehicles within its region. The aggregator takes in the PEV information and optimizes the charging schedule of all vehicles in order to minimize system-wide electricity costs. The centralized architecture allows the aggregator to smooth the aggregated electric load profile (global load) in its region. This architecture makes PEV charging easier, since all of the vehicle data are available to a single entity. While this is a very well-known control architecture, many issues and concerns surround it. While the global load may be smooth, individual vehicles may have peaks in their charging profiles, which could incur high costs for the owner. Since a single entity is managing a large amount of vehicle data, a backup system is required in case of any failures. As

the number of vehicles increase, the complexity increases, which means that significant computational power is required in order to accommodate the large volume of information being transferred and perform the optimization necessary to provide individual PEV charging schedules. One of the biggest issues with this control architecture are privacy concerns. Since an aggregator controls the information and charging schedule, it will be able to access information such as travel patterns of the user. Therefore, unless the users are willing to provide the aggregator with this type of information, a centralized control architecture will be difficult to implement [18], [19].

2.4.3.2 Decentralized Control Architecture

In the decentralized control architecture, each individual PEV creates its own charge schedule based on the local load. Unlike the centralized control architecture, an aggregator is not needed, and this allows each individual vehicle to minimize its charging cost. In this case, the charging schedule is optimized on a local scale rather than on a global scale. Using the decentralized control architecture, privacy concerns are no longer an issue, since the charging schedule resides solely within the user. This leads to a higher user acceptance than the centralized control architecture. Since each vehicle decides on its charge schedule individually, not as much data processing needs to be done. The main issue with the decentralized control architecture is that the charging algorithm does not take into account the global loads. While the charging for each individual PEV may be optimized, this could lead to sudden increases and peaks in the global load, resulting in an aggregated electric load profile that is not as smooth. This is known as the avalanche effect. Due to the scalability and higher user acceptance, the decentralized control architecture is more likely to be utilized and more feasible than the centralized control architecture in real world implementation [18], [19].

2.5 Smart Charging Algorithms Explored in Literature

Many studies have analyzed utilizing smart charging strategies to control PEV charging, on both small and large-scale systems. Studies [19]–[23] evaluated smart charging on residential scales. Mets et al. compared both architectures and benchmarks them against a business-as-usual (BAU) scenario where no smart charging approaches are used, by conducting a simulation on a residential scale of 150 homes. This study found that a local approach reduces the peak load by 26% for a 30% PHEV penetration and that a global approach reduces the peak load by 30% [19]. Mets et al. also examined smart charging on a residential scale of 63 homes and found that peak reductions can range anywhere from 29% to 70% compared to a BAU case [20]. Chen et al. utilized a valley filling approach and evaluates a decentralized algorithm on the valley filling profile on residential load profiles [21]. Alonso et al. focused on applying a genetic algorithm on a residential low-voltage system and found that the smart charging schedule can flatten the overall load profile [22]. Gan et al. used a decentralized charging algorithm on a residential load profile served by Southern California Edison (SCE). This study examined 20 PEVs in 100 homes and found that the decentralized algorithm is able to provide optimal charging profiles [23]. Studies [24]–[28] examined utilizing smart charging on larger scales. Qian et al. analyzed a system consisting of 2840 vehicles on a United Kingdom (U.K.) distribution network and examined how smart charging can reduce the peak load when a 10% and 20% PEV penetration is used. This study found that when charging is not controlled, the peak load increases by 17.9% and 35.8% when a 10% and 20% PEV penetration is used respectively, and that smart charging does not create a new peak load [24]. Kara et al. examined how a centralized smart charging algorithm can decrease the overall peak load for over 2000 PEV chargers, under the assumption that for all PEVs, the arrival and departure time is known, as well as the energy demand profile and determined that smart charging

can decrease the peak load by 37% [25]. Karfopoulos et al. evaluated a decentralized, multi-agent PEV charging strategy on an urban distribution network in Northern Greece with 1200 EVs. This study found that the decentralized approach can perform valley filling functions adequately and also showed that a decentralized approach can achieve results similar to a centralized approach without the use of intense communication requirements and computational resources [26]. Ma et al. used a decentralized charging control strategy to charge large populations of PEVs, showing that the decentralized approach can solve a local problem and converge to a global Nash equilibrium without the use of significant computational resources and communication infrastructure [27]. Ma et al. also showed that a decentralized charging strategy can allow users to optimize their charging schedule locally, while also optimizing the global load [28]. Studies [29]–[31] evaluated smart charging algorithms on state-wide scales and their effects on large-scale GHG emissions. Forrest et al. evaluated how switching from immediate to centralized smart charging affects renewable penetration on the California grid in the year 2050. Using the centralized smart charging algorithm developed by Li et al. [32], this study found that switching to smart charging can increase renewable penetration from 56.7% to 73% since PEV charging is shifted to daytime charging and matches with peak solar production [29]. Tarroja et al. analyzed how the centralized smart charging algorithm developed by Li et al. [32] affects California GHG emissions in the year 2050. This study used 2009 NHTS travel data to represent vehicle travel behavior and scale up the vehicle miles traveled (VMT) based off the projected population in the year 2050. This study found that smart charging can achieve up to 55% GHG emission reductions compared to immediate charging when PEVs are allowed to charge both at home and at work, due to the synchronization of PEV charging with renewable generation [30]. Tarroja et al. also analyzed how the centralized smart charging algorithm developed by Li et al. [32] affects GHG emissions in the year 2050 for

different percentages of PEV penetration combined with different charger powers, specifically two different PEV penetrations (50% and 90%) and with three different charger powers (6.6 kW, 10 kW, and 20 kW). This study found that on average between the three charger powers, 75 MMT CO_2e per year was emitted when a 90% PEV penetration was used, and 96 MMT CO_2e per year was emitted was a 50% PEV penetration was used [31].

Projects have also deployed smart charging algorithms on real vehicles. In 2015, BMW and Pacific Gas and Electric (PG&E) conducted a project called the BMW i ChargeForward Project, with the goal of determining if PEVs could be used as a flexible grid resource to operate and maintain the grid. The project was conducted in the San Francisco Bay Area, with BMW providing PG&E with 100 kW of grid resources and 100 BMW i3's. The vehicles were used for dispatch in 209 demand response events totaling 19.5 MWh [33]. In Toronto, ChargeTO, an electric vehicle smart-charging project, deployed a residential smart charging pilot program. The program was conducted over an 11-month period, where the first six months was baseline vehicle monitoring, and the last five months was paired smart charging. The program included five different PEV models, Tesla Model S, Nissan Leaf, Chevrolet Volt, BMW i3, and Smart Fortwo ED, with 30 PEV owners. During the course of the five months, this project found that 85% of the charging load could be shed at peak load times, or more than 50% of the peak load could be reduced, while still ensuring full customer satisfaction [34].

2.6 Simulation Tools

The models are simulated through the use of Matrix Laboratory (MATLAB) models. The charging algorithms used to produce PEV loads were written by Li Zhang [7], [32]. These PEV load profiles are then used in the HiGRID model written by Fabian Mueller, Josh Eichman, and Brian Tarroja [35].

2.7 Summary

In California, the leading economic sector of GHG emissions is the transportation sector. In order to reduce GHG emissions in the transportation sector, different forms of alternative transportation such as PEVs are necessary. PEVs are a viable form of alternative transportation since they can be refueled at home and can meet most consumers travel demands. As automakers continue to make more vehicle models, PHEV and BEV sales have continued to increase each year [36]. However, as the number of PEVs increase, they are bound to have a significant impact on the electric load. In order to make sure that PEV charging will not cause electrical issues, different charging algorithms are analyzed. As seen in the literature, decentralized smart charging architectures have been mainly been applied to small-scale, residential systems, and studies that focus on large-scale implementation mainly focus on utilizing centralized smart charging architectures. However, in order to meet the climate change goals, decentralized algorithms will need to be applied on larger, state-wide scales. This thesis analyzes the effects of implementing deployable smart charging algorithms on a fleet of PEVs on a small-scale microgrid platform, as well as the effects that PEV smart charging has on the California electric grid.

3. APPROACH

The goals of this thesis are to establish and evaluate a smart charging algorithm on a fleet of plug-in electric vehicles (PEVs) on a microgrid platform, and to project the impacts of PEV smart charging on the California electric grid.

Objective 1. Identify different smart charging algorithms to serve for analysis

Objective 1 will determine which smart charging algorithms will be used in the analysis. Many different smart charging algorithms have been developed. For this study, the smart charging algorithms used were developed by a previous graduate student in the Advanced Power and Energy Program (APEP), Li Zhang. This research utilizes his centralized and decentralized smart charging algorithms.

Objective 2. Modify the decentralized smart charging algorithm in order to deploy it on a fleet of PEVs

Objective 2 will modify the decentralized smart charging algorithm identified in objective 1 in order to deploy it on a small fleet of PEVs. The PEVs used in this study are Kia Souls. This study will utilize a telematics-based approach to deploy the smart charging algorithm. Any barriers associated with the telematics-based approach will also be addressed in objective 2.

Objective 3. Develop and simulate smart charging scenarios within a microgrid

Objective 3 will use the decentralized smart charging algorithm identified in objective 1 to create different scenarios to simulate within a microgrid. To achieve this goal, different cost loads are used to determine how the decentralized smart charging approach affects different building loads within the microgrid. The cost to charge incurred on PEV owners as well as electric grid CO_2 emissions will be analyzed.

Objective 4. Integrate smart charging algorithms into the Holistic Grid Resource Integration and Deployment (HiGRID) model to determine California electric grid emissions.

Objective 4 will determine how centralized and decentralized smart charging approaches affect California's electric grid CO_2 and NO_x emissions. The algorithms will be implemented into the HiGRID model and different scenarios will be simulated to determine California CO_2 and NO_x emissions in the year 2030. The centralized charging scenario will be used as the base scenario, and the decentralized scenarios will be compared to the base scenario.

4. OBJECTIVE 1 RESULTS

Identify different smart charging algorithms to serve for analysis

As seen in the literature, two smart charging architectures have been explored: centralized and decentralized. For this thesis, the main algorithm utilized is the decentralized charging algorithm developed by Li et al. [7]. The centralized charging algorithm developed by Li et al. is explored in objective 4 [32]. Chapter 4 analyzes the two charging algorithms.

4.1 Decentralized Smart Charging Algorithm

The first model used for this thesis is the decentralized smart charging algorithm. In the decentralized charging approach, each vehicle optimizes its own charging schedule based on a cost function. A unique cost function is sent to a PEV each time it plugs in, in order to determine the optimal time to charge based off its dwell period. In this application, the cost function is the net load demand profile, which is the electric load minus renewable generation at each minute. The cost load provided to a vehicle includes any previous loads imposed on the grid by prior vehicles that have plugged in. When the vehicle receives the cost load, it will solve a constrained linear program to determine the optimal time to charge based on its dwell period. The algorithm prioritizes time slots when the net load demand is the lowest, referred to as valley filling. Once the PEV charging schedule has been determined, it is sent to the grid operator, who will add it onto the existing net load profile. Two options to update the cost function are at fixed time intervals or at a fixed number of vehicles in order to minimize the amount of data being transferred between the vehicles and the grid. For example, if the cost function update time is set to 60 minutes, vehicles that plug in between t = 0 and t = 60 minutes will receive a certain cost function. Vehicles that plug in subsequently will receive a different cost function that consists of the net load with the

addition of the PEV charging profiles from the vehicles that plugged in between t = 0 and t = 60 minutes. This process is repeated for an entire year [7].

The decentralized smart charging algorithm is governed by equations 1 through 10. For grid level valley filling, the goal is to minimize the following:

$$min \sum_{i} \left(D(t_i) + X(t_i)\right)^2 \tag{1}$$

where $D(t_i)$ is the electric net load at t_i and $X(t_i)$ is the overall charging power at t_i. Equation 1 is subject to the following constraint:

$$\Delta t \times \sum_{i} X(t_i) = B = \sum_{n} b_n \tag{2}$$

where B is the total charging energy of all PEVs for a day and b_n is the charging energy for an individual PEV. Equation 2 states that the total charging energy of all vehicles (B) is equal to the sum of the overall charging power multiplied by the timeslot. The overall charging power has the following upper bound:

$$X(t_i) \leq R(t_i) \tag{3}$$

where $R(t_i)$ is the product of the amount of plugged in PEVs and individual charging powers. For individual PEV charging, the following cost function is used:

$$\sum_{i} C(t_i) \times x_n(t_i) \tag{4}$$

where $C(t_i)$ is the cost per kWh (DC) at t_i and $x_n(t_i)$ is the charging energy for vehicle n at t_i ($x_n(t_i)$ is a decision variable). In this study, the cost per kWh is proportional to the net load demand. The two constraints are as follows:

$$\sum_i x_n(t_i) = b_n \tag{5}$$

$$0 \le x_n(t_i) \le r_n(t_i) = p_n(t_i) \times \overline{\Delta t_n(t_i)} \times \eta \tag{6}$$

where $p_n(t_i)$ is the charging power, $\Delta t_n(t_i)$ is the time the vehicle is plugged in for, and η is the charging efficiency (assumed to be 85%). Equation 5 states that the amount of energy used during the day (b_n) is equal to total amount of energy sent to the vehicle when it recharges at home $(\sum_i x_n(t_i))$. Equation 6 states that the charging energy at any time slot cannot exceed the maximum allowable charging energy $(r_n(t_i))$.

Two methods for updating the cost load are updating the cost load by fixed time intervals and updating the cost load by a fixed number of vehicles. This is to avoid transmitting large amounts of data due to the large number of vehicles in the system. If the cost function is updated by a fixed time interval, the following equations are used:

$$s_{k-1}(t_i) = \sum_n x_n(t_i)/\eta \forall n \;\; s.t. \;\; T_{k-1} \le ta_n < T_k \tag{7}$$

$$T_k = T_{k-1} + T_{step} \tag{8}$$

where $s_{k-1}(t_i)$ is the aggregated charging profile for step $k-1$, T_k is the time when the cost is updated, ta_n is the home arrival time after the last trip for PEV n, and T_{step} is the time interval for cost function updating. If the cost function is updated by a fixed number of vehicles, the following equations are used:

$$s_{k-1}(t_i) = \sum_n x_n(t_i)/\eta \forall n \;\; s.t. \;\; V_{k-1} < n < V_k \tag{9}$$

$$V_k = V_{k-1} + V_{step} \tag{10}$$

where V_k is the vehicle number when the cost is updated, n is the PEV number, and V_{step} is the vehicle number interval for cost function updating.

4.2 Centralized Smart Charging Algorithm

The second model used for this thesis is the centralized smart charging algorithm. In the centralized charging approach, a central aggregator optimizes the charging of all of the vehicles within its domain. The main goal of the centralized charging algorithm is to minimize the operating costs of the PEV fleet as a whole instead of that for individual PEVs. In this scenario, the algorithm has knowledge of a perfect forecast, assuming that the entire day's travel pattern and dwell period is known, the charging cost at each dwell period is known, and that the cost function for the entire year is known for all vehicles within the system [32].

For the centralized smart charging algorithm, the goal is to minimize the following cost function:

$$\sum_{i=1}^{m} \sum_{j=1}^{seg(i)} f_{ij} \times x_{ij} \tag{11}$$

This is the summation of the total charging cost, where f_{ij} is the charging cost per kWh during the *j*th hour in the *i*th dwelling period and x_{ij} is the state of charge (SOC) increase during the *j*th hour in the *i*th dwelling period.

When using the centralized smart charging algorithm, the following constraints apply:

1. The amount of energy charged must be equal to the amount of energy discharged for the entire day (i.e., 24 hours).

2. For each trip the vehicle makes, the decrease in SOC cannot be larger than the battery capacity.

Similar to how the individual charging energy $x_n(t_i)$ is constrained in the decentralized charging algorithm, the SOC increase (x_{ij}) is constrained by the following equation:

$$0 \leq x_{ij} \leq power_{ij} \times \Delta t_{ij} \times \eta \quad (12)$$

where $power_{ij}$ is the charging power, Δt_{ij} is the dwell period, and η is the charging efficiency.

4.3 Objective 1 Summary

Two smart charging algorithms have been identified to serve for analysis for this study: a centralized smart charging algorithm and a decentralized smart charging algorithm. For both algorithms, the governing equations as well as constraints are listed. The main distinction between the centralized and decentralized charging architectures is that the centralized architecture assumes that all travel patterns and load patterns are known, while the decentralized architecture does not. The decentralized smart charging algorithm has more equations and constraints governing it than the centralized smart charging algorithm. The decentralized smart charging algorithm will be explored in chapters 5 through 7, while the centralized smart charging algorithm will only be explored in chapter 7.

5. OBJECTIVE 2 RESULTS

Modify the decentralized smart charging algorithm in order to deploy it on a fleet of PEVs

The decentralized smart charging algorithm identified in objective 1 will be deployed on a fleet of 10 Kia Souls. The algorithm originally developed by Li et al. [7] was modified by Ramos Muñoz et al. to obtain individual PEV profiles [37]. This allows for the algorithm to be applied on smaller scales, whereas the algorithm developed by Li et al. is mainly used for large-scale simulations. The algorithm modified by Ramos Muñoz et al. will be modified in order send vehicle commands to individual PEVs. Chapter 5 explores what modifications were made to the algorithm as well as the results from the testing.

5.1 Modifications Made to the Algorithm

The main modification made to the algorithm by Ramos Muñoz et al. was the user interface (UI) of the original algorithm. The original algorithm by Li et al. has inputs and information that were mainly used for large-scale applications, such as NHTS travel data. The NHTS data contains information such as the household ID and vehicle ID of each trip and while this information is necessary to simulate large-scale travel patterns, it is not necessary for individual PEV trips. The UI was modified by Ramos Muñoz et al. so that only the necessary input parameters were necessary. The main input parameters necessary to determine individual PEV charging profiles are the arrival time of the PEV, the departure time of the PEV, the distance the PEV will have to travel until the next charge, and the SOC of the PEV. Figure 8 shows the flow chart for the algorithm. Ovals represent inputs, rectangles represent built models, and diamonds represent outputs.

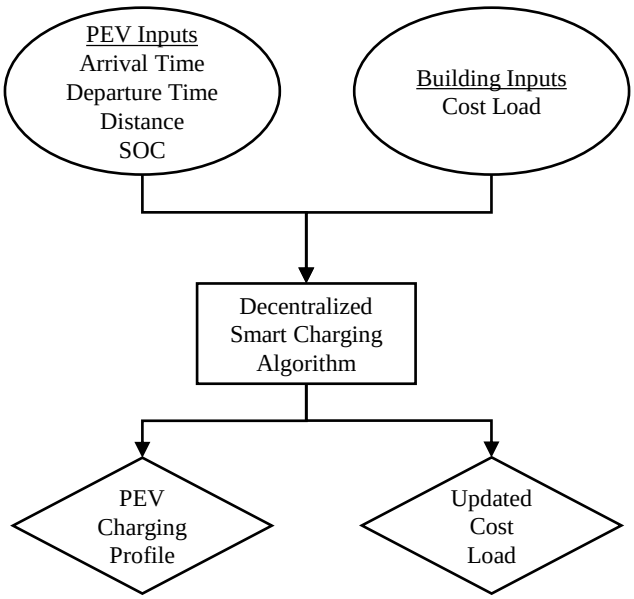

Figure 8. *Algorithm Flow Chart*

5.2 Cost Load and Vehicle Parameters

This section outlines the different parameters that are input into the algorithm.

5.2.1 Cost Load

In order to deploy the charging algorithm, a cost load is required. For this demonstration, the Anteater Instructional Research Building (AIRB) is used. In order to obtain the AIRB data, the MelRok metering system is used [38]. Initially, to obtain an average load profile for the year, 2015 – 2017 data were obtained at a 1-minute interval. However, a 1-minute interval resulted in too much noise in the data. Therefore, data were obtained at a 15-minute interval. However, the cost load in the algorithm has a two-day time span with a 1-minute interval (i.e., 2880 data points). Since a 15-minute interval results in 192 data points for a two-day time span, it was assumed that every 15-minute interval has the same value. Figure 9 and Figure 10 provides an example of the cost load at a 1-minute interval and 15-minute interval.

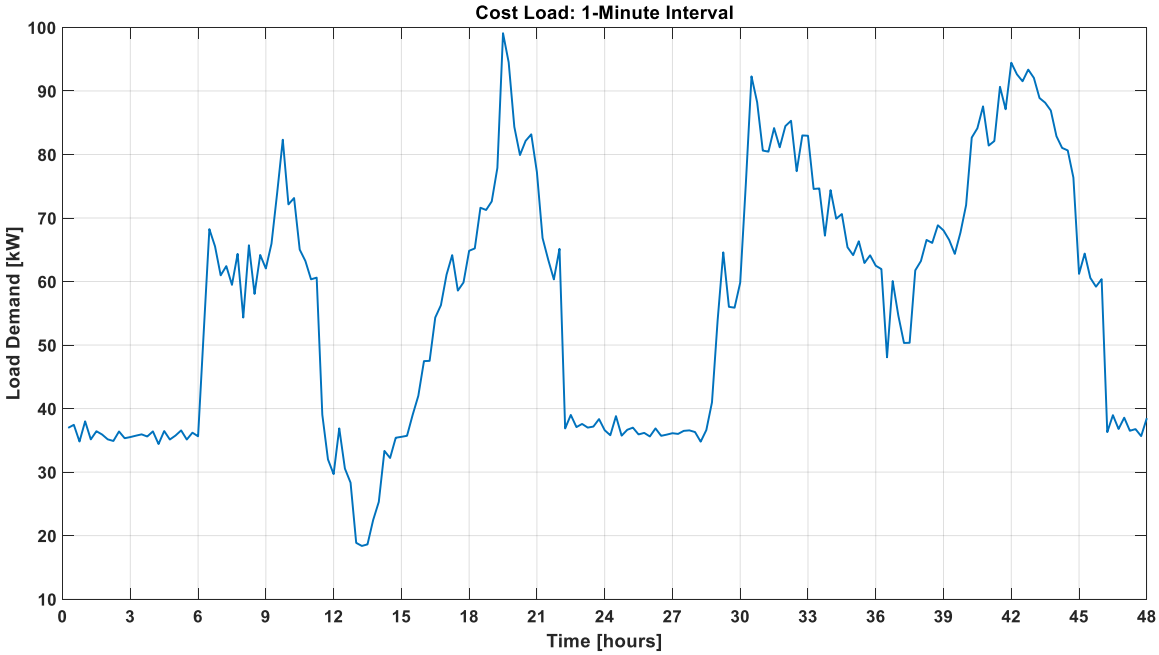

Figure 9. *AIRB Cost Load: 1-Minute Interval (Adapted from Ref. [38])*

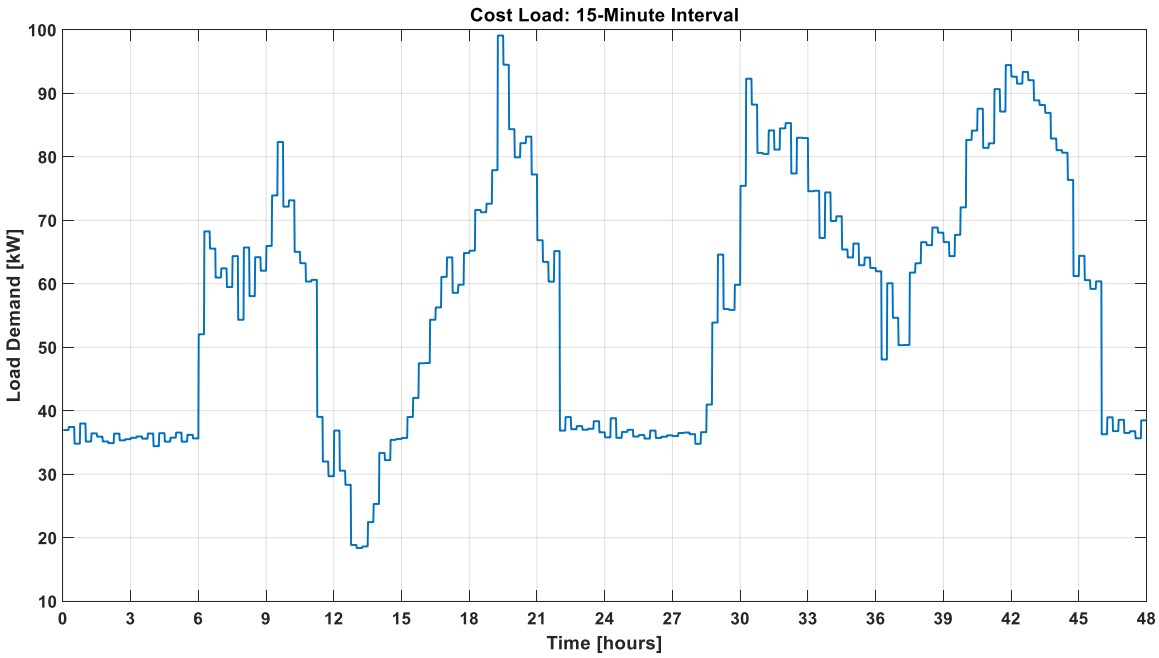

Figure 10. *AIRB Cost Load: 15-Minute Interval (Adapted from Ref. [38])*

5.2.2 Vehicle Data

As stated in the beginning of the chapter, 10 Kia Souls will be used for the demonstration. The 10 vehicles are numbered 105, 117, 118, 119, 120, 121, 122, 123, 124, and 125. In the study done by Li et al. [7], PHEVs and BEVs are used while for this demonstration, only BEVs are used. The simulation parameters used in the study done by Li et al. as well as the Kia Soul characteristics are listed in Table 3.

Table 3. *Vehicle Parameters (From Ref. [7], [39], [40])*

Vehicle Parameters		
Vehicle Type	**All-Electric Range (miles)**	**Battery Capacity (kWh)**
PHEV	40	13.6
BEV	60	18.6
Kia Soul	93	27

5.2.3 Solar Data

In Figure 9 and Figure 10, the cost load depicted is the net load, which is the building electric load minus renewable generation. However, the MelRok metering system does not provide solar data for the Anteater Parking Structure (APS), which is the parking structure adjacent to AIRB that has solar panels attached to the top floor. In order to determine the net load, solar data from the Multipurpose Science & Technology Building (MSTB) were used as a proxy for AIRB, since it is available on the MelRok metering system.

To see if the MSTB solar data could be used as a proxy for APS, it had to be determined whether or not the MSTB solar profile followed the same trend as the APS solar profile. From a previous study, a week of solar data from summer 2015 were available for APS. Using the MelRok metering system, the same week of MSTB solar data were obtained. Figure 11 shows both the APS and MSTB solar profiles.

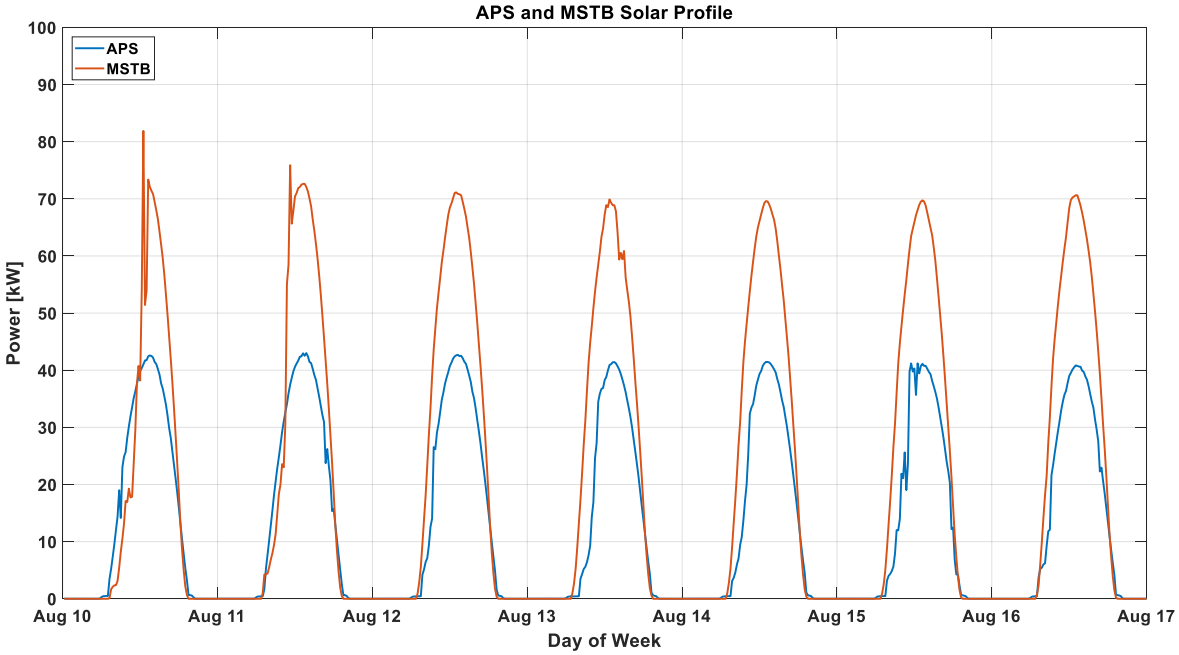

Figure 11. *APS and MSTB Solar Profile (Adapted from Ref. [38])*

As seen in Figure 11, the APS and MSTB solar profile follow a similar trend, but have minor differences. Both profiles experience minor deviations, but overall, the differences in their profiles do not have a significant effect on the overall results. Once it was determined that the APS and MSTB solar profile follow similar trends, a scaling factor was calculated by dividing the MSTB solar profile by the APS solar profile. A scaling factor for each day of that week was calculated, and the week was averaged to determine an average scaling factor. For this study, it is assumed that the average scaling factor can be applied to each day of the year. Each day of the yearlong MSTB solar profile was divided by the average scaling factor in order to obtain a solar profile for APS. Figure 12 shows the scaling profile used.

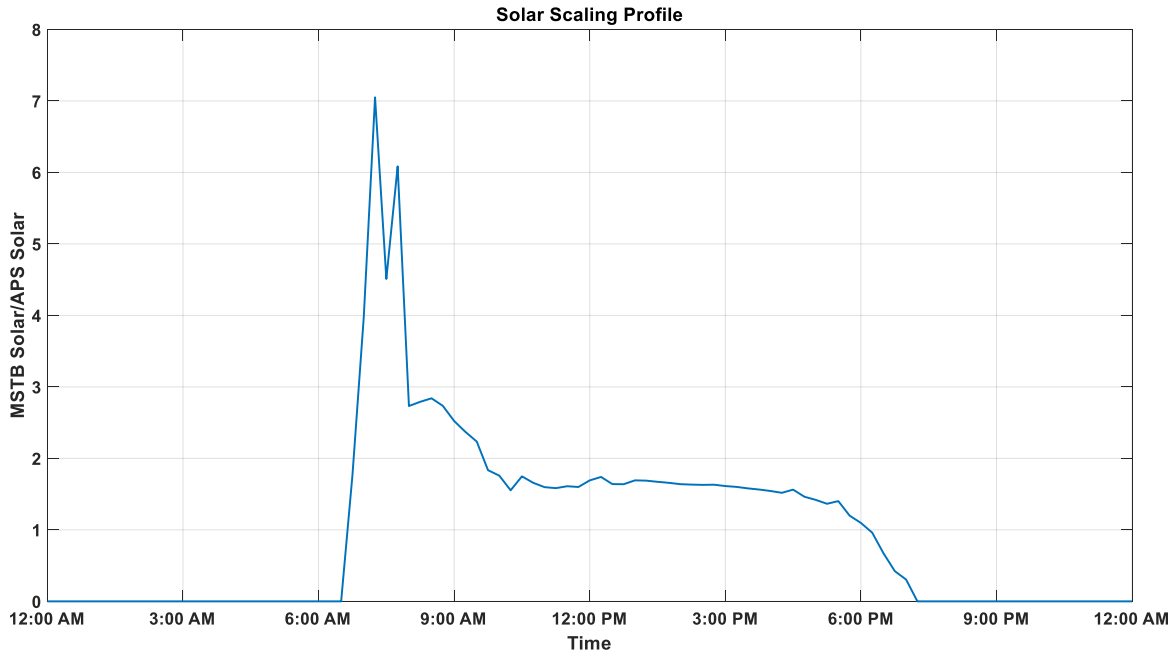

Figure 12. *Solar Scaling Profile*

5.2.4 Cost Updating

As stated in section 4.1, two methods for updating the cost load are updating the cost by fixed time intervals and updating the cost by a fixed number of vehicles. For this demonstration however, due to the low number of vehicles, the cost can be updated after each vehicle rather than after a fixed number of vehicles. To update the cost load, the PEV charging profile from the first vehicle is added to the original cost load. This becomes the updated cost load. The updated cost load is then sent back to the algorithm, where the next vehicle's charging profile is created based off the updated cost load. This process is repeated depending on the number of vehicles. Figure 13 shows how the cost load is updated.

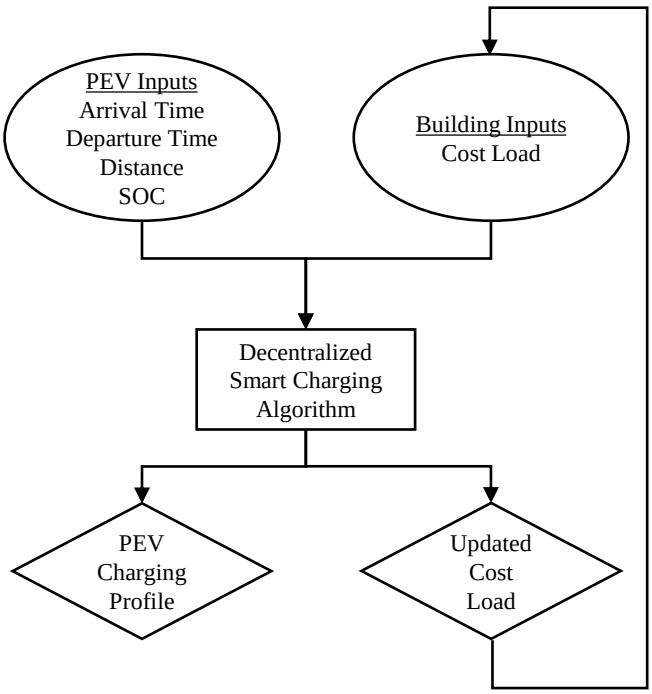

Figure 13. *Cost Load Updating*

5.3 Modifications made for Deployment

In order to deploy the algorithm, the vehicles need to be able to receive the commands from the algorithm and the algorithm needs to be able to receive the necessary input parameters. In order to achieve this, the on-board telematics will be used to send and receive information. Figure 14 shows the information flow. First, the user will input the necessary parameters: their dwell period and next trip distance. When the vehicle plugs in, the current SOC and time they plug in will be obtained. These data are sent to the PEV smart charging algorithm, where it will use the cost load to determine the charging schedule, which gets sent back to the PEVs.

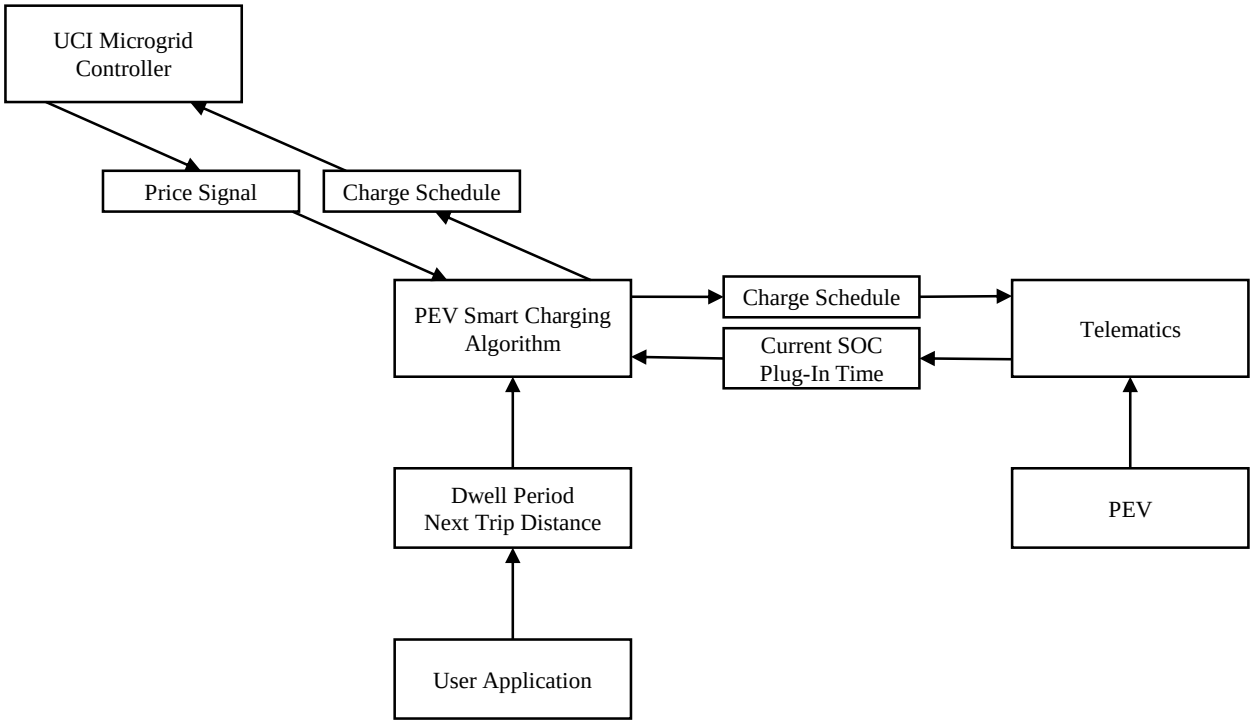

Figure 14. *Information Flow*

5.3.1 User Application and SQL Database

In order for users to input their travel plans, a user application had to be developed. Figure 15 shows the application programming interface (API), where the users can input their departure time, as well as their planned trip distance. The plug-in time as well as current SOC are obtained via telematics.

Once the user inputs their departure date/time and planned trip distance, the information is sent to the SQL database. Figure 16 and Figure 17 show an example of the SQL database with the vehicle trip information as well as the vehicle status.

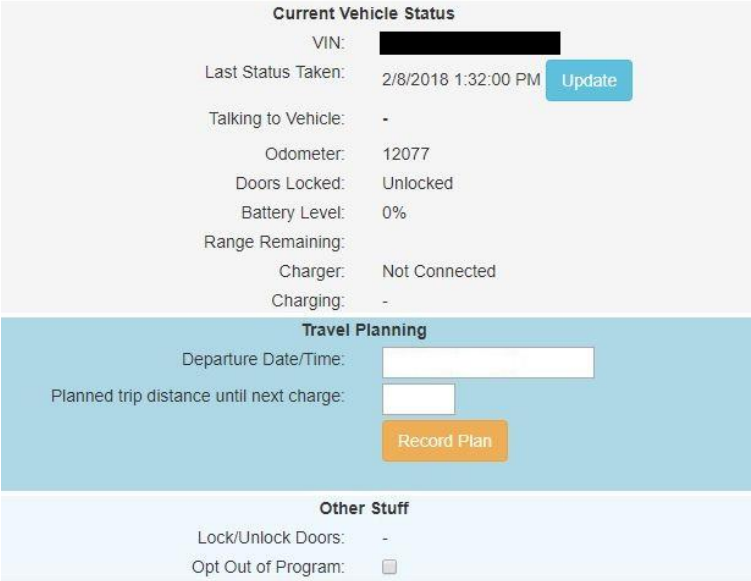

Figure 15. *Online API*

	Id	VehicleInfoId	TripDepartureTime	TripDistance	TimeStampEntered
9	9	120	NULL	24	2017-12-01 15:37:00
10	10	120	NULL	10	2017-12-28 17:06:00
11	11	120	NULL		2018-01-04 11:43:00
12	12	120	NULL	15	2018-01-04 11:43:00
13	13	120	NULL		2018-01-04 11:43:00
14	14	120	NULL	20	2018-01-04 12:12:00
15	15	120	NULL	10	2018-01-08 10:27:00
16	16	120	NULL	26	2018-01-09 11:58:00
17	17	120	2018-01-11 05:00:00	10	2018-01-10 19:33:00
18	18	120	2018-01-11 08:00:00	4.5	2018-01-10 19:35:00
19	19	120	2018-01-11 20:00:00	20	2018-01-11 13:14:00
20	20	120	2018-01-12 05:00:00	20	2018-01-11 14:13:00
21	21	120	2018-01-11 20:00:00	20	2018-01-11 14:35:00
22	22	121	2018-01-16 17:00:00	20	2018-01-16 10:52:00
23	23	120	2018-01-16 17:00:00	25	2018-01-16 11:57:00
24	24	105	2018-01-16 19:00:00	30	2018-01-16 15:05:00
25	25	117	2018-01-16 20:00:00	15	2018-01-16 15:11:00
26	26	120	2018-01-16 21:00:00	2	2018-01-16 20:12:00
27	27	120	2018-01-18 12:00:00	20	2018-01-18 08:17:00

Figure 16. *Vehicle Trip Information*

	Id	VehicleInfoId	VehicleStatus	VehicleMileage	VehicleRangeRemaining	VehicleStatusDoorLocked	evStatusBatteryStatus	evStatusBatteryPlugin	evStatusBatteryCharge	VehicleChargingTimeRemaining	VehicleTimeStamp	StatusTimeStamp
1	257	120	success	11563	50	1	62	0	0	0	2017-12-11 05:07:07.000	2017-12-10 21:07:00
2	258	120	success	11686	88	1	100	0	0	0	2017-12-15 18:55:08.000	2017-12-15 10:55:00
3	259	120	success	11686	88	1	100	0	0	0	2017-12-15 19:04:16.000	2017-12-15 11:04:00
4	261	120	success	11686	88	1	100	0	0	0	2017-12-15 19:21:30.000	2017-12-15 11:22:00
5	262	120	success	11686	88	1	100	0	0	0	2017-12-15 20:12:11.000	2017-12-15 12:12:00
6	266	120	success	11686	88	1	100	0	0	0	2017-12-15 20:15:15.000	2017-12-15 12:15:00
7	269	120	success	11689	78	1	99	0	0	0	2017-12-15 20:45:03.000	2017-12-15 12:45:00
8	272	120	success	11689	83	1	94	0	0	0	2017-12-15 21:15:33.000	2017-12-15 13:16:00
9	275	120	success	11689	83	1	94	0	0	0	2017-12-15 21:45:26.000	2017-12-15 13:45:00
10	278	120	success	11695	72	1	93	0	0	0	2017-12-15 22:15:00.000	2017-12-15 14:15:00
11	281	120	success	11695	76	1	88	0	0	0	2017-12-15 22:45:02.000	2017-12-15 14:45:00
12	284	120	success	11695	76	1	88	0	0	0	2017-12-15 22:56:02.000	2017-12-15 14:56:00
13	287	120	success	11695	76	1	88	0	0	0	2017-12-15 22:57:30.000	2017-12-15 14:58:00
14	293	120	success	11702	75	0	87	0	0	0	2017-12-16 00:14:43.000	2017-12-15 16:15:00
15	296	120	success	11702	75	0	87	2	1	590	2017-12-16 00:16:46.000	2017-12-15 16:17:00
16	297	120	success	11702	75	0	87	2	0	0	2017-12-16 00:17:38.000	2017-12-15 16:18:00
17	298	120	success	11702	75	0	87	2	0	0	2017-12-16 00:18:40.000	2017-12-15 16:19:00
18	299	120	success	11705	75	0	87	2	0	0	2017-12-16 00:19:24.000	2017-12-15 16:19:00

Figure 17. *Vehicle Status*

The vehicle's arrival time is defined as when the charger is plugged into the vehicle and the vehicle begins charging. To determine the vehicle's arrival time, the columns labeled "evStatusBatteryStatus", "evStatusBatteryPlugin", and "evStatusBatteryCharge" are used. If the value in "evStatusBatteryStatus" is less than 100 (i.e., SOC is less than 100%), the value in "evStatusBatteryPlugin" switches from 0 to 2 (i.e., the charger is plugged in), and the value in "evStatusBatteryCharge" switches from 0 to 1 (i.e., the vehicle begins charging), this indicates that the vehicle has begun charging, and the value in "StatusTimeStamp" is used as the arrival time (e.g., rows 14 and 15 in Figure 17). To determine the SOC during the arrival time, the value under "evStatusBatteryStatus" is multiplied by 27 (Kia Soul battery capacity) and divided by 100.

In order to determine the vehicle's arrival time and SOC, the vehicle status needs to be updated at a certain time interval. The update interval can be seen in "StatusTimeStamp" by examining the time difference between the value in row *n* and *n+1*. This is referred to as the "poll rate" or "polling", which affects the accuracy of the arrival time and SOC sent to the algorithm.

5.3.2 Vehicle Commands

Once each vehicle has a charge profile, the charge commands are sent to the vehicles. Vehicle commands are sent according to the charging profile. Figure 18 and Table 4 show an example of vehicle charging commands for two vehicles.

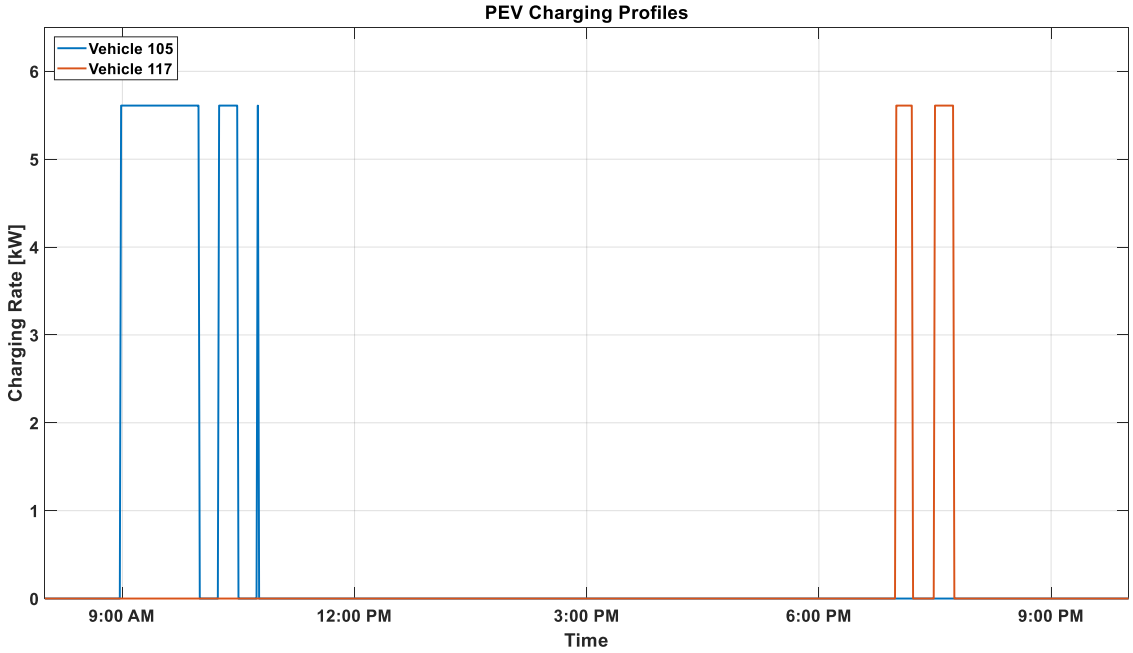

Figure 18. *PEV Charging Profiles*

Table 4. *Vehicle Charge Commands*

Vehicle Charge Commands		
Vehicle ID	**Time**	**Command**
105	8:59 AM	On
105	10:00 AM	Off
105	10:15 AM	On
105	10:30 AM	Off
105	10:45 AM	On
105	10:46 AM	Off
117	7:00 PM	On
117	7:13 PM	Off
117	7:30 PM	On
117	7:45 PM	Off

For example, in Figure 18, vehicle 105 has three charging periods and vehicle 117 has two charging periods. This means that three “on/off” commands will be sent for vehicle 105, and two “on/off” commands will be sent for vehicle 117. Since the cost load and charging profiles have a 1-minute resolution, the algorithm runs every minute. The algorithm checks the time on the

computer and if the time corresponds to the same time as a charge command, the command is sent. To ensure that the charger is turned on or off, the algorithm checks the vehicle status in between each on/off or off/on command and if the vehicle has not been turned on or off, it will issue another command. For example, if at 9:00 AM vehicle 105 has not begun charging, the algorithm will issue another on command. This is set up as a fail-safe in case the vehicle does not receive the initial command. Figure 19 shows the updated flow chart for the algorithm with a connection to the SQL database.

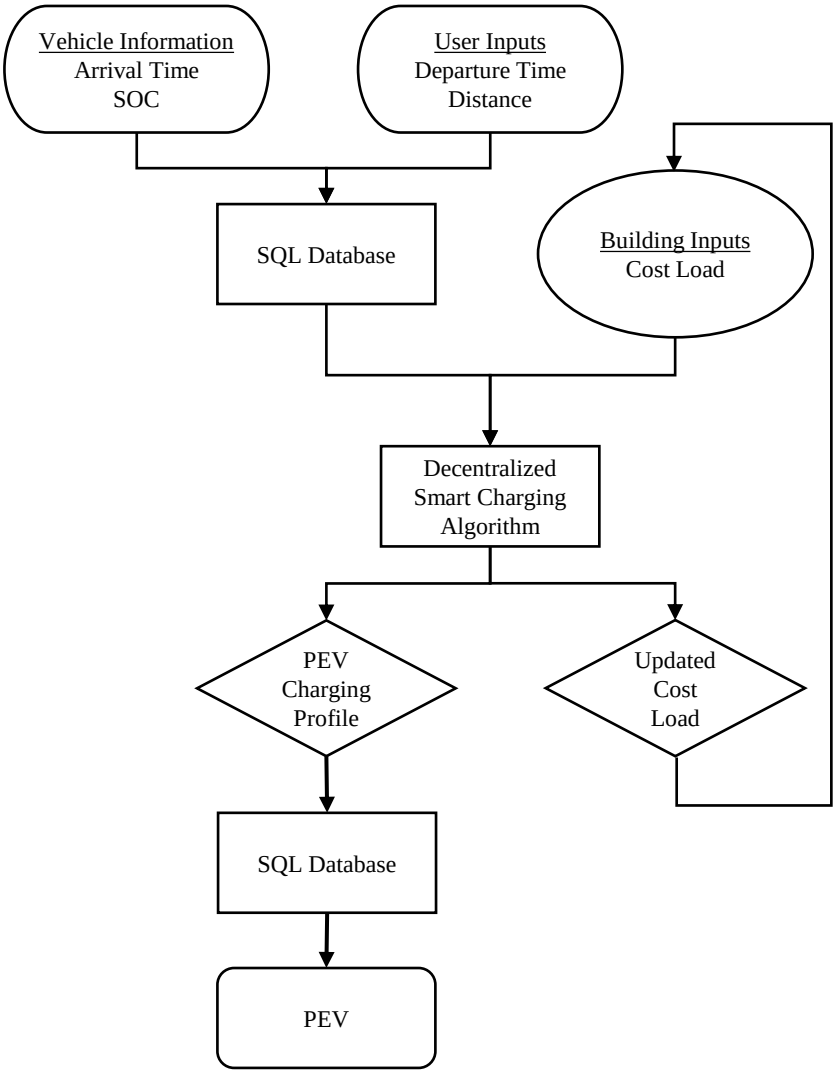

Figure 19. *Algorithm Flow Chart with Connection to SQL Database*

5.4 Edge Cases

When modifying the algorithm, upon initial testing, three edge cases were discovered.

5.4.1 Sorting Priority

The first edge case that must be taken into consideration is the sorting priority. When the algorithm was modified for multiple vehicles, the sorting priority became an issue. Depending on the order of the vehicles that arrive, the cost load can be affected in different ways. Therefore, in order to make sure the cost load is updated in a consistent manner, the following order is used: The first vehicle to arrive receives the first charge profile. If two or more vehicles arrive at the same time, the vehicle with the earliest departure time receives the first charge profile. If two or more vehicles arrive at the same time and have the same departure time, the vehicle with the farthest travel receives the first charging profile. The vehicles with the least flexibility receive first priority.

5.4.2 Initial Plug-In

The second edge case is when the vehicle initially plugs in, the charger needs to be turned off. When the charger is plugged in the vehicle begins charging immediately, but the charge profile most likely will not require the vehicle to be charged immediately. Therefore, the algorithm will check to see if the vehicle should be charged when it initially plugs in. If not, the algorithm will send an “off” command to the vehicle. However, the poll rate dictates how long the vehicle will initially charge before the algorithm can send an off command. For example, if a vehicle plugs in at 8:32 AM and the poll rate is set to 5 minutes, the algorithm will use 8:35 AM as the arrival time. If the charge profile does not have an on command at 8:35 AM, the algorithm will issue an off command. In this scenario, the vehicle will charge for 3 minutes before the charger is turned off (Figure 20b). If the poll rate is set to 30 minutes, the algorithm will use 9:00 AM as the arrival

time. If the charge profile does not have an on command at 9:00 AM, the algorithm will issue an off command. In this scenario, the vehicle will charge for 28 minutes before the charger is turned off (Figure 21b). In situations where the initial SOC is close to maximum, if the poll rate is not small enough the vehicle could finish charging completely on the initial plug in. In Figure 20a and Figure 21a, the top plot represents the ideal charging profile, while Figure 20b and Figure 21b represents the charging profile with the poll rate taken into consideration.

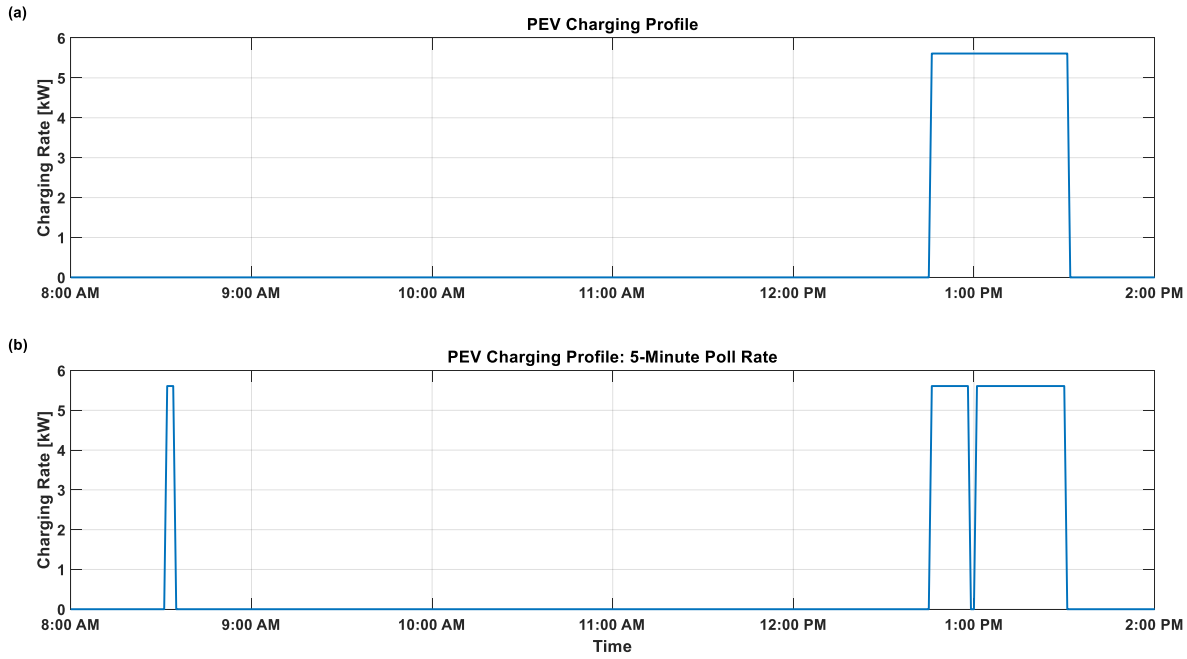

Figure 20. *PEV Charging Profile: 5-Minute Poll Rate*

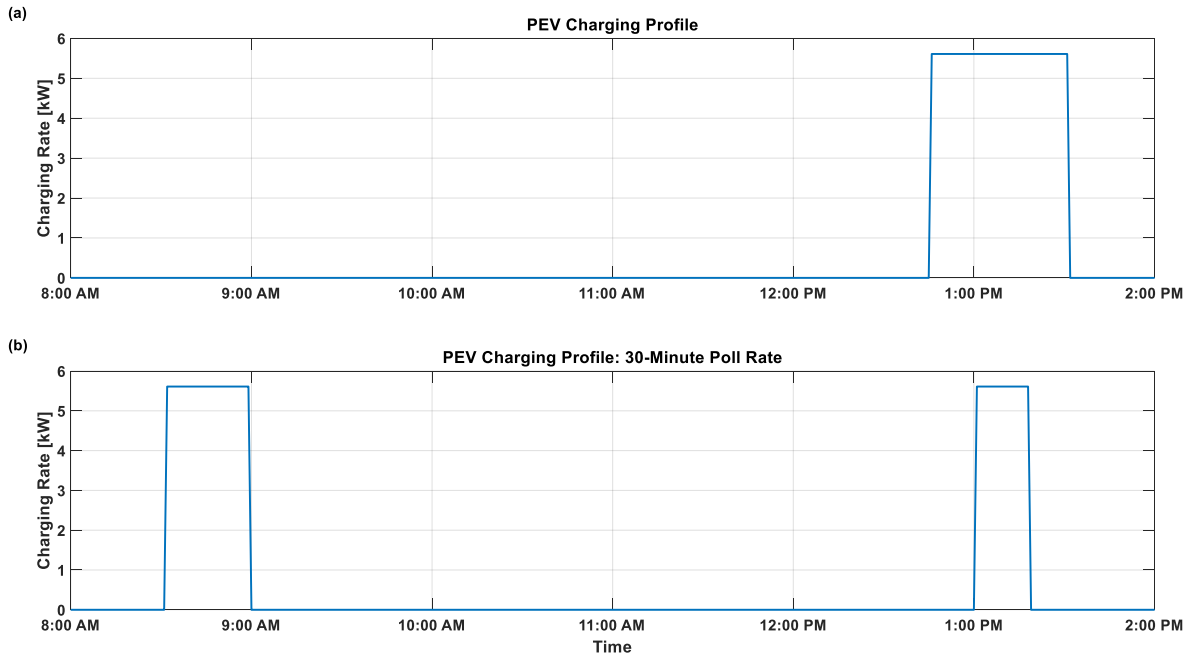

Figure 21. *PEV Charging Profile: 30-Minute Poll Rate*

5.4.3 Overnight Charging

The third edge case is if the vehicle needs to charge overnight. If a vehicle's dwell period occurs overnight (e.g., arrive Monday at 6:00 PM and depart Tuesday at 5:00 AM), the charge profile will occur overnight, such as in Figure 22. Figure 22a shows the PEV charging profile while Figure 22b shows the cost load before and after the PEV charging profile.

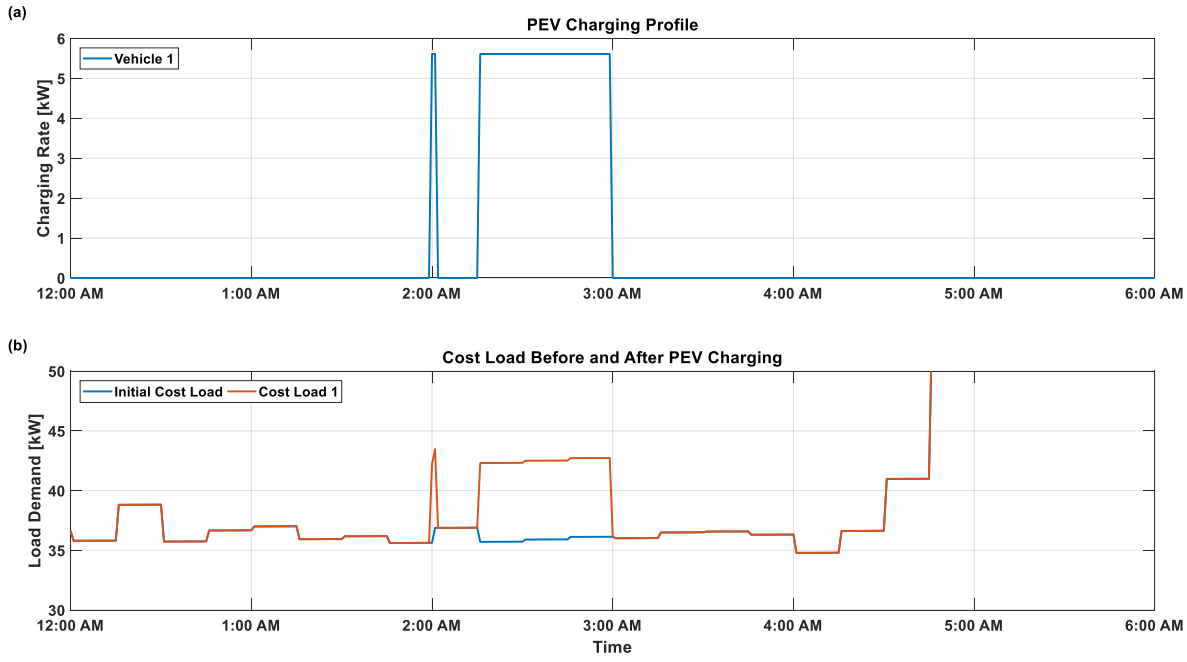

Figure 22. *Overnight Charging*

However, the cost load changes when the next day arrives. For example, if the current day is Monday, the cost load consists of Monday and Tuesday, and when Tuesday arrives, the cost load consists of Tuesday and Wednesday. Since the algorithm only takes into account the time and not the date, when Tuesday arrives, the arrival time of the vehicle will be shifted to Tuesday at 6:00 PM, rather than being kept at Monday at 6:00 PM and the departure time will be shifted to Wednesday at 5:00 AM, rather than being kept at Tuesday at 5:00 AM. The charge profile would then be set to charge overnight on Tuesday. In this case, since the departure time of the vehicle is 5:00 AM on Tuesday, the vehicle would never charge. In order to ensure that the vehicle will be charged, when Tuesday arrives (i.e., 12:00 AM on Tuesday), the arrival time of the PEV will be set to 12:02 AM, while keeping the departure time the same. Using this method, the charge profile changes slightly (since the dwell period is no longer the same length) but remains fairly similar. Figure 23a shows the PEV charging profile when the arrival time is set to 12:02 AM.

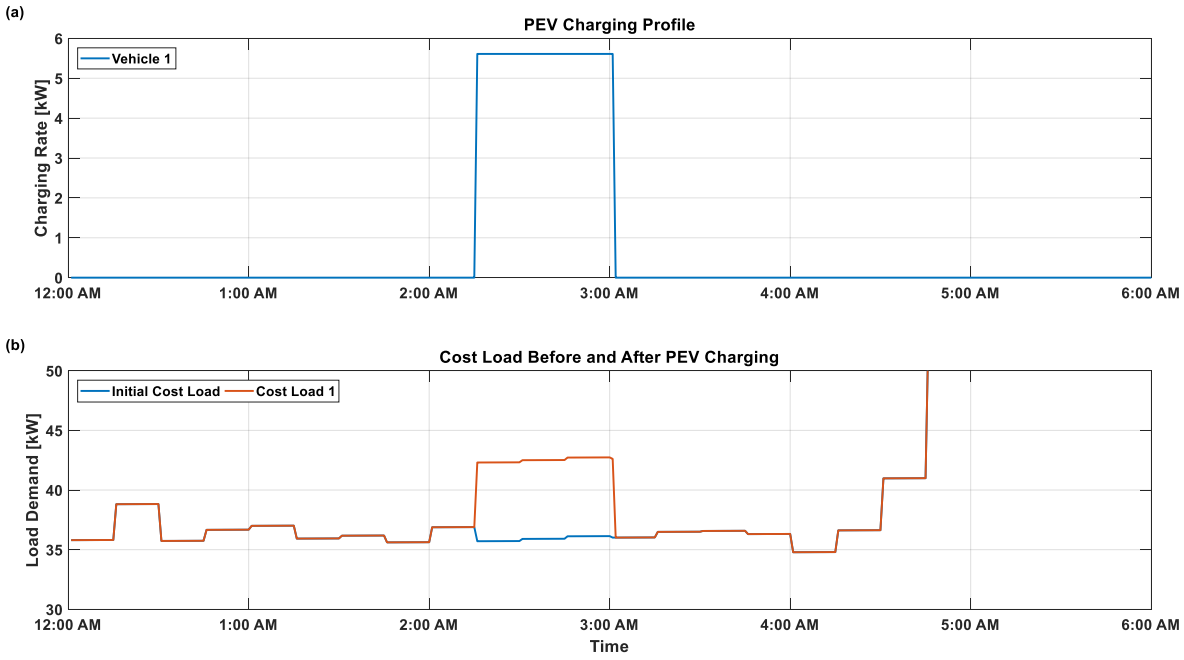

Figure 23. *Overnight Charging with Modified Arrival Time*

5.5 Results

5.5.1 Vehicle Response Time

The first test was to determine the response time of the vehicle. The initial test was carried out on vehicle 121. Commands were sent to the vehicle via MATLAB commands. Figure 24 and Figure 25 show how the vehicle responded to the commands.

3	85	121	AUTO	ON	success	1968857f-86e0-4c1f-b473-0ed7739e92a8	2018-01-18 11:01:32.467
4	86	121	AUTO	OFF	success	dd7f5c04-4822-4d8a-86a4-73af61550849	2018-01-18 11:35:29.183
5	87	121	AUTO	ON	success	203d3763-2989-4695-a6fe-26502b79c323	2018-01-18 11:42:24.700

Figure 24. *Vehicle 121 Commands*

	Id	VehicleInfoId	VehicleStatus	VehicleMileage	VehicleRangeRemaining	VehicleStatusDoorLocked	evStatusBatteryStatus	evStatusBatteryPlugin	evStatusBatteryCharge	VehicleChargingTimeRemaining	VehicleTimeStamp	StatusTimeStamp
2043	14347	121	success	11359	37	1	52	2	0	0	2018-01-18 19:00:54.000	2018-01-18 11:01:00
2044	14351	121	success	11359	37	1	52	3	1	0	2018-01-18 19:10:24.000	2018-01-18 11:10:00
2045	14356	121	success	11359	37	1	53	3	1	0	2018-01-18 19:20:38.000	2018-01-18 11:21:00
2046	14363	121	success	11367	39	1	54	2	1	125	2018-01-18 19:30:21.000	2018-01-18 11:30:00
2047	14371	121	success	11367	40	1	56	2	0	0	2018-01-18 19:40:53.000	2018-01-18 11:41:00
2048	14375	121	success	11367	41	1	57	2	1	65	2018-01-18 19:50:35.000	2018-01-18 11:51:00

Figure 25. *Vehicle 121 Status*

For the initial test, the vehicle poll rate was set at 10 minutes. This means that every 10 minutes the vehicle status is updated. The initial on command was sent at 11:01 and at 11:10, the value in evStatusBatteryCharge became 1 indicating the charger has been turned on. At 11:35, an off command was sent and at 11:41, the value became 0 indicating the charger has been turned off.

To determine how long it takes for the vehicles to respond to the commands, four other vehicles were selected for testing to send vehicle commands to. Table 5 shows when both "on" and "off" commands were sent and how long it took the vehicles to respond.

Table 5. *Vehicle Charge Command Response Times*

Vehicle Charge Command Response Times				
Vehicle ID	**Off Sent**	**Off Received**	**On Sent**	**On Received**
119	11:24:18 AM	11:27:00 AM	11:27:38 AM	11:29:58 AM
120	11:15:22 AM	11:17:56 AM	11:18:34 AM	11:21:33 AM
122	11:39:45 AM	11:41:55 AM	11:42:38 AM	11:45:24 AM
124	11:04:40 AM	11:06:02 AM	11:09:06 AM	11:12:27 AM

On average, it took the vehicles 2 minutes and 12 seconds to respond to the off commands and 2 minutes and 51 seconds to respond to the on commands. However, these tests were performed while the vehicles were enclosed in a parking structure, which could affect the latency.

5.5.2 Battery Testing

In order to obtain a more accurate arrival time and SOC, the poll rate was decreased to 5 minutes from 10 minutes. However, a 5-minute poll rate caused the vehicle's auxiliary battery to deplete within 2 to 3 days. Each time the vehicle's status was polled, the on-board telematics turn on, causing an increase in the amperage. To determine the amperage increase, tests were performed on the vehicle using a multimeter.

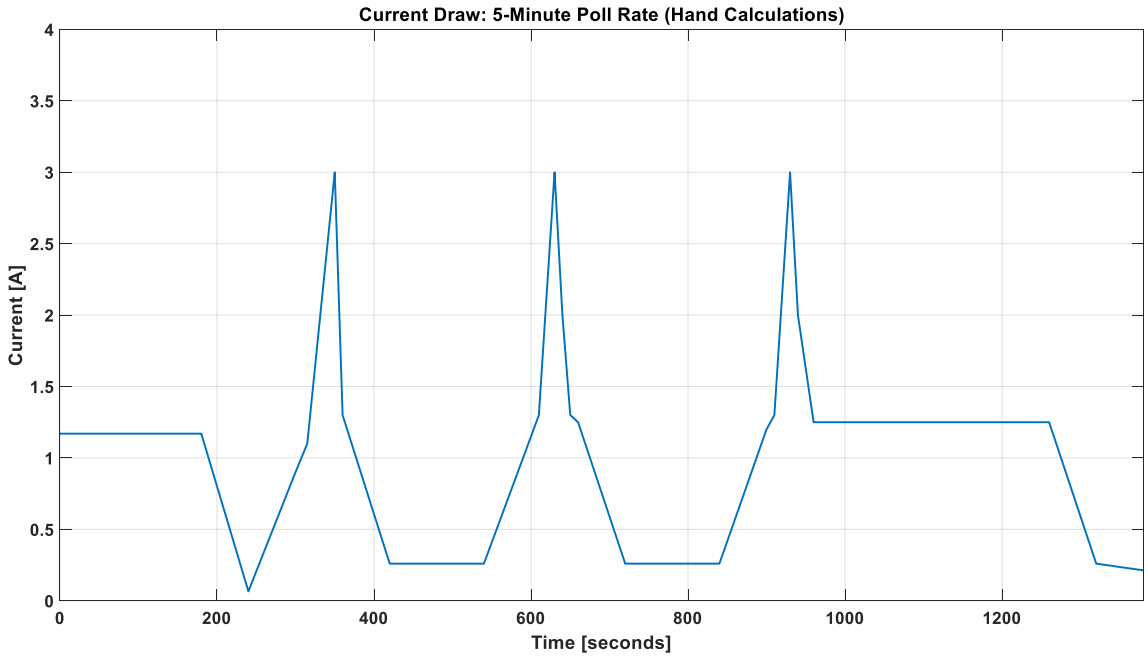

Figure 26. *Current Draw: 5-Minute Poll Rate (Hand Calculations)*

As seen in Figure 26, each time the vehicle information was polled, the amperage increased to 3 amps from a baseline of ~260 milliamps. This results in 0.047 Amp-hours drawn from the battery during the poll period. The poll period refers to the increase in amperage each time the vehicle's information is polled from the baseline of ~260 milliamps until it decreases back to the baseline amperage. To retrieve more data points, the vehicle's auxiliary battery was attached to a shunt resistor, which was connected to an Arduino to record the amps. Figure 27 through Figure 30 show the results for a 5, 10, 15, and 20-minute poll rate, respectively.

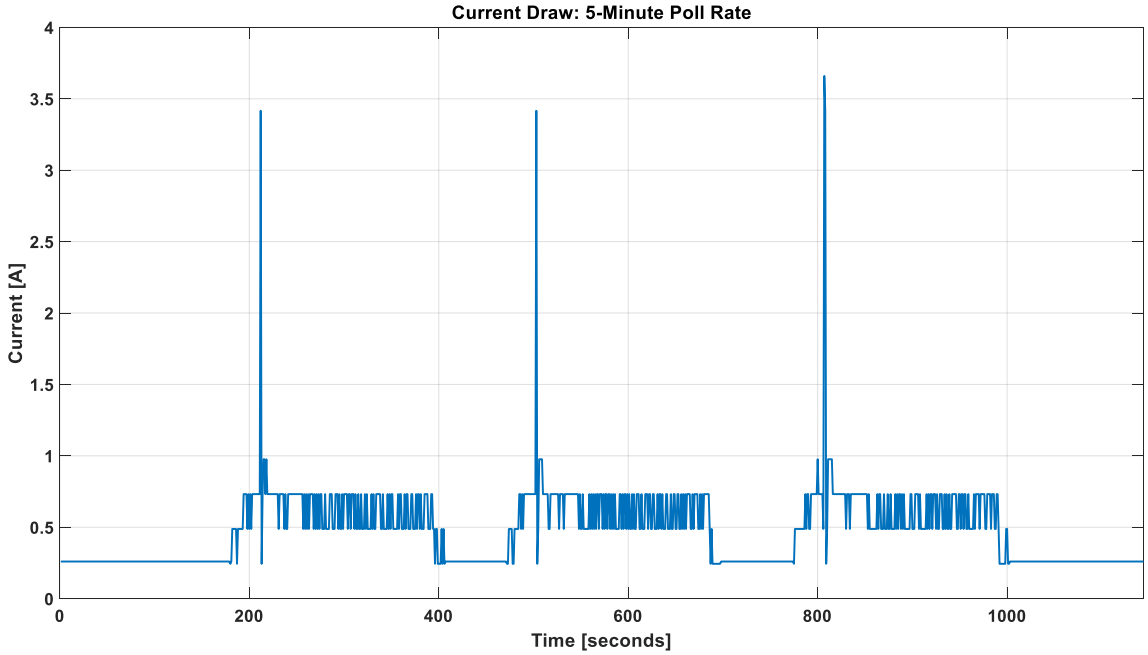

Figure 27. *Current Draw: 5-Minute Poll Rate*

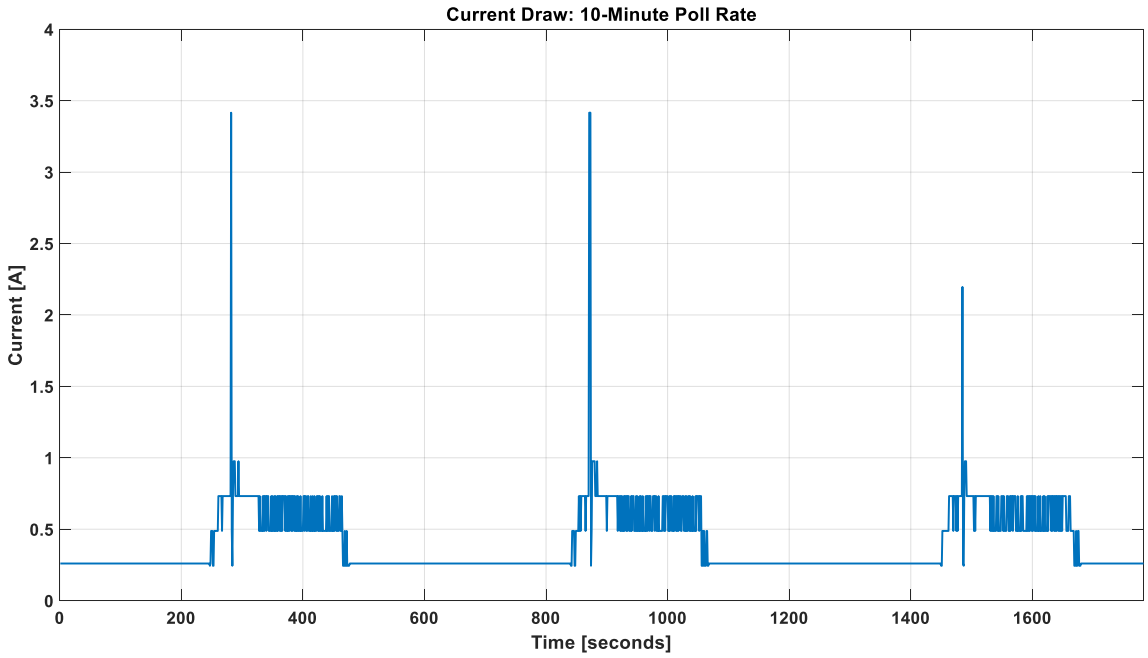

Figure 28. *Current Draw: 10-Minute Poll Rate*

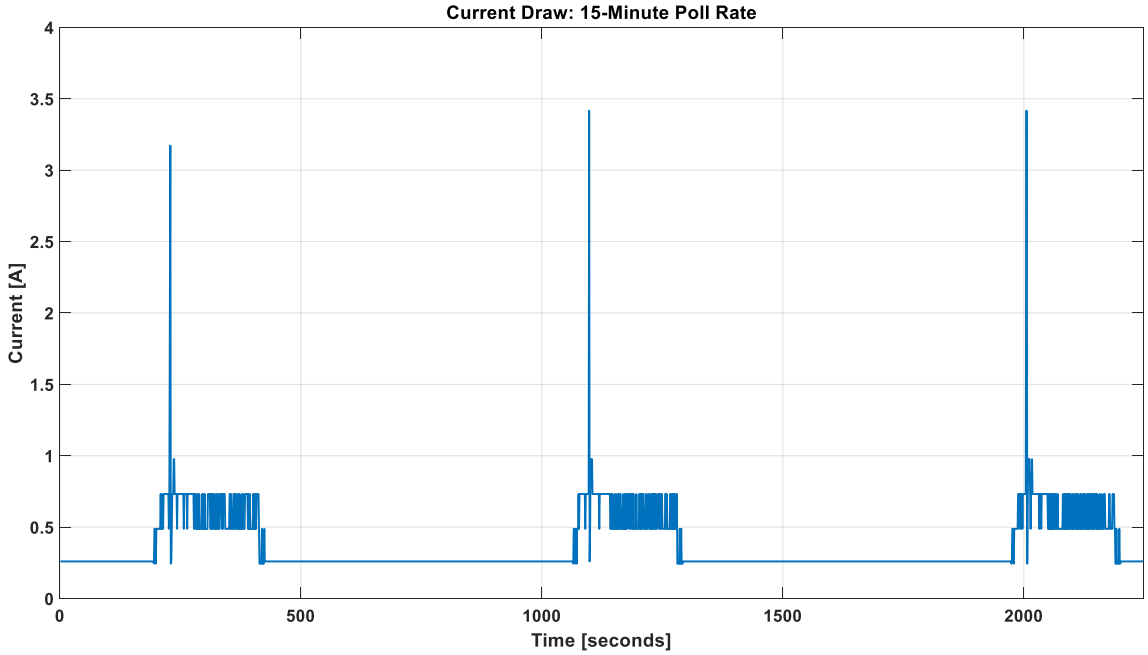

Figure 29. *Current Draw: 15-Minute Poll Rate*

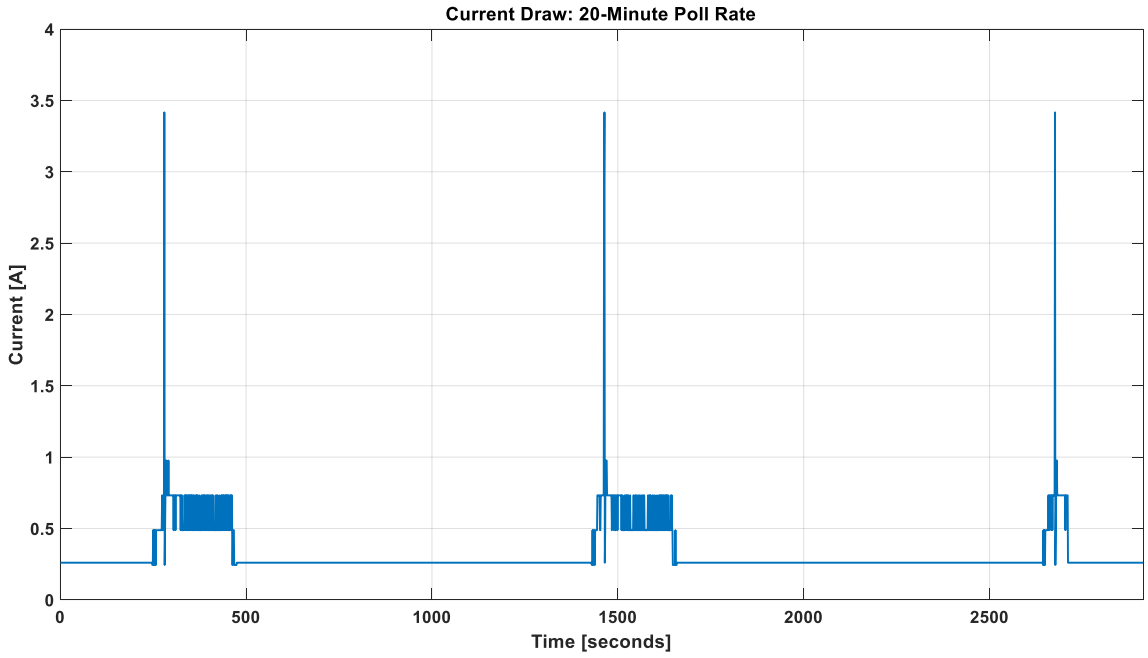

Figure 30. *Current Draw: 20-Minute Poll Rate*

In Figure 27 through Figure 30, the average amp-hour during each poll period was 0.039. The average amp-hour during each break period was also calculated. The break period refers to the period between each polling rate, when the amperage is at the baseline. The combined amp-hours of the poll period and break period is referred to as a single cycle. The number of cycles is used to determine approximately how many days the battery will last before it is depleted, assuming the battery has not been charged. To determine the number of days before the battery is depleted, the following calculations are used:

Table 6. *Kia Soul Auxiliary Battery (From Ref. [41], [42])*

Kia Soul Auxiliary Battery		
Voltage (V)	**Reserve Capacity (min)**	**Battery Capacity (Amp-hours)**
12	120	50

$$Battery\ Capacity\ [A \cdot h] = Reserve\ Capacity\ [min] \times 25\ [A] \times \frac{1}{60}\left[\frac{hours}{min}\right]$$

$$Break\ Period\ [A \cdot h] = 0.26\ [A] \times Break\ Period\ [s] \times \frac{1}{3600}\left[\frac{hours}{s}\right]$$

$$Poll\ Period\ Amp - Hours\ = 0.039\ [A \cdot h]$$

$$\frac{Total\ Amp - Hours}{Cycle} = \frac{(Break\ Period\ Amp - hours + Poll\ Period\ Amp - hours)}{1\ Cycle}\left[\frac{A \cdot h}{cycle}\right]$$

$$\#\ of\ Cycles = \frac{Battery\ Capacity}{\left(\frac{Total\ Amp - Hours}{Cycle}\right)}\left[\frac{A \cdot h}{\left(\frac{A \cdot h}{cycle}\right)}\right]$$

$$Days\ before\ Depletion = \frac{\#\ of\ Cycles\ [Cycle] \times \left(\frac{Poll\ Rate}{Cycle}\right)\left[\frac{min}{cycle}\right]}{1440\ \left[\frac{min}{day}\right]}$$

Table 7 and Figure 31 show approximately how many days the battery will last before it is fully depleted based on the poll rate.

Table 7. *Poll Rate Characteristics*

Poll Rate Characteristics					
Poll Rate	**Break Period A·h**	**Poll Period A·h**	**Total A·h**	**# of Cycles**	**Days before Depletion**
5 Minutes	0.005	0.039	0.044	1133	3.93
10 Minutes	0.027	0.039	0.066	758	5.26
15 Minutes	0.048	0.039	0.087	577	6.00
20 Minutes	0.070	0.039	0.109	459	6.37

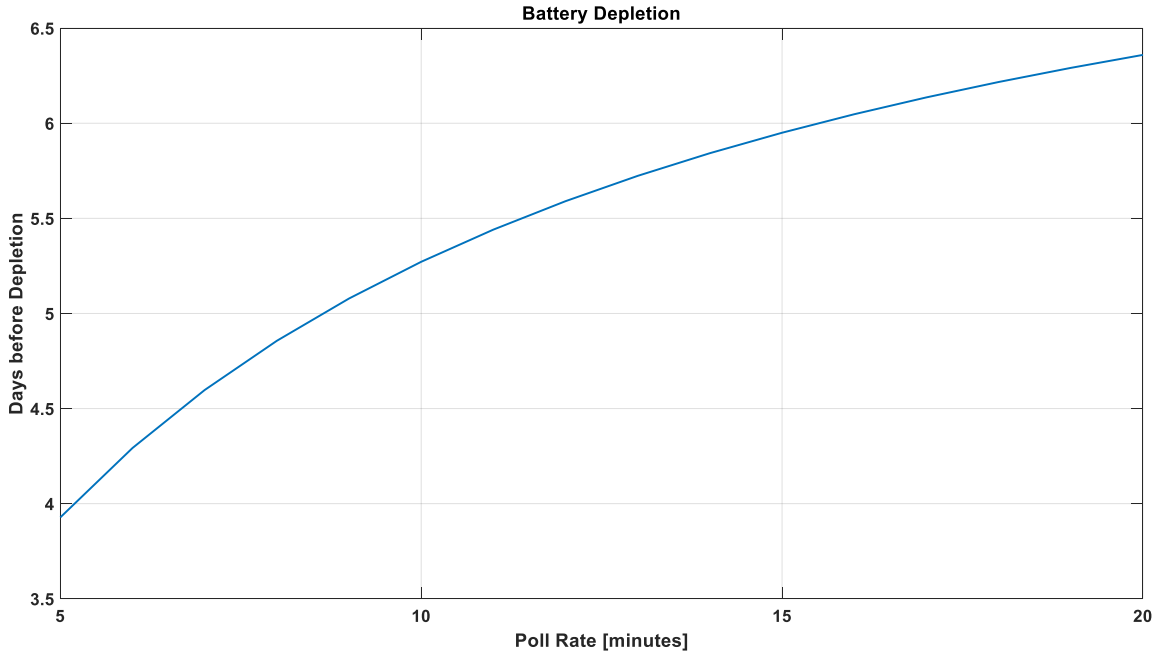

Figure 31. *Battery Depletion*

5.6 Poll Rate Effect on Charging Schedules and Cost Load

The poll rate can affect how the overall profile is shaped. In order to simulate how the poll rate affects the net load, the 2009 NHTS data were used to represent vehicle travel patterns [16].

These data were filtered for work related travel. Figure 32 through Figure 34 show arrival and departure times, as well as VMT.

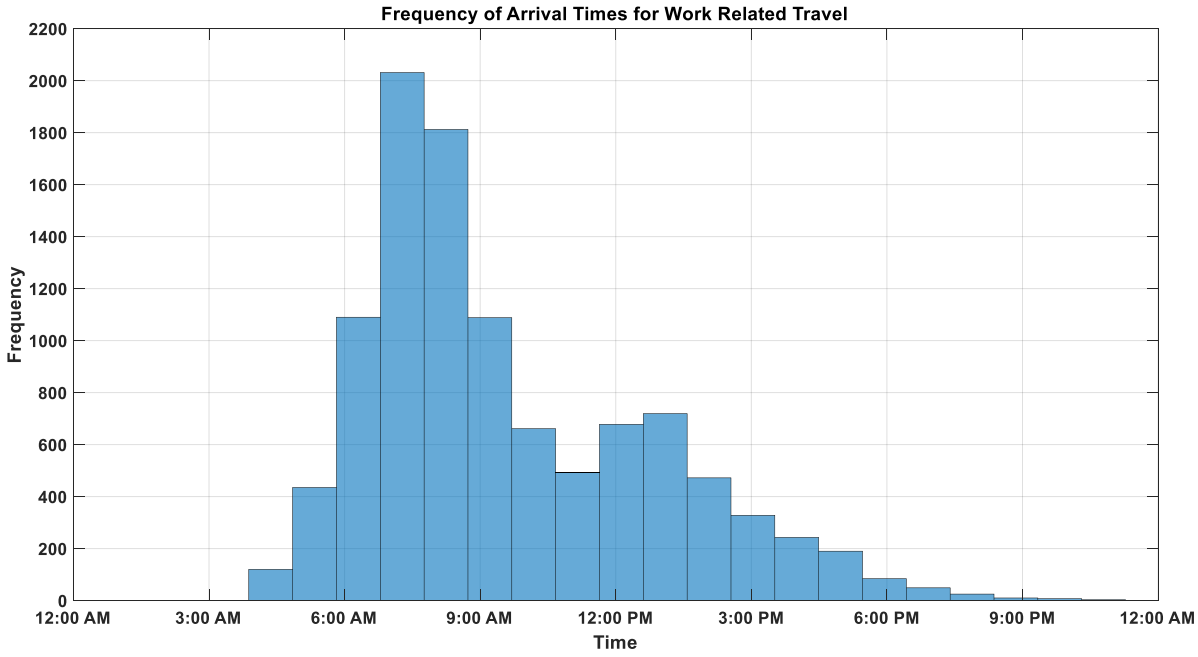

Figure 32. *Arrival Times for Work Related Travel (Adapted from Ref. [16])*

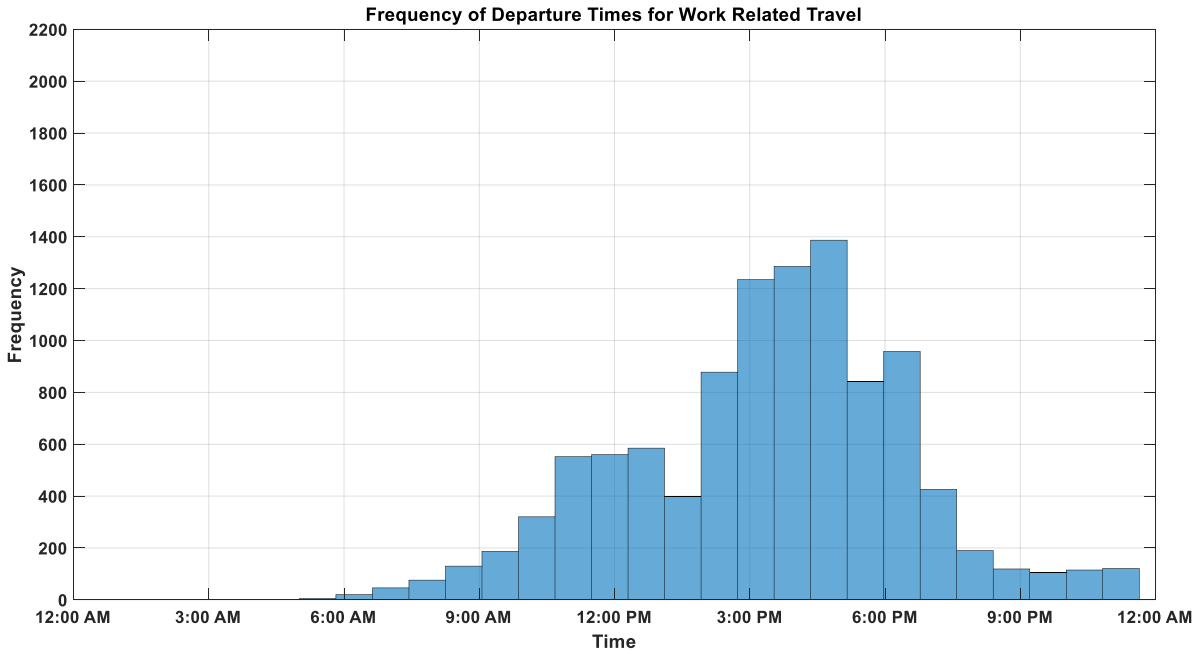

Figure 33. *Departure Times for Work Related Travel (Adapted from Ref. [16])*

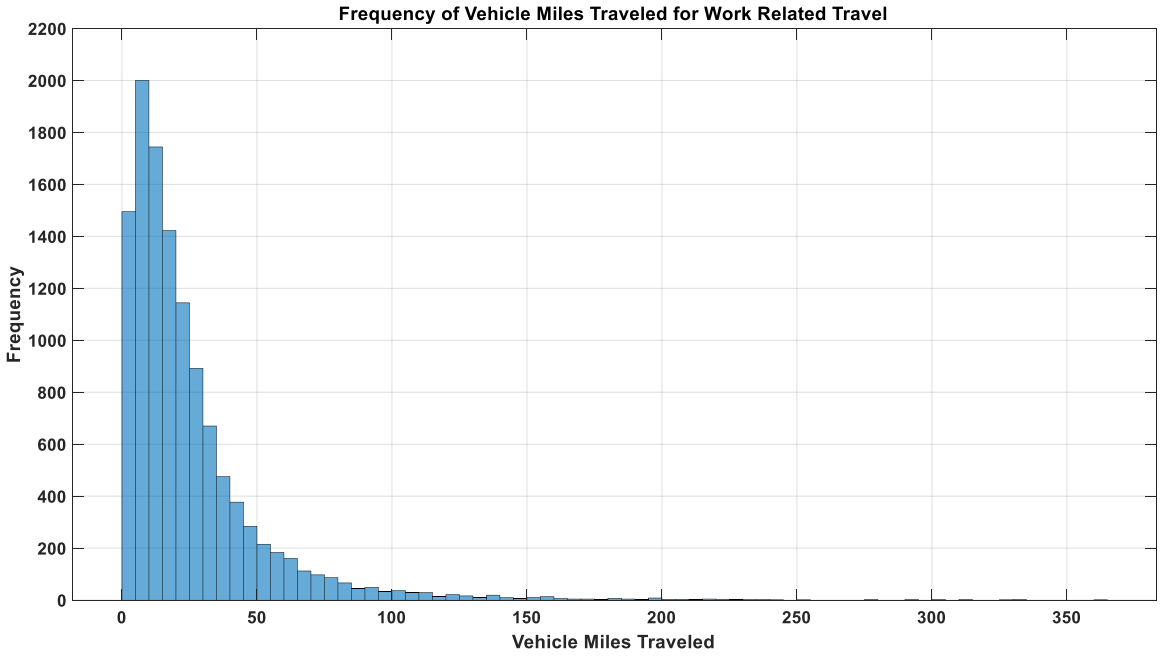

Figure 34. *Vehicle Miles Traveled for Work Related Travel (Adapted from Ref. [16])*

As seen in Figure 34, the majority of VMT for work related travel is less than 30 to 40 miles. For the following simulations, the VMT were limited to 30 miles to ensure that the vehicles will not travel more than the allowable range. Figure 35 through Figure 38 show the effects of a 5, 10, 15, and 20-minute poll rate on the cost load when 500 vehicles are simulated, respectively.

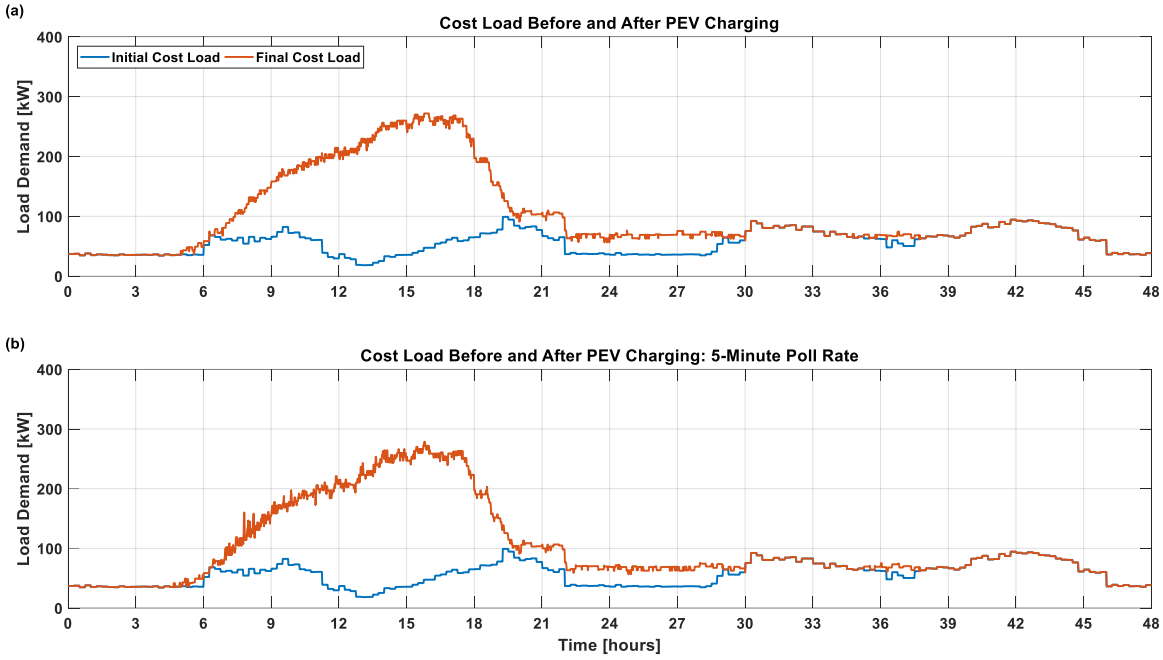

Figure 35. *Cost Load Before and After PEV Charging: 5-Minute Poll Rate*

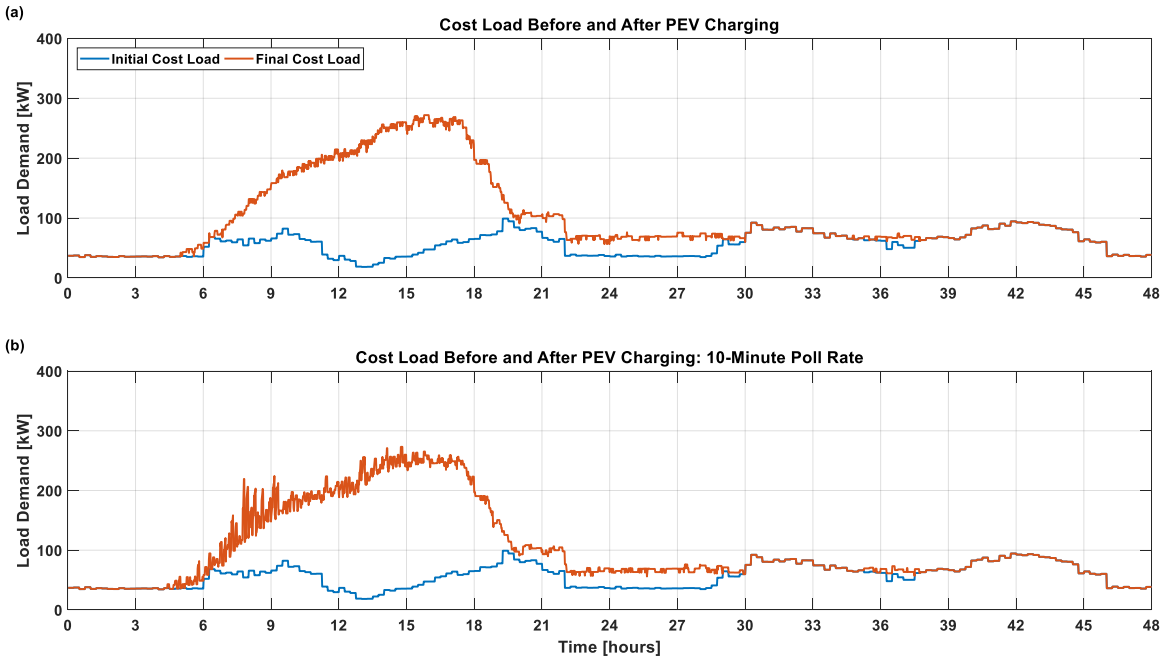

Figure 36. *Cost Load Before and After PEV Charging: 10-Minute Poll Rate*

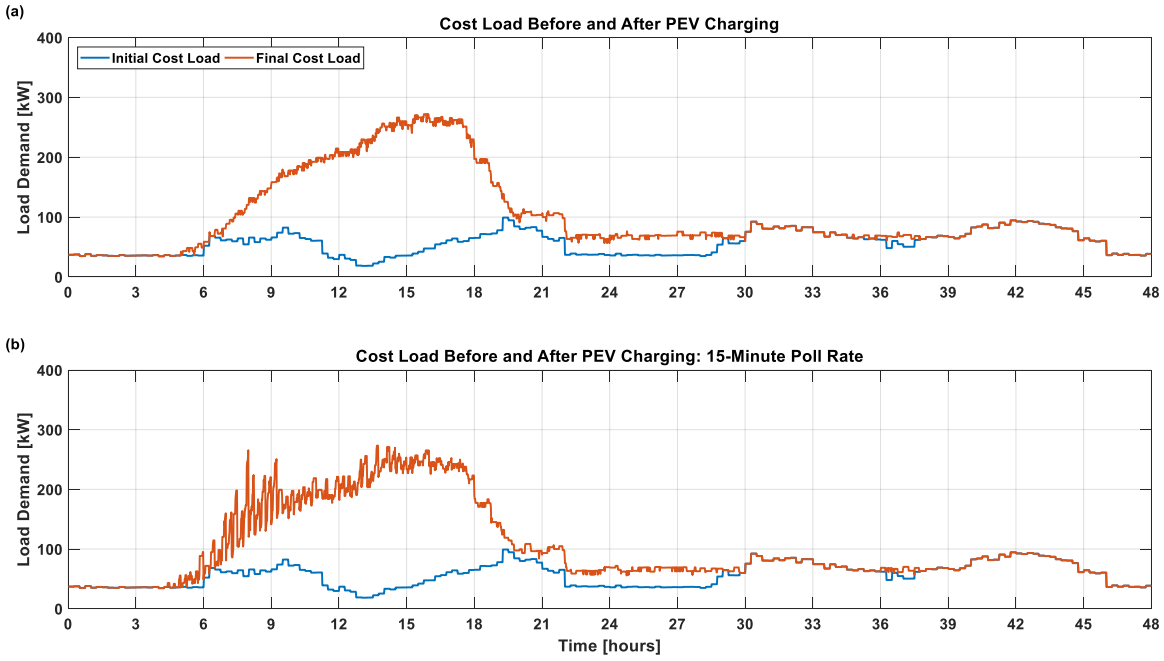

Figure 37. *Cost Load Before and After PEV Charging: 15-Minute Poll Rate*

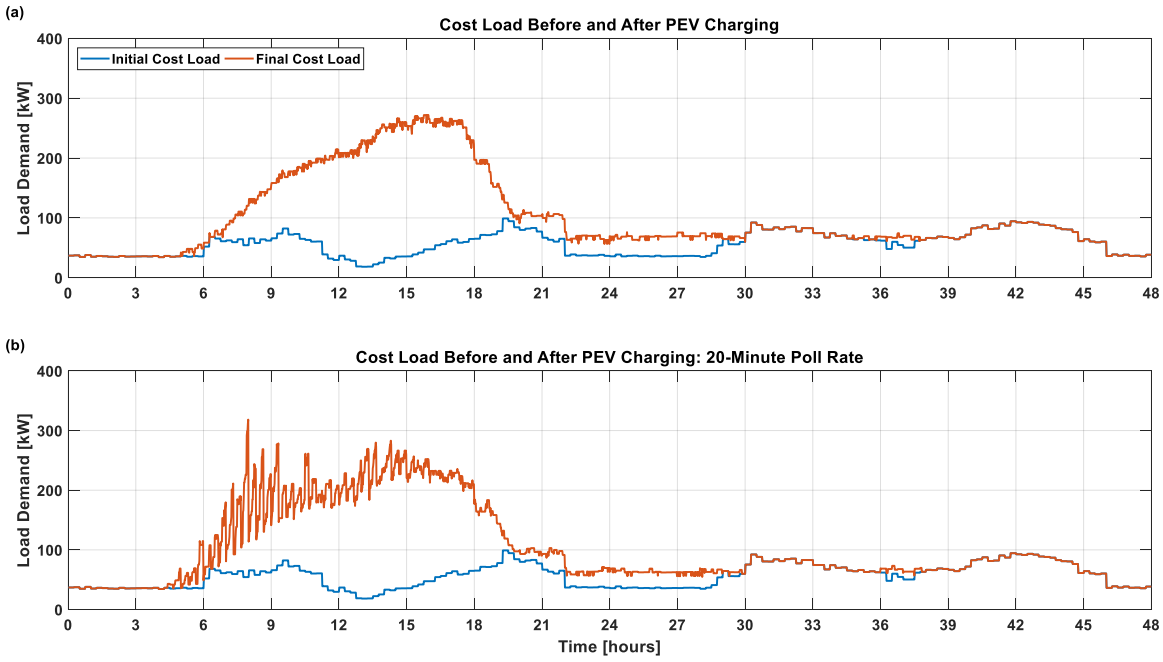

Figure 38. *Cost Load Before and After PEV Charging: 20-Minute Poll Rate*

In Figure 35 through Figure 38, subplots "a" show the ideal profile, where the poll rate does not affect that charging profiles and subplots "b" show the profile when the poll rate is taken into account. It is clear that as the poll rate increases, the profile becomes more unstable. The majority of the "spikes" in the cost load occurs around 8 AM – 9 AM, corresponding with the majority of arrival times, as seen in Figure 32.

5.7 Objective 2 Summary

As seen in sections 5.5.2 and 5.6, the poll rate has a significant effect on both the battery as well as the accuracy of the results. While a 1-minute poll rate would be the most ideal, it is not possible since it takes on average 3.8 minutes to obtain the vehicle status. As seen earlier, a 5-minute poll rate caused the auxiliary battery to deplete within 2-3 days. Therefore, for this demonstration, a 10-minute poll rate should be used. This will provide the most accurate results without putting too much strain on the battery.

One potential solution to address the poll rate issue would be to use the EVSE to obtain the vehicles' status rather than the vehicles' on-board telematics system. This would remove the need to use the telematics system to obtain the status since once the vehicle plugs in, the vehicles' status can get sent to the algorithm from the EVSE side. Another potential solution would be to use a "hybrid" polling approach. Using this approach, the poll rate can be set to 5 minutes when the vehicles are plugged in, and reverted back to 20 minutes once they have finished charging.

While this demonstration is for 10 vehicles, the algorithm can be scaled up to larger scales, such as what has been done in [7]. When deploying the algorithm on a small fleet of vehicles such as the demonstration, the computation time is not extensive and the cost load can be updated after each vehicle. However, as the number of vehicles scale up, if the cost load is to be updated after each vehicle, significant computation power will be needed. Therefore, as the number of vehicles increase, to avoid transmitting large amounts of data, the cost load should be updated after a fixed number of vehicles or a fixed time step.

6. OBJECTIVE 3 RESULTS

Develop and simulate smart charging scenarios within a microgrid

The decentralized smart charging algorithm identified in objective 1 will be used to create and simulate different smart charging scenarios. Chapter 6 explores how the decentralized smart charging algorithm affects different building loads on a microgrid.

6.1 University of California, Irvine Microgrid

The microgrid used for analysis in this thesis is the University of California, Irvine's (UCI) microgrid. The UCI microgrid serves more than 30,000 members as well as a variety of building types such as residential, office, and research buildings. As seen in Figure 39, a wide array of different technologies have been installed on UCI's microgrid such as gas and steam turbines, electric vehicle chargers, solar PV, etc. [43].

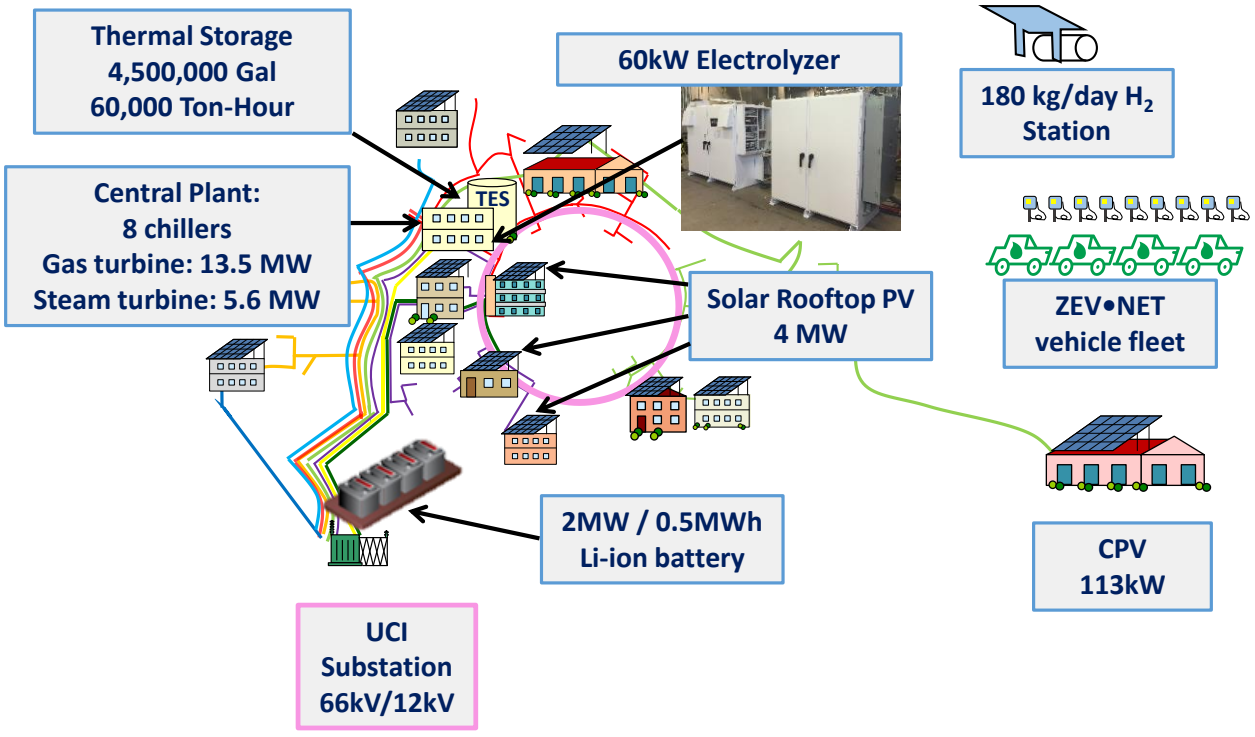

Figure 39. *UCI Microgrid (From Ref. [43])*

6.2 Cost Loads: Time-Of-Use Rate Structure & Building Loads

For these simulations, three different cost loads were selected to evaluate how the smart charging algorithm impacts UCI's electric load: Southern California Edison's (SCE) Time-Of-Use (TOU) rate structure, a proposed future TOU rate structure, and different building loads. Using different cost loads will shape the net load profile in different ways.

6.2.1 SCE TOU Rate Structure

The first cost load used is the TOU rate structure provided by SCE. This is used to estimate how much it will cost each individual PEV to charge. While UCI charges each vehicle based on how long they are parked for ($2.50/hour [44]), in order for it to be practical to use the SCE TOU rate structure as a cost load, it is assumed that the vehicles will be charged based on how much energy they use rather than how long they are parked for. If vehicle owners were charged based on their dwell period, using this rate structure as a cost load would not be practical since work dwell periods typically last around 8 hours. In this scenario, vehicles will attempt to charge at the lowest cost, which may not necessarily occur when the net load is at the lowest. The SCE TOU rate structure is broken up into three categories and two seasons: off-peak, mid-peak, on-peak, and the winter (10/1 – 5/31) and summer (6/1 – 9/30) seasons. These costs consist of peak cost and transmission and distribution charges. For both seasons, holidays and weekends use off-peak costs [45]. Figure 40 shows the SCE TOU rate structure for both seasons and all three categories along with a generic normalized solar profile. As seen in Figure 40, the costs tend to be the cheapest when renewable generation is at a minimum, meaning that the net load will not be at the lowest value.

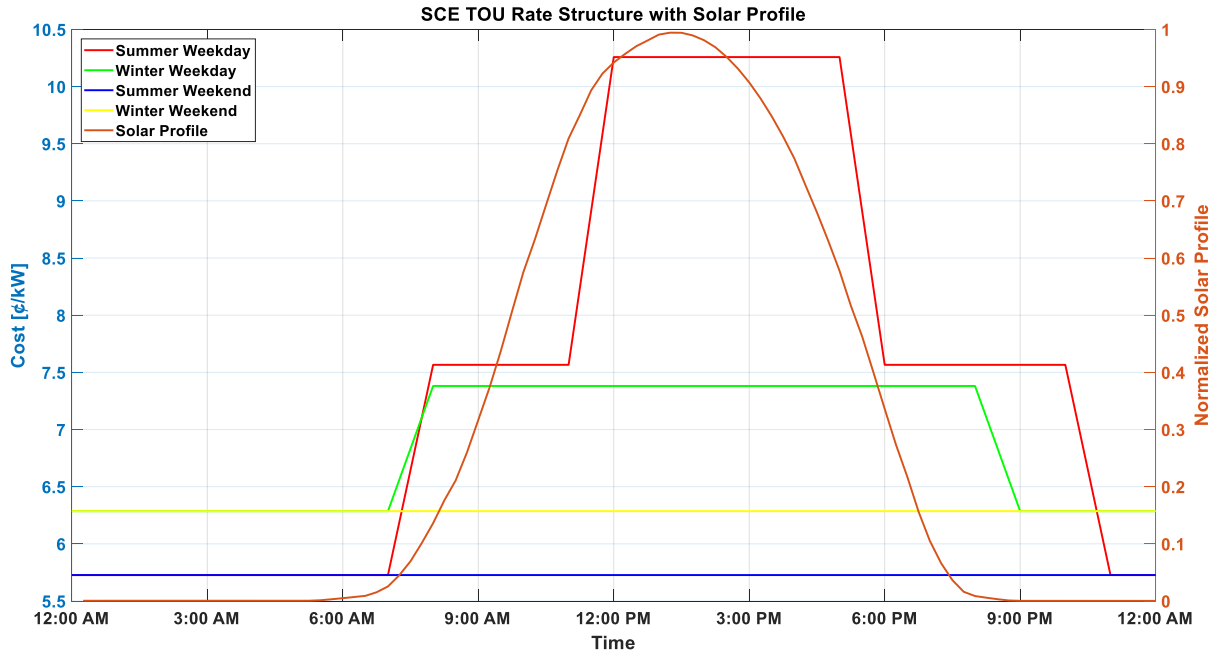

Figure 40. *SCE TOU Rate Structure with Solar Profile*

6.2.2 Future TOU Rate Structure

The second cost load used is a proposed future TOU rate structure. The way TOU rate structures are designed is important since it can encourage electric loads to coordinate better with solar production. The California Public Utilities Commission (CPUC) aims to shift PEV charging to times of the day that utilize low-cost renewable energy in order to better assist the grid. However, commercial TOU rates that are currently used were not constructed with renewable generation and integration taken into consideration. Therefore, investor owned utilities (IOUs) such as San Diego Gas and Electric, Pacific Gas and Electric, and Southern California Edison have proposed shifting their peak TOU rates to late afternoon and into the evening, such as 4 PM – 9 PM. This will provide better alignment with the "duck curve" since peak prices would be shifted to expected peak periods, as seen in Figure 4 [46]–[48].

This proposed rate structure will alter the costs such that the cost will be the lowest when renewable generation is maximized and the highest when renewable generation is minimized. In this scenario, vehicles will also attempt to charge at the lowest cost. However, in contrast to the SCE TOU rate structure, this rate structure tends to be the lowest when the net load is at the lowest. For this rate structure it is assumed that the SCE on-peak and off-peak hours/rates will switch for the summer season, and the mid-peak and off-peak hours/rates will switch for the winter season. Weekend and holidays will still use off-peak costs. Figure 41 shows the proposed future TOU rate structure along with the same normalized solar profile shown in Figure 40. Note how the lowest rates corresponds with peak solar production.

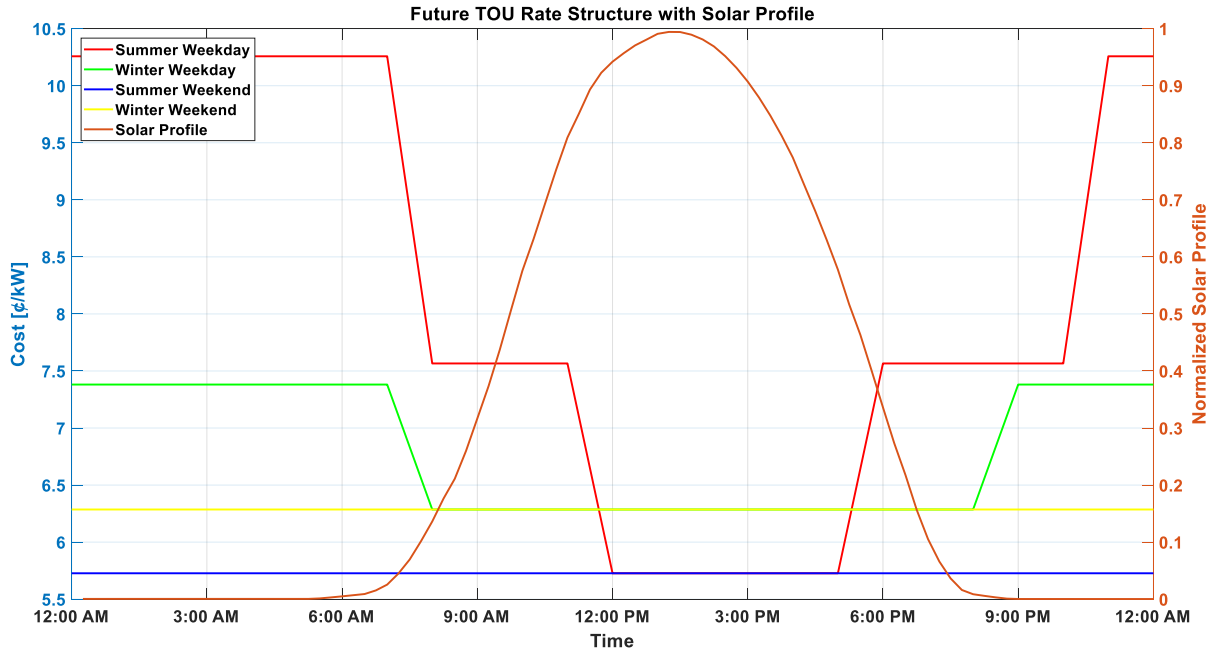

Figure 41. *Future TOU Rate Structure with Solar Profile*

6.2.3 Building Profiles

The third cost load used are different building profiles. In this scenario, vehicles will attempt to charge when the net load is the lowest. The six buildings selected already have EVSEs

installed. Table 8 lists each building as well as the number of chargers located at each building. Figure 42 and Figure 43 shows each building's electric load profile and where the chargers are located, respectively. When using the building profiles as the cost load, both the SCE and future TOU rate structure will be used to determine how much it will cost the vehicles to charge.

Table 8. *UCI Buildings with EVSEs (From Ref. [44])*

UCI Buildings with EVSEs	
Building	**Number of Chargers**
A. Anteater Parking Structure (APS)	20
B. East Campus Parking Structure (ECPS)	20
C. Mesa Parking Structure (MPS)	14
D. Multipurpose Science Technology Building (MSTB)	6
E. Student Center Parking Structure (SCPS)	12
F. Social Science Parking Structure (SSPS)	38

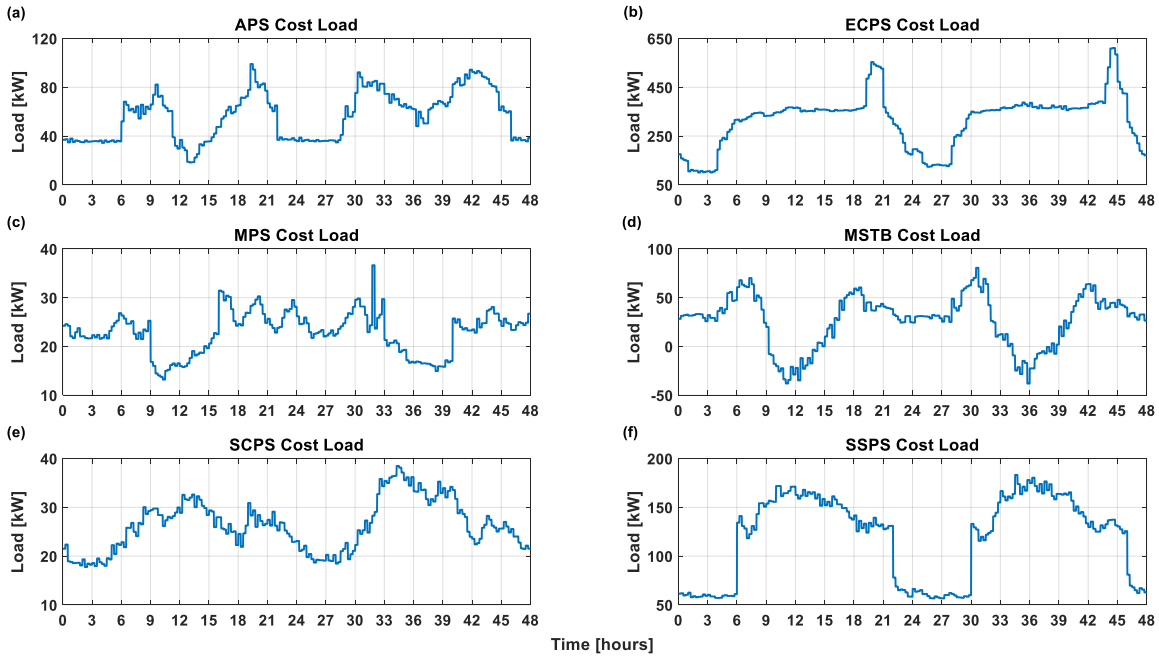

Figure 42. *UCI Building Electric Load Profiles (Adapted from Ref. [38])*

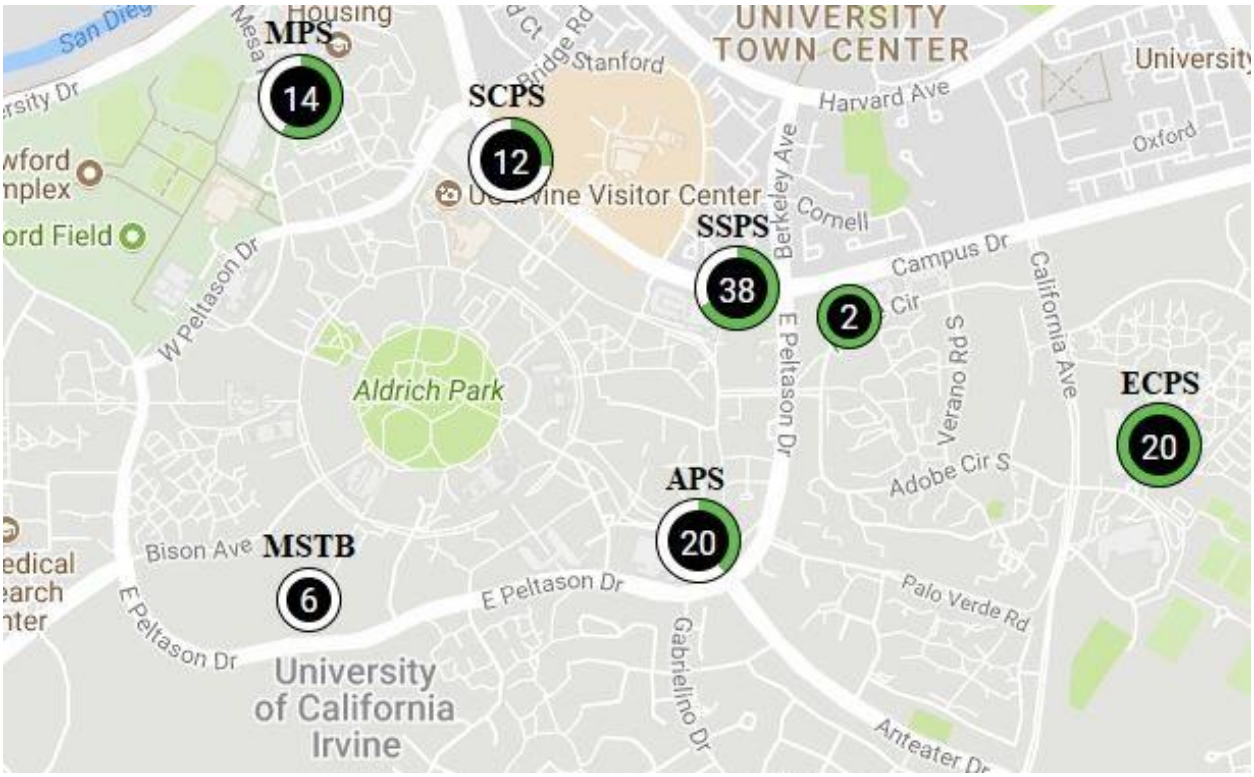

Figure 43. *UCI EVSE Charger Locations (From Ref. [44])*

6.3 Simulation Scenarios

For the following simulations, the goal is to determine how smart charging will impact the electric load at the six different building locations. As seen in section 5.6 the poll rate can have a significant effect on the overall net load depending on what it is set to. However, two potential solutions for this issue are noted in section 5.7. For the following simulations two cases are considered: a base case where it is assumed that no poll rate is necessary and the vehicles follow the exact charge profile they are given, and a case where a poll rate of 10 minutes is used and the vehicles follow a charge profile with the poll rate taken into consideration. The case with the poll rate taken into consideration will be benchmarked against the base case to determine how the poll rate affects the overall net load.

6.4 Metrics: Cost to Charge and Electric Grid CO_2 Emissions

To determine the impact that smart charging has, two different metrics are examined: the cost to charge the vehicles and the electric grid CO_2 emissions that result from PEV charging.

6.4.1 Cost to Charge

The first metric analyzed is the cost to charge the vehicles. This metric reflects the costs that PEV owners will incur when they charge their vehicles and allows owners to see the difference in cost when a poll rate is taken into consideration versus when no poll rate is needed. The rate structures shown in section 6.2.1 and 6.2.2 are used to determine the charging costs.

6.4.2 Electric Grid CO_2 Emissions

The second metric analyzed is the electric grid CO_2 emissions. This metric is used to determine the emissions that come from the electric grid as a result of PEV charging. To determine the electric grid CO_2 emissions, an emissions factor (EF) based on California Independent System Operator (CAISO) data were created. To create an emissions factor, renewable production data for California were obtained from the CAISO Renewables Watch, which provides hourly power production data from the California grid for a specified day for specific resource types [49]. The resource types are separated into two categories, zero-carbon and carbon technologies. Zero-carbon technologies that are considered are solar, wind, and geothermal, while carbon-technologies that are considered are thermal and import resources. It is assumed that thermal resources emit carbon at a rate of 1232.35 pounds per MWh [50], and import resources emit carbon at a rate of 782.2 pounds per MWh [51]. Using these carbon-technology emissions factors, an hourly resolved emissions factor for the entire year was produced using the following calculation:

$$\frac{\left(Thermal\ [MWh] * Theraml\ EF\ \left[\frac{lb}{MWh}\right]\right) + \left(Import\ [MWh] * Import\ EF\ \left[\frac{lb}{MWh}\right]\right)}{(Renewables + Nuclear + Thermal + Imports + Hydro)[MWh]}$$

Using these calculations, the emissions factor produced had a maximum, minimum, and average rate of 821.67, 424.18, and 660.96 pounds per MWh, respectively. However, since the average emissions factor produced was higher than the 2014 Emissions and Generation Resource Integrated Dataset (eGRID) rate of 568.6 pounds per MWh for California, the estimated time resolved emissions factor was normalized to the eGRID value [52]. Figure 44a and Figure 44b shows a winter and summer example for typical CO_2 emissions factors where each tick mark represents midnight.

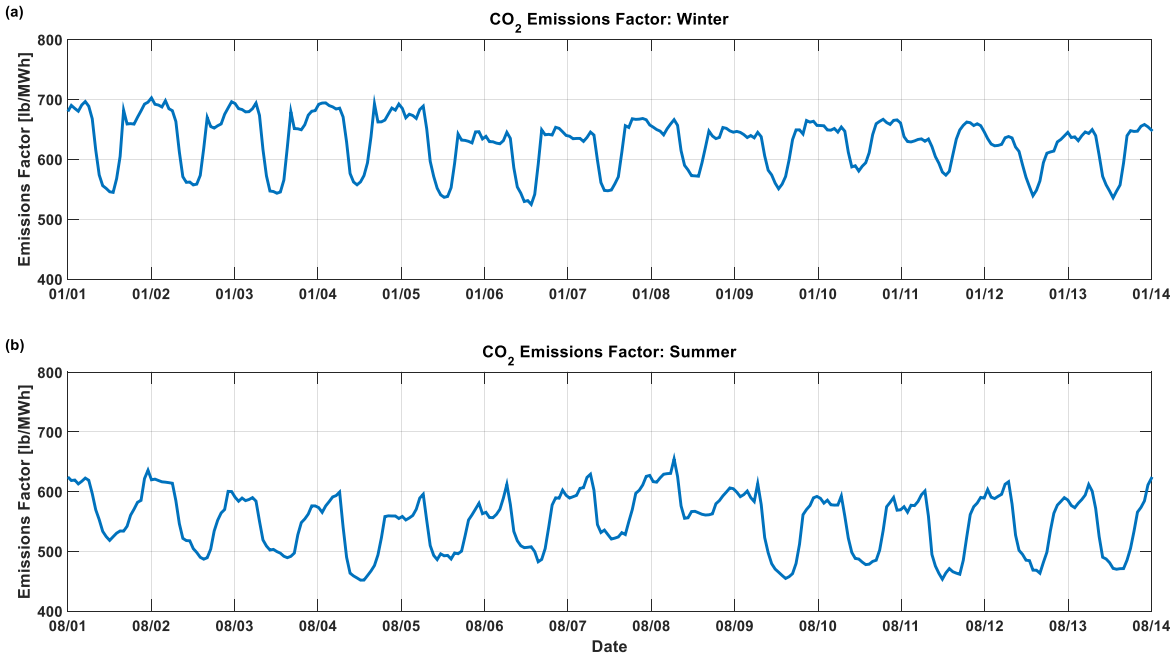

Figure 44. *Winter and Summer CO_2 Emissions Factor*

6.5 Simulation Results

Five sets of scenarios were simulated with increasing vehicle traffic, starting from 100 vehicles at each location up to 900 vehicles, increasing in increments of 200 vehicles. For the following simulations it is assumed that the number of chargers is proportional to the number of vehicles. The following simulations were simulated on August 9th. Figure 45 shows an example of

the cost load before and after PEV charging for three different cost loads for 500 vehicles. Figure 45a uses the building profile as the cost load, Figure 45b uses the SCE TOU rate structure as the cost load, and Figure 45c uses the future TOU rate structure as the cost load. This specific example uses APS for the building cost load. Figure 46 shows the same plots as Figure 45 but with a 10-minute poll rate. Figure 47 and Figure 48 shows the average electric grid CO_2 emissions and cost to charge per two days for all cost loads, respectively. In each figure, the legend represents which cost load was utilized. Table 9 and Table 10 shows the percent change between the scenarios with and without the poll rate for the averaged values presented in Figure 47 and Figure 48, respectively. Positive values indicate a percent increase and negative values indicate a decrease, respectively. Table 11 and Table 12 show the number of simulations performed and the average standard deviation (STD) for each simulated vehicle traffic level for the average electric grid CO_2 emissions and cost to charge for all cost loads, respectively. To view individual values for each cost load, refer to Table 25 through Table 52 in the appendix.

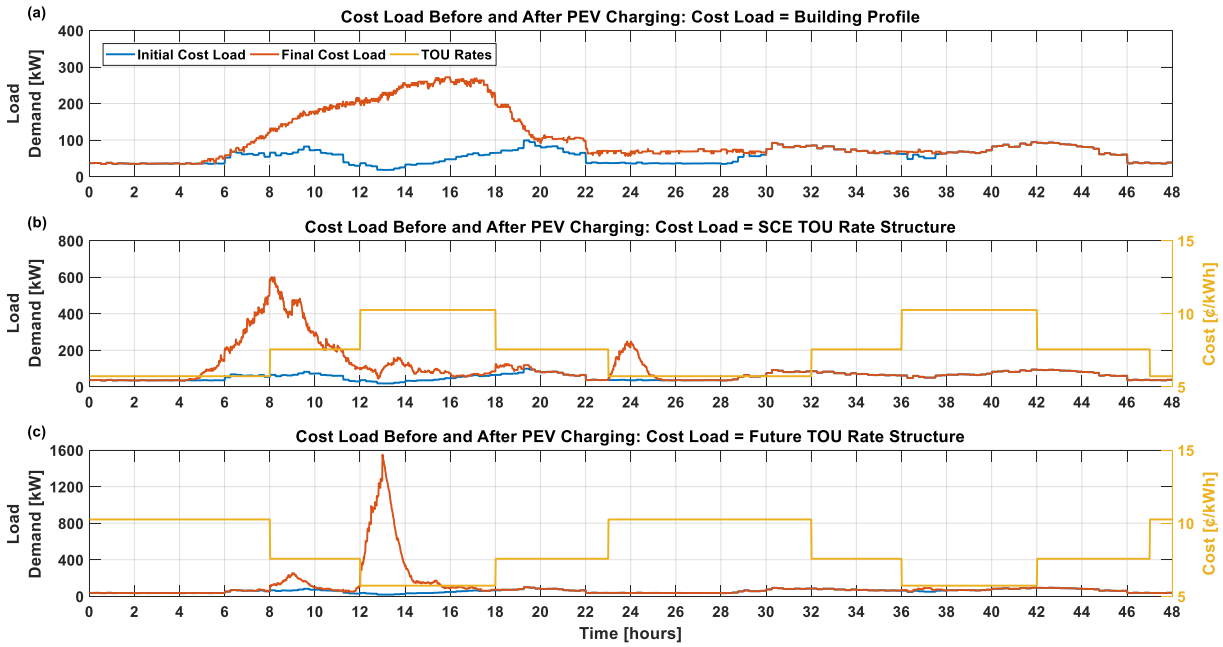

Figure 45. *Cost Load Before and After PEV Charging for APS*

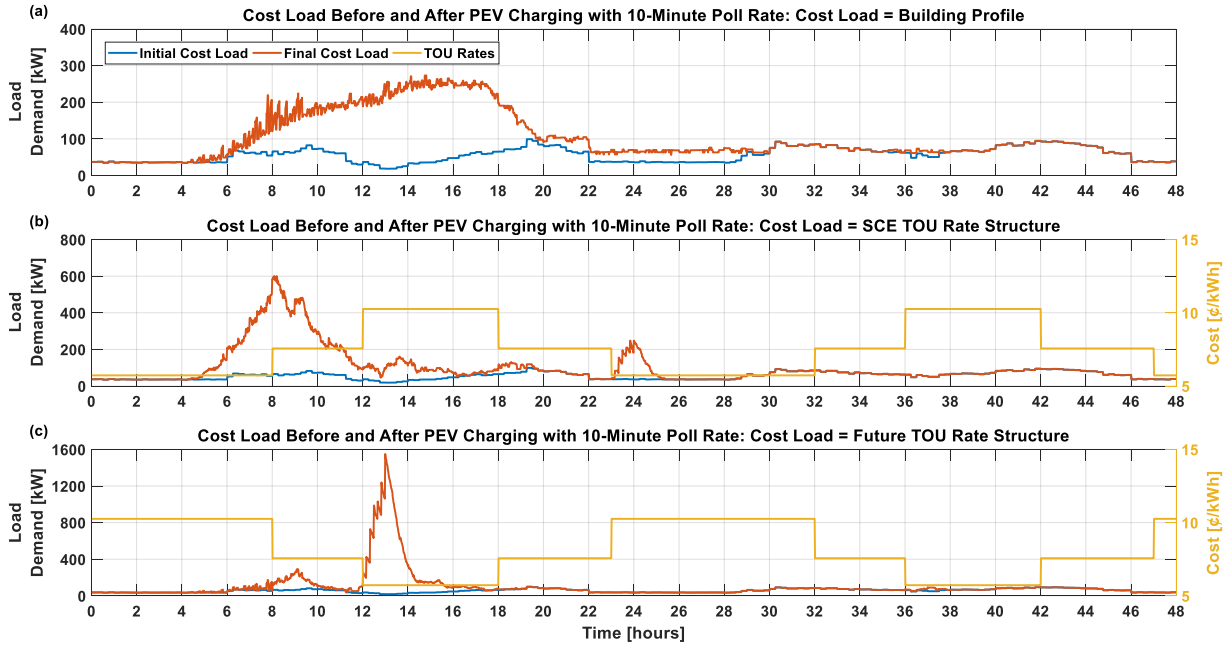

Figure 46. *Cost Load Before and After PEV Charging for APS: 10-Minute Poll Rate*

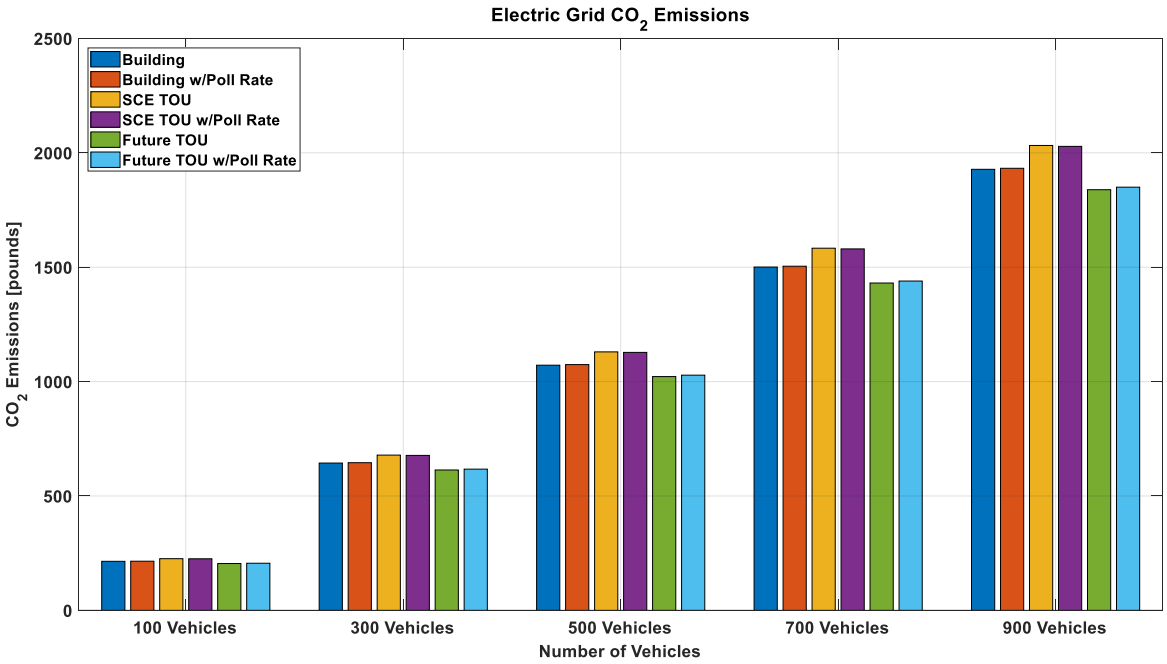

Figure 47. *Electric Grid CO_2 Emissions*

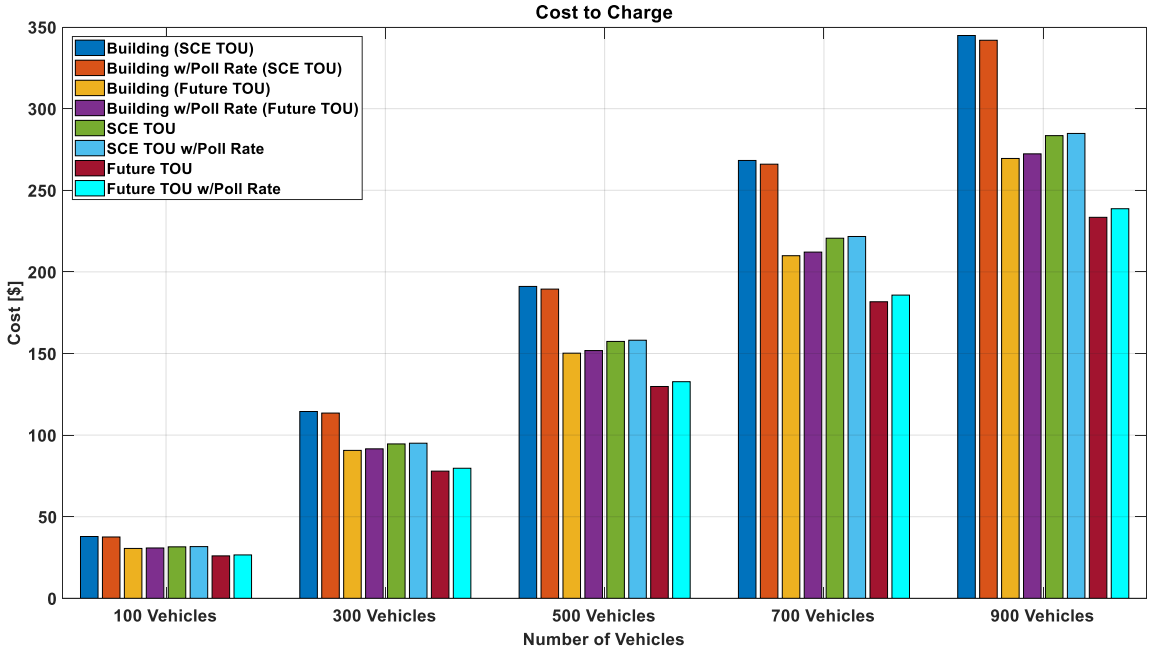

Figure 48. *Cost to Charge*

Table 9. *Electric Grid CO_2 Emissions Percent Change*

Electric Grid CO_2 Emissions Percent Change			
Vehicles	**Building**	**SCE TOU**	**Future TOU**
100	0.22	-0.19	0.60
300	0.24	-0.20	0.61
500	0.24	-0.20	0.61
700	0.24	-0.20	0.60
900	0.23	-0.20	0.60

Table 10. *Cost to Charge Percent Change*

Cost to Charge Percent Change				
Vehicles	**Building SCE TOU**	**Building Future TOU**	**SCE TOU**	**Future TOU**
100	-0.78	0.93	0.47	2.24
300	-0.84	1.04	0.47	2.26
500	-0.86	1.06	0.47	2.26
700	-0.85	1.06	0.48	2.25
900	-0.84	1.05	0.47	2.25

Table 11. *Electric Grid CO_2 Emissions Standard Deviation*

Electric Grid CO_2 Emissions Standard Deviation (%)							
Veh	**Sim**	**Bldg**	**Bldg w/PR**	**SCE**	**SCE w/PR**	**Future**	**Future w/PR**
100	500	6.33	6.31	6.33	6.34	6.25	6.22
300	500	3.66	3.65	3.69	3.70	3.60	3.59
500	300	2.75	2.74	2.76	2.76	2.71	2.70
700	150	2.37	2.37	2.33	2.33	2.40	2.39
900	100	2.13	2.12	2.15	2.15	2.09	2.08

Table 12. *Cost to Charge Standard Deviation*

Cost to Charge Standard Deviation (%)									
Veh	**Sim**	**Bldg SCE**	**Bldg SCE w/PR**	**Bldg Future**	**Bldg Future w/PR**	**SCE**	**SCE w/PR**	**Future**	**Future w/PR**
100	500	6.51	6.54	6.52	6.45	6.77	6.73	6.37	6.25
300	500	3.79	3.80	3.75	3.70	3.89	3.87	3.68	3.61
500	300	2.78	2.79	2.81	2.78	2.87	2.85	2.73	2.69
700	150	2.41	2.42	2.49	2.46	2.52	2.50	2.42	2.38
900	100	2.17	2.19	2.14	2.10	2.30	2.29	2.13	2.08

In Figure 45a, when using the SCE TOU rate structure as the cost load, the vehicles tend to charge in the morning. This is typically when vehicles plug in upon arrival, centering around 8:00 AM. In Figure 45b, when using the future TOU rate structure as the cost load, vehicles tend

to shift their charge schedules to the middle of the day around 12:00 PM – 3:00 PM. In Figure 45c, when using the building profile as the cost load, the charge schedules are distributed throughout the day in order to fill the valley and minimize the load. Depending on which cost load is utilized, the final cost loads are shaped in different ways, which affects the electric grid CO_2 emissions and cost to charge as seen in Figure 47 and Figure 48. When the building profile is used as the cost load, the CO_2 emissions that result are the second to highest, and the cost to charge is either the highest or third to highest, depending on which rate structure is used. When the SCE TOU rate structure is used as the cost load, the CO_2 emissions that result are the highest, and the cost to charge is the second to highest. When the future TOU rate structure is used as the cost load, both the CO_2 emissions and cost to charge are the lowest out of the three cost loads.

In Table 9, "building profile", "SCE TOU rate", and "future TOU rate" each refer to which cost load was used. In Table 10, "building SCE TOU" and "building future TOU" refer to the cost load when the building profile was used with the SCE TOU rate structure and future TOU rate structure, respectively. When the poll rate is taken into consideration, emissions increase slightly when the building profile and future TOU rate structure are used as the cost load since vehicles will charge briefly when the emissions factor is higher. If the SCE TOU rate structure is used to determine the cost to charge when the building profile is used as the cost load, the cost will decrease slightly since the cost is cheaper when the emissions factor is higher. When the future TOU rate structure is used to determine the cost to charge when the building profile is used as the cost load, the cost increases since with this rate structure the cost is more expensive when the emissions factor is higher. When the SCE TOU rate structure is used as the cost load, emissions slightly decrease since vehicles will charge slightly into the period when the emissions factor is

lower. The poll rate forces the vehicles to charge slightly into the more expensive rate period, which coincides with a lower emissions factor, leading to an increase in the cost to charge.

In Table 11 and Table 12, "veh" represents the number of vehicles simulated, "sim" represents the number of simulations performed at that vehicle traffic, "bldg" represents the building cost load, and "PR" represents poll rate. In Table 12, "bldg SCE" represents the building profile using the SCE TOU rate structure to determine the cost to charge and "bldg future" represents the building profile using the future TOU rate structure to determine the cost to charge. In both tables, as the number of vehicles increased, the number of simulations that needed to be performed decreased. Higher simulated vehicle traffic shows less variability between all simulations, indicated by the decreasing standard deviation. With the standard deviation ranging between 2% and 6%, most outliers that would have appeared in the simulations have been filtered out.

6.6 Objective 3 Summary

From the perspective of CO_2 emissions and cost, using the future TOU rate structure appears to be the ideal cost load to use to charge the vehicles. However, if this cost load is used, a large peak occurs in the middle of the day, more than twice as much as the peak that occurs when the SCE TOU rate structure is used as the cost load and more than five times as much as the peak that occurs when the building profile is used as the cost load. For the grid operator, this is difficult to manage, as power plants would have to ramp up quickly in order to meet the sudden demand. To benefit both the grid operator and vehicle owners, the building profiles should be used as the cost load but with a real time pricing structure implemented (i.e., the cost should be the lowest when the net load is the lowest and vice versa). For all cost loads, the poll rate does not have a significant effect on the resulting CO_2 emissions and cost to charge.

7. OBJECTIVE 4 RESULTS

Integrate smart charging algorithms into the Holistic Grid Resource Integration and Deployment (HiGRID) model to determine California electric grid emissions.

As seen in the literature presented in section 2.5, studies that used a centralized smart charging architecture have mainly focused on large-scale implementation and have been used to demonstrate the benefits of smart charging approaches when compared to non-smart charging approaches. However, as seen in the literature, many barriers associated with the centralized smart charging architecture prevent it from being implemented in real life systems. On the other hand, decentralized smart charging architectures have mainly been examined on small-scale residential systems, but are more feasible and likely to be implemented in real life systems since they do not face the same challenges that centralized smart charging architectures face.

In order to meet California's climate change goals, it will be necessary to be able to implement decentralized architectures on larger, state-wide scales. This leads to the question of whether or not decentralized smart charging approaches can achieve the same system-wide benefits of an ideal centralized smart charging approach. Chapter 7 explores the difference between a centralized and decentralized approach when implemented on a large-scale system. The electric grid greenhouse gas and criteria pollutant emissions associated with the decentralized smart charging algorithm are benchmarked against the centralized smart charging algorithm to determine whether or not decentralized smart charging approaches can achieve the same benefits as centralized smart charging approaches in the year 2030.

7.1 Model Implementation

As stated earlier, this chapter focuses on the two different charging algorithms developed by Li et al: the centralized and decentralized smart charging algorithm [7], [32]. Both algorithms

are integrated into the HiGRID model developed by Eichman et al. and Shaffer et al. to determine the electric grid CO_2 and NO_x emissions [35], [53], [54]. Figure 49 shows a model flow chart of the overall approach. Rectangles represent built models, ovals represent outputs, and rounded rectangle shapes represent input parameters.

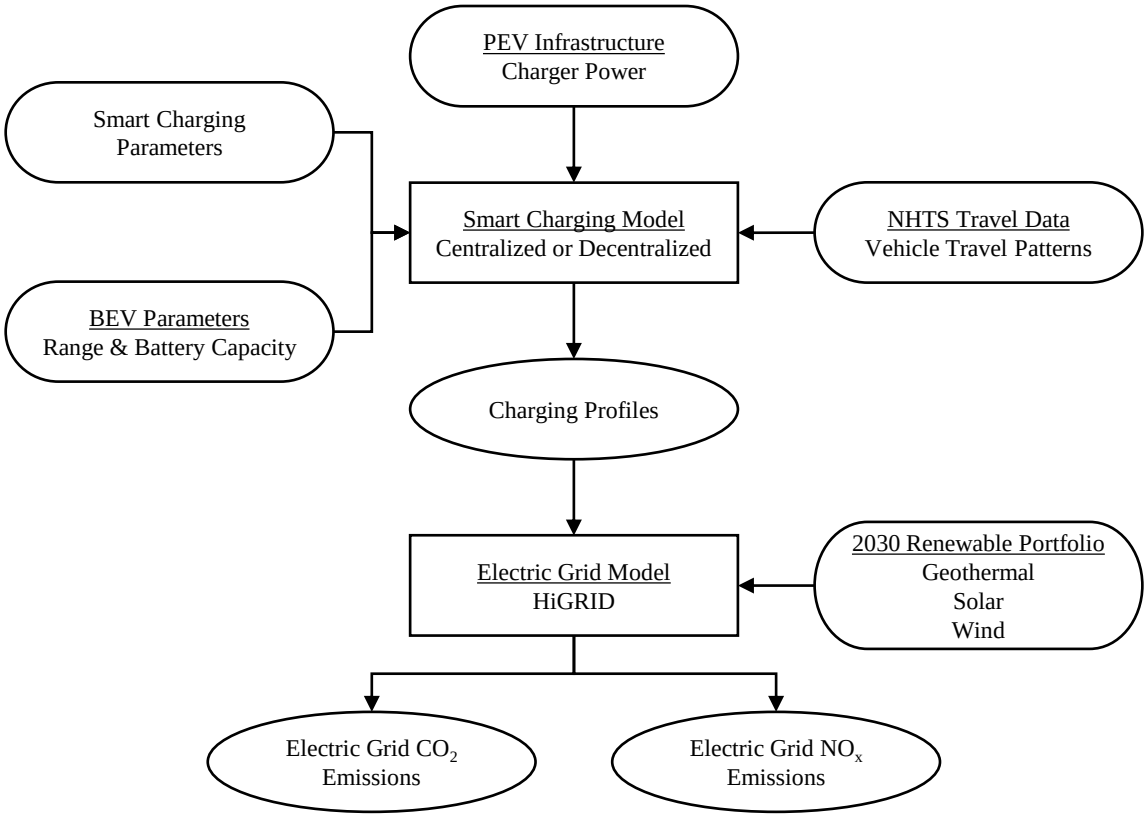

Figure 49. *Model Flowchart*

First, the necessary parameters for the smart charging algorithms are identified. For this study, it is assumed that all of the PEVs are BEVs. The main parameters related to the BEVs are their range and battery capacity, which for this study use fleet averaged values presented in sections 7.2.2 and 7.2.3. Each BEV follows a travel pattern based off of the 2009 NHTS data [16]. The smart charging parameters that are altered are explained in sections 7.2.2 and 7.2.3. Note that the BEV parameters and PEV infrastructure parameters are common between both algorithms. Once the charging parameters have been decided they are then sent to the charging algorithm where the

aggregated charging profile is calculated. The aggregated charging profile is then sent to HiGRID, where the electric grid CO_2 and NO_x emissions from the electric grid are calculated.

7.1.1 Holistic Grid Resource Integration and Deployment (HiGRID) Model

The HiGRID model serves as the main tool for the analyses in this chapter. HiGRID is a model developed at UCI as part of a California Energy Commission (CEC) sponsored project to determine any barriers that arise when integrating increasing renewable resources into the electric grid. It is an hourly resolved model that simulates the electric grid in response to different renewable portfolios. Analyses can be carried out on small-scale systems such as college campuses, all the way to the entire California electric grid, depending on the input parameters. HiGRID produces hourly resolved outputs such as electric power generation, fuel consumption, and part-load condition for grid resources over the course of a year. From these outputs, electric grid CO_2 and NO_x emissions can be calculated. Figure 50 shows an example of a time series output from HiGRID. Two different classes of power plants are peakers, which are fast responding, simple cycle power plants and load followers, which are moderate responding combined cycle power plants [35].

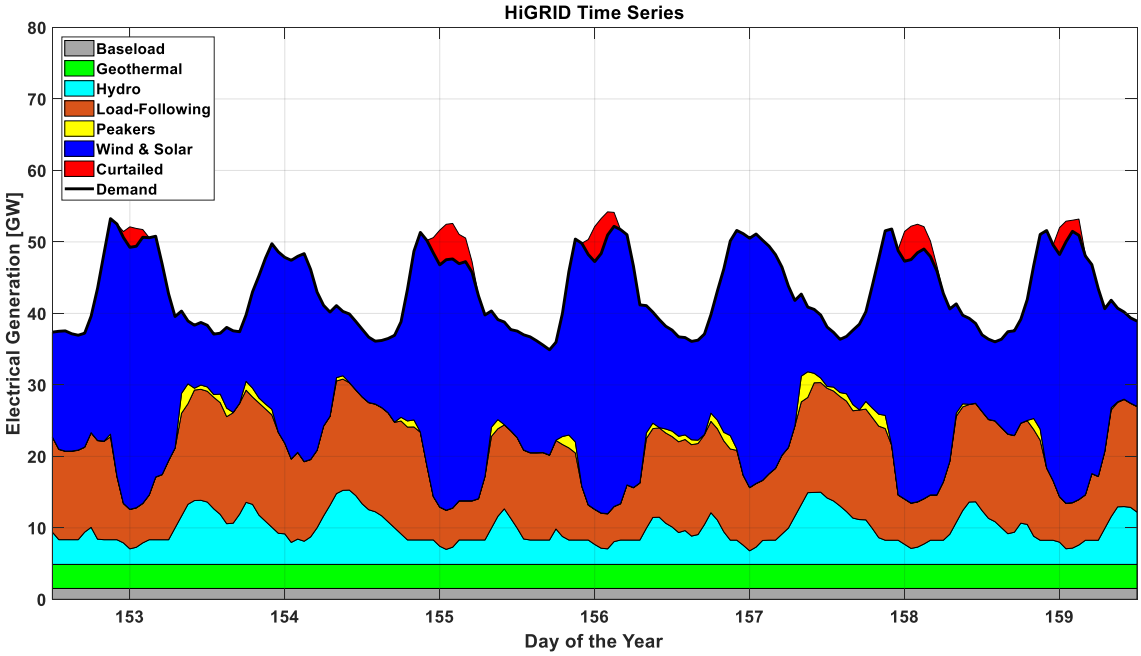

Figure 50. *HiGRID Time Series Output*

7.2 Simulation Scenario Parameters

Section 7.2 covers the different parameters that were used in the HiGRID model, as well as both the centralized and decentralized smart charging algorithms.

7.2.1 HiGRID Scenario Parameters

The main parameter that affects the net load are the capacities of renewable generation technologies installed on the electric grid. To determine the potential renewable generation capacity in 2030, data from the Energy + Environmental Economics (E3) California PATHWAYS Model were used. The E3 pathways model is a tool to determine different pathways to reach an 80% reduction in GHG emissions by the year 2050. The “Straight Line” scenario from the Pathways study, which is a trajectory that achieves a linear progression towards an 80% GHG reduction in California by 2050, was used for this study [55]. Table 13 lists the predicted renewable generation capacities for 2030 from this scenario.

Table 13. *E3 2030 Renewable Generation Capacity*

E3 2030 Renewable Generation Capacity (MW)			
Geothermal	**Solar**	**Wind**	**Rooftop PV**
3105	20850	20790	11800

The second parameter that affects the overall load is the projected PEV load in 2030, which is also taken from the E3 Pathways study. For the year 2030, the projected annual PEV load is 3.96×10^4 GWh [55], which corresponds to 7.7 million PEVs deployed in the California light-duty transportation sector.

7.2.2 Smart Charging Scenario Parameters: Common

The behavior of the centralized and decentralized smart charging algorithms in terms of their ability to shape the electric vehicle charging load profile is commonly affected by various parameters, listed in Table 14.

Table 14. *Smart Charging Parameters*

Smart Charging Parameters	
Parameter	**Value**
Charging Infrastructure Location Availability	Home & Workplace
Charger Power (kW)	10
Vehicle Range (miles)	200
Vehicle Efficiency (kWh/mile)	0.34

For this study the following assumptions are used for both charging algorithms:

- All vehicles commute to their workplace and are able to charge at both home and work locations. At both locations, a 10-kW charger is used to recharge the vehicles.
- All vehicles have a range of 200 miles with an energy consumption per mile of 0.34, resulting in a 68-kWh battery for each vehicle.

7.2.3 Smart Charging Scenario Parameters: Decentralized

The decentralized smart charging algorithm has additional parameters that are not included in the centralized charging algorithm. Table 15 lists the parameters specifically designed for the decentralized smart charging algorithm.

Table 15. *Decentralized Smart Charging Parameters*

Decentralized Smart Charging Parameters	
Parameter	**Value**
Continuous Charging	On/Off
Error Prediction	On/Off
Final Error Type	Variable: 1 through 4
Maximum Error (MW)	Variable: 184 up to 9195
Cost Function Update Time (min)	Variable: 30 up to 1440
Forecast Length (hours)	Variable: 6, 8, 10, 12
Forecast Type	Variable: 1 through 3

The continuous charging parameter dictates whether or not the vehicle will have multiple charging periods. Turning this parameter on means that the vehicle will continuously charge even if a peak occurs during the charging period. The error prediction parameter allows the algorithm to account for errors that occur while predicting the load since it is not possible to predict the load 100% perfectly. This parameter is not present in the centralized algorithm since a perfect forecast is assumed. The final error type parameter is used to determine how the error is calculated. Final error type 1 through 3 utilize a random number generator, while final error type 4 is dependent on the maximum error. The maximum error parameter is the maximum allowable error in MW. The cost function update time interval parameter is the frequency at which the cost function provided by the electric grid to the individual vehicle is recalculated and transmitted. This parameter value is influenced by two limitations: the accuracy of the cost function and the data/information volume transfer limit. The forecast length parameter is how far the error is forecasted in determining the cost function from the time when a PEV is plugged in to the electric grid. The forecast type

parameter is the type of forecast the forecast length parameter is. Forecast type 1 is a random forecast error, forecast type 2 is a linear reducing forecast error, and forecast type 3 is an exponentially reducing forecast error.

7.3 Sensitivity Analysis

To determine the effect of each parameter in decentralized smart charging algorithm, a sensitivity analysis had to be done. To perform the sensitivity analysis, an initial decentralized case is chosen, and each parameter from the initial case is varied and the CO_2 and NO_x emissions are compared to the centralized case. The values for the initial decentralized case are listed in Table 16. Table 17 through Table 23 shows the absolute percent difference in CO_2 and NO_x emissions compared to the centralized case.

Table 16. *Decentralized Smart Charging Parameters: Initial Case*

Decentralized Smart Charging Parameters: Initial Case	
Parameter	**Value**
Continuous Charging	Off
Error Prediction	On
Final Error Type	4
Maximum Error (MW)	3000
Cost Function Update Time (min)	30
Forecast Length (hours)	12
Forecast Type	3

Table 17. *Continuous Charging: CO_2 and NO_x Percent Difference*

Continuous Charging: CO_2 and NO_x Percent Difference		
Value	**CO_2**	**NO_x**
On	3.06%	4.33%

For the continuous charging parameter, the parameter was turned on. As shown in Table 17, turning the continuous charging parameter on affects the emissions. CO_2 emissions experienced around a 3% change and NO_x emissions experienced around a 4% change.

Table 18. *Error Prediction: CO_2 and NO_x Percent Difference*

Error Prediction: CO_2 and NO_x Percent Difference

Value	CO_2	NO_x
On	0.29%	1.07%

For the error prediction parameter, the parameter was turned off. As shown in Table 18, turning the error prediction parameter off did not have a significant impact on emissions. CO_2 emissions experienced around a 0.3% change and NO_x emissions experienced around a 1% change.

Table 19. *Final Error Type: CO_2 and NO_x Percent Difference*

Final Error Type: CO_2 and NO_x Percent Difference		
Value	**CO_2**	**NO_x**
1	0.08%	1.84%
2	0.28%	1.11%
3	0.28%	1.12%

For the final error type parameter, the values were set to 1, 2, and 3. As shown in Table 19, changing the final error type parameter did not have a significant impact on emissions. For all values, CO_2 emissions experienced around a 0.3% change and NO_x emissions experienced around a 1% to 2% change.

Table 20. *Maximum Error: CO_2 and NO_x Percent Difference*

Maximum Error: CO_2 and NO_x Percent Difference		
Value	**CO_2**	**NO_x**
184	0.27%	1.09%
552	0.28%	1.07%
920	0.27%	1.09%
1839	0.29%	1.05%
2759	0.28%	1.08%
3678	0.30%	1.08%
4598	0.29%	1.09%
5517	0.30%	1.07%
6436	0.29%	1.09%
7356	0.28%	1.08%
8275	0.29%	1.08%
9195	0.30%	1.08%

For the maximum error parameter, the values were set to a certain percentage of the maximum aggregated value of the PEV load. The following values show 1%, 3%, 5%, 10%, 15%,

20%, 25%, 30%, 35%, 40%, 45%, and 50%. As shown in Table 20, changing the maximum error parameter did not have a significant impact on emissions. CO_2 emissions experienced around a 0.3% change, and NO_x emissions experienced around a 1% change.

Table 21. *Cost Function Update Time: CO_2 and NO_x Percent Difference*

Cost Function Update Time: CO_2 and NO_x Percent Difference		
Value	**CO_2**	**NO_x**
45	0.28%	1.09%
60	0.28%	1.14%
90	0.23%	1.38%
120	0.16%	1.95%
180	0.56%	3.70%
240	1.41%	6.98%
300	1.35%	6.13%
360	2.99%	11.18%
540	3.80%	12.75%
720	3.60%	12.58%
1080	6.18%	19.95%
1440	7.49%	23.67%

For the cost function update time parameter, the values were set to 45, 60, 90, 120, 180, 240, 300, 360, 540, 720, 1080, and 1440 minutes. As shown in Table 21, varying the cost function update time has a significant impact on emissions. As the values increased, both CO_2 and NO_x percent difference increased.

Table 22. *Forecast Length: CO_2 and NO_x Percent Difference*

Forecast Length: CO_2 and NO_x Percent Difference		
Value	**CO_2**	**NO_x**
6	0.28%	1.09%
8	0.28%	1.09%
10	0.28%	1.09%

For the forecast length parameter, the values were set to 6, 8, 10, and 12 hours. As shown in Table 22, changing the forecast length parameter did not have a significant impact on emissions. For all values, CO_2 emissions experienced around a 0.3% change and NO_x emissions experienced around a 1% change.

Table 23. *Forecast Type: CO_2 and NO_x Percent Difference*

Forecast Type: CO_2 and NO_x Percent Difference		
Value	**CO_2**	**NO_x**
1	0.30%	1.07%
2	0.28%	1.09%

For the forecast type parameter, the values were set to 1 and 2. As shown in Table 23, changing the forecast type parameter did not have a significant impact on emissions. For all values, CO_2 emissions experienced around a 0.3% change and NO_x emissions experienced around a 1% change.

7.4 Results: CO_2 and NO_x Emissions

From the sensitivity analysis, it is clear that emissions were not sensitive to most of the parameters. Most parameters only experienced a 0.3% change in CO_2 emissions and 1% change in NO_x emissions. However, when compared to the other parameters the continuous charging parameter and cost function update parameter were more sensitive.

7.4.1 CO_2 Emissions

Figure 51 and Figure 52 shows the year 2030 electric grid CO_2 emissions for the scenario where the continuous charging parameter and cost function update time are varied, respectively. The blue and red bars represent CO_2 emissions resulting from load following (LF) power plant generation and startups respectively, while the yellow and green bars represent CO_2 emissions caused by peaker (PK) power plant generation and startups respectively. Load following power plants are slower responding power plants while peaker power plants are faster responding power plants. In both figures, base refers to the centralized case that the decentralized case is being compared against.

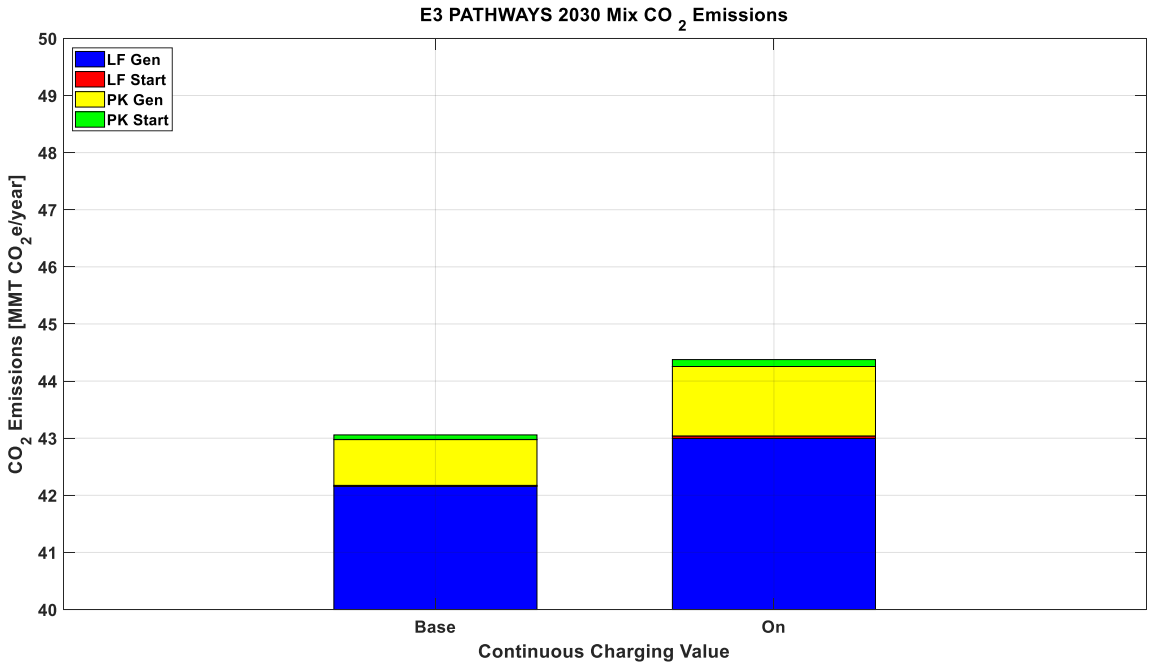

Figure 51. *CO_2 Emissions Breakdown: Continuous Charging*

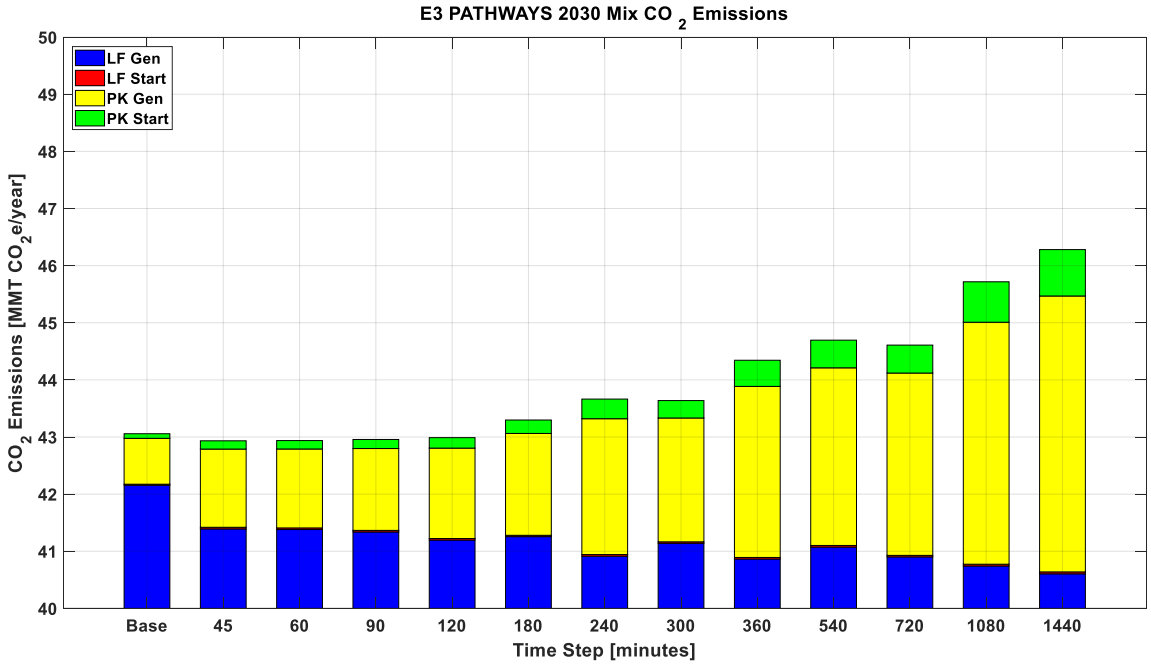

Figure 52. *CO_2 Emissions Breakdown: Cost Function Update Time*

In Figure 51, it is clear that when the continuous charging parameter is turned on, the CO_2 emissions increase. This is expected since when this parameter is turned on, the vehicles will attempt to charge, even if a peak occurs in the net load. When this occurs, the use of peaker plants increase, which is indicated by the increasing yellow and green segments. In the base case, about 2% of total CO_2 emissions are caused by peaker plants and when the continuous charging parameter is turned on, about 3% of total CO_2 emissions are caused by peaker plants.

In Figure 52, the general trend is that CO_2 emissions increase as the cost function update time increases. While a few cases exist where the CO_2 emissions decrease as the cost function update time increase, such as when the time step increases from 240 minutes to 300 minutes, this is primarily due to HiGRID being able to optimize the dispatch solution to increase the use of load following plants vs peaker plants. However, this does not occur often, and the main trend indicates that CO_2 emissions increase as the update time step increases. The main source of the increase in CO_2 emissions is caused by the use of peaker plants. This is indicated by the increasing yellow and green segments, while the blue segments stay relatively constant. This is expected since as the time step increases, there can be significant changes in the electric load between the first and second update interval. This can significantly alter how the vehicles decide on their charging schedules. For example, if the update interval is long and many vehicles plug in during that update interval, the vehicles during the current update interval will not be able to take into account the impacts when determining their charging schedules; only the vehicles that plug in during the second update interval will. As sudden changes in the electric load occur, it becomes more difficult to smoothen the load due to the peaks caused by the aggregated charging profiles, resulting in the increased use of peaker plants. The impact of CO_2 emissions caused by peaker plants becomes more evident the longer the time step is, such as when comparing the base case to the case with

the longest time step (1440-minute time step). In the base case, about 2% of total CO_2 emissions are caused by peaker plants while in the case where the time step is set to 1440 minutes, about 12% of total CO_2 emissions are caused by peaker plants. For all cases, the majority of peaker plant emissions are from electricity generation. Note that for both the centralized and decentralized charging algorithms when the continuous charging parameter and cost function update parameter are varied, the emissions caused by load following plant startups is negligible when compared to the overall emissions, since load following plants do not need to restart very often.

Figure 53 and Figure 54 show examples of the net load and total load (net load + PEV load) profiles for the scenario where the continuous charging parameter and cost function update time are varied, respectively. Figure 53a and Figure 54a shows the profiles when the centralized algorithm is used. Figure 53b shows the profiles when the decentralized charging algorithm is used when the continuous charging parameter is turned on. Figure 54b and Figure 54c shows the profiles when the decentralized charging algorithm is used with a 45-minute and 300-minute time step, respectively.

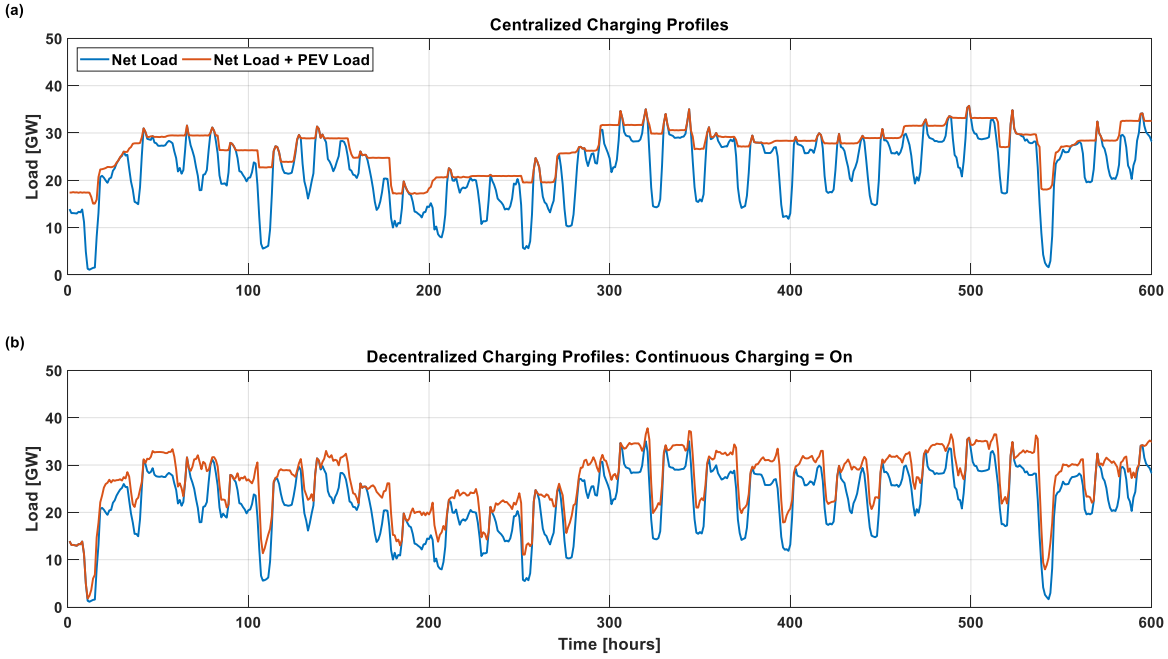

Figure 53. *Centralized and Decentralized Charging Profiles: Continuous Charging*

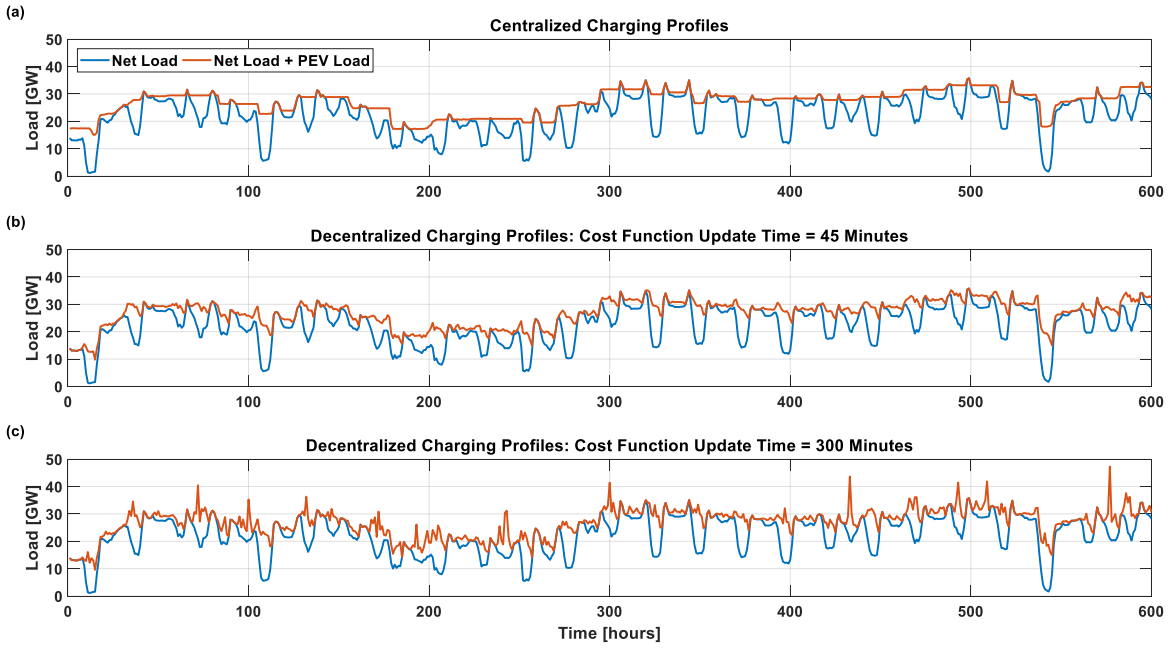

Figure 54. *Centralized and Decentralized Charging Profiles: Cost Function Update Time*

In Figure 53a and Figure 54a, using the centralized charging algorithm to charge the vehicles produces a relatively smooth profile with minimal peaks. This reduces the need for startups from the load following or peaker plants, as seen in the base case in Figure 51 and Figure 52. In Figure 53b, when the continuous charging parameter is turned on, the vehicles will charge even when a peak occurs in the net load. This does not occur when the centralized charging algorithm is used. Creating new peaks leads to the increased use of peaker plants, indicated by the increase in peaker plant generation and start up CO_2 emissions. In Figure 54b, using the decentralized charging algorithm to charge the vehicles when a 45-minute time step is used produces a profile that follows a trend similar to the profile produced from the centralized charging algorithm. The peaks are relatively small but the overall profile is more variable, which leads to an increase in the use of peaker plants. This is indicated by the increase in peaker plant generation and start up CO_2 emissions when a 45-minute time step is used when compared to the base case. In the bottom plot in Figure 54c, using the decentralized charging algorithm to charge vehicles when a 300-minute time step is used produces a profile that has many peaks and is generally more variable than the cases represented in Figure 54a and Figure 54b. It is clear that the major peaks tend to happen when valleys in the net load occur since all of the vehicles charge at that time.

The variability seen in Figure 53 and Figure 54 directly affect how power plants on the electric grid are dispatched. Figure 55 and Figure 56 presents a 12-day time series of how the electric grid resources are dispatched. Figure 55a and Figure 56a shows the electric grid resource dispatch for the centralized case. Figure 55b shows the electric grid resource dispatch for the decentralized case when the continuous charging parameter is turned on, and Figure 56b and Figure 56c shows the electric grid resource dispatch for the decentralized case when the cost function update time is set to 45 minutes and 300 minutes, respectively.

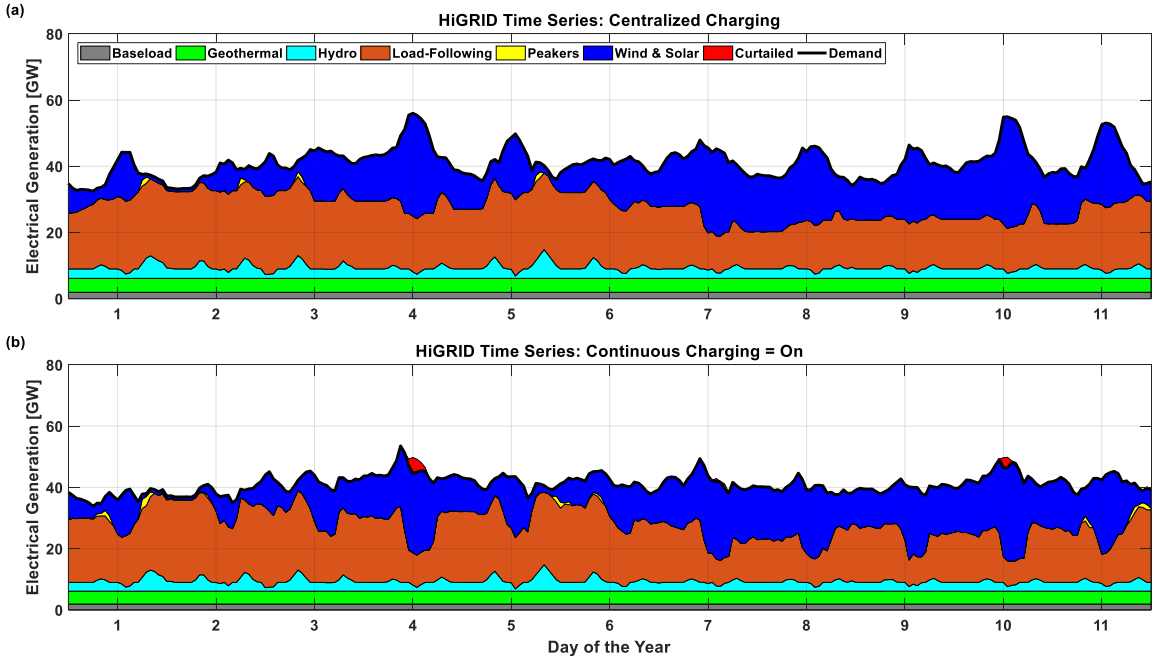

Figure 55. *HiGRID Time Series Output: Continuous Charging*

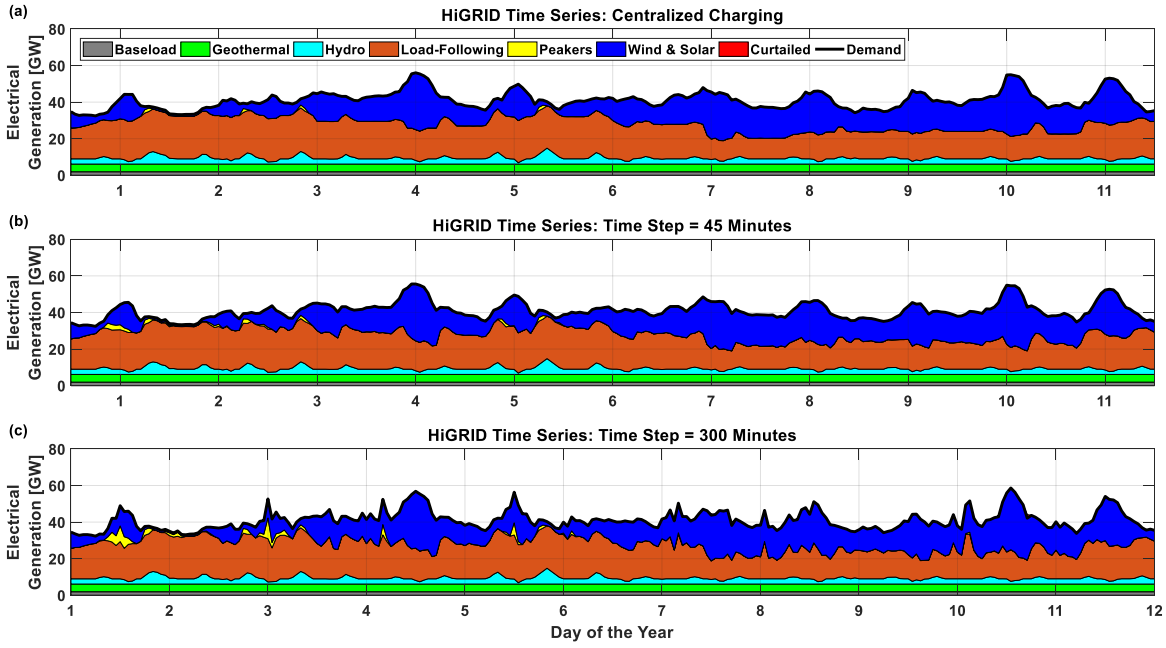

Figure 56. *HiGRID Time Series Output: Cost Function Update Time*

As seen in Figure 55a and Figure 56a, using the centralized algorithm allows for steady state operation of load following power plants with minimal variability. In Figure 55b, using the decentralized algorithm with the continuous charging parameter turned on causes an increase in the variability of load following power plants as well as an increase in the use of peaker plants. A portion of the electrical generation is curtailed as well, as seen in days 4 and 10. In Figure 56b, using the decentralized algorithm with a cost function update time of 45 minutes still allows for smooth operation of load following and peaker plants. However, in Figure 56c when the cost function update time is increased to 300 minutes, load following plants do not operate as smoothly and experience increased variability, and the use of peaker plants increase as well in order to meet the electric load demand.

Table 24 lists the number of power plant start up events for both load following and peaker plants over the course of a year. As the time step increases the profiles have more peaks, which leads to an increase in the number of peaker start up events. Load following plant start up events remain fairly consistent, averaging about 2700 starts per year, with the exception of the base case.

Table 24. *Power Plant Start Up Events: Cost Function Update Time*

Power Plant Start Up Events: Cost Function Update Time		
Update Time Step	**Peaker Start Ups (#)**	**Load Following Start Ups (#)**
Base (Centralized)	11047	1581
45	19605	2735
60	19989	2731
90	21549	2650
120	24848	2591
180	31920	2251
240	46681	2747
300	41412	2450
360	62143	2633
540	65770	2702
720	66409	2580
1080	96129	3017
1440	110236	3273

These results show that when using the decentralized smart charging algorithm on a large fleet of PEVs on California's electric grid, if the continuous charging parameter is turned on, a slight increase in CO_2 emissions occurs due to the increased use of peaker plants when vehicles charge during the peaks in the net load. If the cost function update time parameter is varied, it can only provide the same emissions benefits as the centralized smart charging algorithm when the cost function is updated at frequent intervals. From a practical standpoint, this means that the communications infrastructure must be able transfer large amounts of data frequently and reliably.

7.4.2 NO_x Emissions

Figure 57 and Figure 58 shows the year 2030 electric grid NO_x emissions for the scenario where the continuous charging parameter and cost function update time are varied, respectively. The blue and red bars represent NO_x emissions resulting from load following (LF) power plant generation and startups respectively, while the yellow and green bars represent NO_x emissions caused by peaker (PK) power plant generation and startups respectively. In both figures, base refers to the centralized case that the decentralized case is being compared against.

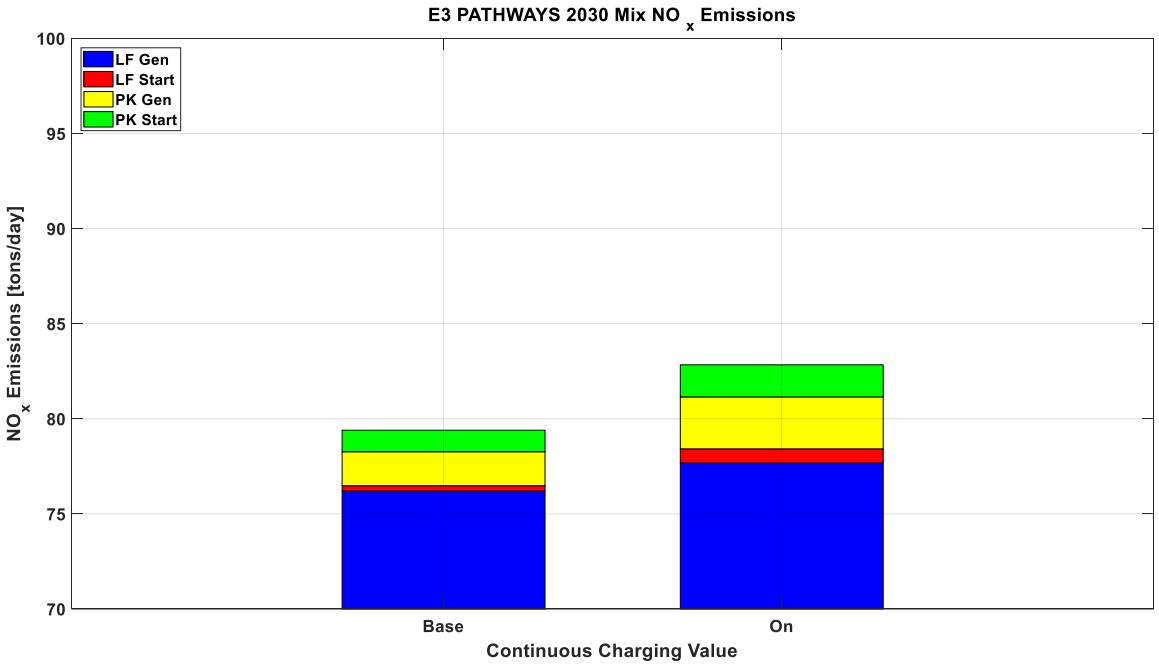

Figure 57. *NO_x Emissions Breakdown: Continuous Charging Value*

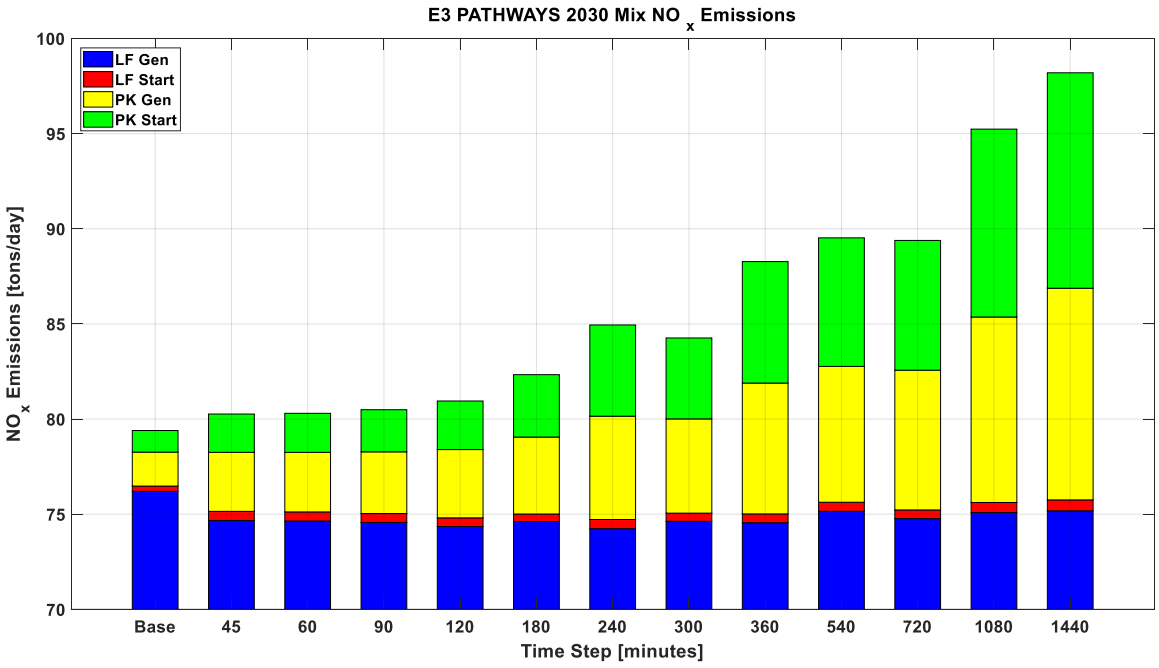

Figure 58. *NO_x Emissions Breakdown: Cost Function Update Time*

Similar to Figure 51 and Figure 52, it is clear that when the continuous charging parameter is turned on and the time step increases, the NO_x emissions increase as well. While a few cases exist where the NO_x emissions decrease as the cost function update time increase, such as when the time step increases from 240 minutes to 300 minutes, this is primarily due to HiGRID being able to optimize the dispatch solution to increase the use of load following plants vs peaker plants. However, this does not occur often, and the main trend indicates that NO_x emissions increase as the update time step increases. The main source of the increase in NO_x emissions is caused by the increase in use of peaker plants in both Figure 57 and Figure 58. For the base case, about 4% of total NO_x emissions are caused by peaker plants. When the continuous charging parameter is turned on, about 5% of NO_x emissions are caused by peaker plants. In the case where the cost function update time is set to 1440 minutes in Figure 58, about 23% of total NO_x emissions are caused by peaker plants. One key difference between the CO_2 emissions and NO_x emissions is the percentage of emissions caused by peaker plant startups when compared to the total emissions caused by peaker plants. About 9% to 15% of peaker plant CO_2 emissions are caused by startups, while about 40% to 50% of peaker plant NO_x emissions are caused by startups for both scenarios. In California, thermal combustion based power plants are used on the electric grid and each time they start up, NO_x emissions are produced. When the net load demand drops, these power plants go offline and when they need to go online again, clean-up equipment such as selective catalytic reduction restart and need to reach certain operating temperatures in order to be effective for post-combustion NO_x cleanup. During this time, significant NO_x emissions can occur since natural gas is being burned as the clean-up equipment is to returning to its optimal operating temperature.

These results show that when using the decentralized smart charging algorithm on a large fleet of PEVs on California's electric grid, a slight increase in NO_x emissions occurs due to the

increased use of peaker plants when the continuous charging parameter is turned on. When the cost function update time is varied, it can provide similar emissions benefits as the centralized smart charging algorithm only when the cost function update time is varied at frequent intervals. Since power plant startups affect NO_x emissions more than CO_2 emissions, the decentralized algorithm was not able to match the exact performance of the centralized algorithm when varying the cost function update time.

7.5 Real World Implications

When trying to deploy smart charging algorithms in real world systems, a major component that must be considered is the willingness of PEV owners to participate. Implementing a decentralized architecture addresses the privacy concerns of letting a central aggregator know individual travel plans, but this method requires frequent communication with the electric grid in order to achieve the same results. To ensure that the potential benefits of smart PEV charging are realized on a system wide basis, it is important to have adequate communication infrastructure as well as the support of information updating. Many components must be taken into consideration when implementing different types of communication infrastructure, such as the type of technology (wired vs. wireless), the range of the technology, the security and reliability of the technology, and the cost and transfer rate of the data. Different types of communication technologies that have been explored and can be considered for smart charging applications are ZigBee, Power Line Communication (PLC), Digital Subscriber Line (DSL), Wi-Fi, and cellular communication technologies such as 3G and LTE [26], [56]–[58]. To see the advantages and disadvantages of some of the technologies listed, refer to Güngör et al [56].

Frequent communication with the electric grid means that the PEV profiles must be transferred to the grid operator frequently. In order for a decentralized charging architecture to be

feasible, the communication infrastructure would need to consist of low data costs and fast transfer rates. If the data costs are incurred on the PEV owners and if the costs are high, this may deter PEV owners from participating. As the number of PEVs in the system increase, if the aggregated PEV profiles cannot be transferred fast enough, the grid operators will not be able to update the cost load frequently enough.

7.6 Objective 4 Summary

Two smart charging architectures were deployed to see how they impact electric grid GHG and criteria pollutant emissions that result from PEV charging. A centralized algorithm that is assumed to have a perfect forecast of the electric net load is used as a benchmark for a decentralized algorithm to be compared against. The decentralized algorithm does not have a perfect forecast of the electric net load and does not have the advantage of central optimization but is more feasibly deployable in real world systems. The decentralized algorithm is compared against the centralized algorithm to determine whether or not decentralized architectures can provide the same emissions benefits as a centralized architecture on the California electric grid in the year 2030.

It was found that only the continuous charging parameter and cost function update time parameter had an effect on overall emissions. When the continuous charging parameter was turned on, emissions increased since vehicles would charge even when a peak load in the electric net load occurred. When the cost function update time was varied, emissions would generally increase as the cost function update time increased since the net load would experience more instabilities. If the cost function update time is updated frequently enough, then the decentralized algorithm can achieve the same emissions benefits as the centralized architecture. For both parameters, the main cause of emissions increase is due to the increased use of peaker plants, since these fast responding plants are used to meet sudden changes that occur in the net load.

8. SUMMARY AND CONCLUSIONS

8.1 Summary

In California, the largest economic sector contributing to the increase in anthropogenic GHG emissions is the transportation sector. Major reforms must be made in the transportation sector in order to reduce GHG emissions. Electric vehicles, a subset of which are PEVs, have been identified as one of the forefront solutions in reducing GHG emissions since they have several advantages compared to their ICE counterparts, such as reduced usage in petroleum and reduced tailpipe emissions. However, while PEVs offset tailpipe emissions, their batteries must be recharged, which leads to an increase in the electric demand. If all of the PEVs recharge at the same time, this will lead to sudden peaks in the electric net load. Grid operators would need to ramp up power plants quickly in order to meet the sudden demand in electricity, subsequently leading to an increase in electric grid CO_2 emissions. To ensure that PEVs will not have a significant impact on the electric load, "smart" charging protocols are necessary to manage PEV charging schedules.

Two different smart charging algorithms were explored in this study: decentralized and centralized. For the decentralized smart charging algorithm, PEV charging profiles are optimized based on a cost function derived from a local load. This minimizes costs on the local load but may not minimize costs on the global load. For the second algorithm, the centralized smart charging algorithm, PEV charging profiles are optimized based on a cost function derived from a global load. This minimizes costs on the global load but may not minimize costs on the local load.

The decentralized smart charging algorithm was modified so that it could be deployed on a fleet of Kia Soul PEVs on the UCI microgrid. To create charging schedules for each vehicle, the vehicles' status was obtained by using the on-board telematics system to send the vehicles' SOC

and arrival time to the algorithm. However, the vehicles' status could only be obtained every *x* minutes, which is referred to as the poll rate. To obtain the most accurate results, the poll rate was initially set to 5 minutes. Upon initial testing however, it was discovered that a 5-minute poll rate would deplete the vehicles' auxiliary battery in 2 to 3 days.

Since it was discovered that the poll rate can alter how PEV charging schedules are determined, simulations were performed with a 10-minute poll rate since a 10-minute poll rate would not deplete the battery quickly. To determine whether or not the poll rate has a significant impact on the electric load, simulations were performed on different cost loads on the UCI campus with varying PEV traffic loads. Six different buildings were chosen to serve as the location for PEVs to charge: APS, ECPS, MPS, MSTB, SCPS, and SSPS. At each building, three different cost loads were tested: the SCE TOU rate, a proposed future TOU rate, and the building profiles. Two different metrics were used to determine the impact that the poll rate has: electric grid CO_2 emissions and the cost to charge PEVs. The results showed that the poll rate did not have a significant effect on either metric. Electric grid CO_2 emissions experienced a 0.2% to 0.6% percent change, while the cost to charge the vehicles experienced 0.5% to 2.2% change when the poll rate was considered.

In order to reduce GHG emissions on a state-wide scale, these smart charging algorithms will need to be deployed on larger fleets of vehicles. As addressed earlier, the decentralized charging algorithm is considered a "field-deployable" algorithm since it is more likely to be used in practice compared to the centralized charging algorithm. However, the centralized charging algorithm is a more ideal algorithm since it has a more accurate forecast of the electric net load and can manage the charging of all PEVs. To determine whether or not the decentralized charging algorithm could provide the same benefits as the centralized charging algorithm, both algorithms

were simulated on the California electric grid in the year 2030 with an increased population of PEVs. It was shown that the decentralized algorithm had two main parameters that influence electric grid emissions. If the vehicles are allowed to continuously charge, they will increase emissions compared to the centralized algorithm since vehicles will still charge even when a peak in the electric load occurs. If vehicles cannot communicate with the grid frequently enough, emissions will increase since the grid operator will not be able to update the cost load frequently. When the communication with the grid is high, the decentralized charging algorithm can provide the same emissions benefits as the centralized charging algorithm.

Many barriers and challenges are associated with introducing an increasing number of PEVs into the market. Deploying PEV smart charging algorithms on the electric grid is a way to address some of these challenges. This thesis demonstrates that while many obstacles are associated with smart charging, if implemented correctly, they have a great potential in reducing GHG and criteria pollutant emissions.

8.2 Conclusions

- **A decentralized smart charging architecture is a more viable option for real life deployment than a centralized smart charging architecture**

  While a centralized smart charging algorithm has the ability to provide more accurate results, many barriers are associated with it. Utilizing a decentralized smart charging algorithm addresses these barriers. In the centralized architecture, vehicle owners would have to disclose their travel patterns to a central operator, which could lead to privacy concerns. In the decentralized architecture, the travel patterns solely reside with the vehicle owner and does not need to be disclosed to a central operator. In the centralized architecture, as the number of vehicles scale up, the computation power required to satisfy

all vehicle demands would scale up as well. This issue is not present in the decentralized architecture

- **Using telematics to obtain the vehicles' status can cause issues to the vehicles' auxiliary battery as well as affect the accuracy of the charging profiles**

  The need to obtain the vehicles' status proved to be a major barrier associated with a telematics-based approach. If the vehicles' status is updated frequently, this leads to a more accurate charging schedule, but also leads to battery degradation. On the other hand, if the vehicles' status is not updated frequently enough, this could lead to inaccurate charging schedules. A potential solution to this issue is to obtain the vehicles' status from the EVSE side rather than obtaining it from the vehicle side. If the vehicles' status could get sent to the algorithm upon initial plug-in, this would eliminate the need to obtain the vehicles' status through polling. Another solution would be to use a "hybrid" approach when polling the vehicles. For example, the polling rate could be set to 5 minutes when the vehicle is plugged in, and when the vehicle is not plugged in it can be reverted to 20 minutes. This approach assumes that poll rates can occur for individual vehicles rather than for the entire fleet of vehicles.

- **Using a real time pricing structure is the most effective way to reduce costs for PEV owners as well as reduce emissions**

  With the way the current TOU rate structures are set up, the cheapest prices tend to happen when renewable generation is minimized, and the highest prices occur when renewable generation is maximized. This deters PEV owners from charging their vehicles when the grid is producing its power renewably. Using a rate structure that shifts the cheapest prices to when renewable generation is maximized will reduce costs for PEV owners as well as

reduce emissions. However, this can lead to sudden peaks occurring in the electric load. A real time pricing structure would be the best solution to reduce costs for PEV owners, reduce emissions, and reduce peaks in the electric load. This type of rate structure would incentivize vehicles to charge when the grid is the cleanest as well as fill the valley that occurs in the middle of the day, making it easier for grid operators to manage the load.

- **The decentralized smart charging algorithm can provide the same benefits as the centralized algorithm when programmed correctly**

  In order for the decentralized smart charging algorithm to achieve the same results as the centralized smart charging algorithm, it must be tuned accordingly. The most important parameter that must be taken into consideration when using the decentralized smart charging algorithm is to ensure that communication with the electric grid occurs frequently enough. Practically, this means that the proper telematics infrastructure would have to be established to make sure that information can be transferred quick enough.

REFERENCES

[1] U. S. EPA, “Global Greenhouse Gas Emissions Data.” [Online]. Available: https://www.epa.gov/ghgemissions/global-greenhouse-gas-emissions-data. [Accessed: 28-Aug-2017].

[2] J. Friedrich, M. Ge, and A. Pickens, “This Interactive Chart Explains World’s Top 10 Emitters, and How They’ve Changed,” 2017. [Online]. Available: http://www.wri.org/blog/2017/04/interactive-chart-explains-worlds-top-10-emitters-and-how-theyve-changed. [Accessed: 12-Mar-2018].

[3] U. S. EPA, “Sources of Greenhouse Gas Emissions,” 2017. [Online]. Available: https://www.epa.gov/ghgemissions/sources-greenhouse-gas-emissions. [Accessed: 11-Aug-2017].

[4] C. A. R. Board, “California Greenhouse Gas Emission Inventory - 2017 Edition,” 2017. [Online]. Available: https://www.arb.ca.gov/cc/inventory/data/data.htm. [Accessed: 11-Aug-2017].

[5] C. A. R. Board, “Assembly Bill 32 Overview,” 2014. [Online]. Available: https://www.arb.ca.gov/cc/ab32/ab32.htm. [Accessed: 08-Jan-2018].

[6] E. G. B. Jr., “GOVERNOR BROWN ESTABLISHES MOST AMBITIOUS GREENHOUSE GAS REDUCTION TARGET IN NORTH AMERICA.” [Online]. Available: https://www.gov.ca.gov/news.php?id=18938. [Accessed: 08-Jan-2018].

[7] L. Zhang, F. Jabbari, T. Brown, and S. Samuelsen, “Coordinating plug-in electric vehicle charging with electric grid: Valley filling and target load following,” *J. Power Sources*, vol. 267, pp. 584–597, 2014.

[8] U.S. Department of Energy, “The History of the Electric Car,” 2014. [Online]. Available: https://energy.gov/articles/history-electric-car. [Accessed: 15-Aug-2017].

[9] The National Academies of Science, *Overcoming Barriers to Deployment of Plug-in Electric Vehicles*. 2015.

[10] U.S. Department of Energy, “Developing Infrastructure to Charge Plug-In Electric Vehicles.” [Online]. Available: https://www.afdc.energy.gov/fuels/electricity_infrastructure.html. [Accessed: 16-Aug-2017].

[11] U.S. Department of Energy, “Charging Plug-in Electric Vehicles at Home.” [Online]. Available: https://www.afdc.energy.gov/fuels/electricity_charging_home.html. [Accessed: 16-Aug-2017].

[12] A. Lantero, “How Microgrids Work,” 2014. [Online]. Available: https://www.energy.gov/articles/how-microgrids-work. [Accessed: 17-Aug-2017].

[13] Y. Bhandari, S. Chalise, J. Sternhagen, and R. Tonkoski, “Reducing fuel consumption in microgrids using PV, batteries, and generator cycling,” *IEEE Int. Conf. Electro Inf. Technol.*, pp. 7–10, 2013.

[14] W. Su, Z. Yuan, and M. Y. Chow, “Microgrid planning and operation: Solar energy and wind energy,” *IEEE PES Gen. Meet. PES 2010*, pp. 1–7, 2010.

[15] California Energy Commission, “California Energy Commission – Tracking Progress: Resource Flexibility,” 2015.

[16] U. D. of Transportation, “National Household Travel Survey,” 2009. [Online]. Available: http://nhts.ornl.gov/download.shtml. [Accessed: 08-Mar-2018].

[17] C. ISO, “What the duck curve tells us about managing a green grid,” *Calif. ISO, Shap. a Renewed Futur.*, pp. 1–4, 2016.

[18] J. García-Villalobos, I. Zamora, J. I. San Martín, F. J. Asensio, and V. Aperribay, “Plug-in electric vehicles in electric distribution networks: A review of smart charging approaches,” *Renew. Sustain. Energy Rev.*, vol. 38, pp. 717–731, 2014.

[19] K. Mets, T. Verschueren, W. Haerick, C. Develder, F. De Turck, and F. De Turck, “Optimizing smart energy control strategies for plug-in hybrid electric vehicle charging,” *2010 IEEE/IFIP Netw. Oper. Manag. Symp. Work.*, pp. 293–299, 2010.

[20] K. Mets, R. D’Hulst, and C. Develder, “Comparison of Intelligent charging algorithms for electric vehicles to reduce peak load and demand variability in a distribution grid,” *J. Commun. Networks*, vol. 14, no. 6, pp. 672–681, 2012.

[21] N. Chen, C. W. Tan, and T. Q. S. Quek, “Electric Vehicle Charging in Smart Grid Optimality and Valley-Filling Algorithms,” vol. 8, no. 6, pp. 1073–1083, 2014.

[22] M. Alonso, H. Amaris, J. G. Germain, and J. M. Galan, “Optimal charging scheduling of electric vehicles in smart grids by heuristic algorithms,” *Energies*, vol. 7, no. 4, pp. 2449–2475, 2014.

[23] L. Gan, U. Topcu, and S. H. Low, “Optimal Decentralized Protocols for Electric Vehicle Charging,” *IEEE Trans. Power Syst.*, vol. 28, no. 2, pp. 940–951, 2013.

[24] K. Qian, C. Zhou, M. Allan, and Y. Yuan, “Modeling of load demand due to EV battery charging in distribution systems,” *IEEE Trans. Power Syst.*, vol. 26, no. 2, pp. 802–810, 2011.

[25] E. C. Kara, J. S. Macdonald, D. Black, M. Bérges, G. Hug, and S. Kiliccote, “Estimating the benefits of electric vehicle smart charging at non-residential locations: A data-driven approach,” *Appl. Energy*, vol. 155, pp. 515–525, 2015.

[26] E. L. Karfopoulos and N. D. Hatziargyriou, “A multi-agent system for controlled charging of a large population of electric vehicles,” *IEEE Trans. Power Syst.*, vol. 28, no. 2, pp.

1196–1204, 2013.

[27] Z. Ma, D. Callaway, and I. Hiskens, “Decentralized charging control for large populations of plug-in electric vehicles,” *Decis. Control (CDC), 2010 49th IEEE Conf.*, vol. 21, no. 1, pp. 67–78, 2010.

[28] Z. Ma, D. Callaway, and I. Hiskens, “Decentralized Charging Control of Large Populations of Plug-in Electric Vehicles,” *Ieee Trans. Control Syst. Technol.*, vol. 21, no. 1, pp. 67–78, 2013.

[29] K. E. Forrest, B. Tarroja, L. Zhang, B. Shaffer, and S. Samuelsen, “Charging a renewable future: The impact of electric vehicle charging intelligence on energy storage requirements to meet renewable portfolio standards,” *J. Power Sources*, vol. 336, pp. 63–74, 2016.

[30] B. Tarroja, B. Shaffer, and S. Samuelsen, “The importance of grid integration for achievable greenhouse gas emissions reductions from alternative vehicle technologies,” *Energy*, vol. 87, pp. 504–519, 2015.

[31] B. Tarroja, L. Zhang, V. Wifvat, B. Shaffer, and S. Samuelsen, “Assessing the stationary energy storage equivalency of vehicle-to-grid charging battery electric vehicles,” *Energy*, vol. 106, pp. 673–690, 2016.

[32] L. Zhang, T. Brown, and S. Samuelsen, “Evaluation of charging infrastructure requirements and operating costs for plug-in electric vehicles,” *J. Power Sources*, vol. 240, pp. 515–524, 2013.

[33] S. (BMW) Kaluza, D. (PG&E) Almeida, and P. (PG&E) Mullen, “BMW i ChargeForward: PG&E’s Electric Vehicle Smart Charging Pilot,” 2017.

[34] FleetCarma, “Residential Smart Charging Pilot in Toronto ChargeTO.”

[35] J. D. Eichman, F. Mueller, B. Tarroja, L. S. Schell, and S. Samuelsen, “Exploration of the integration of renewable resources into California’s electric system using the Holistic Grid Resource Integration and Deployment (HiGRID) tool,” *Energy*, vol. 50, no. 1, pp. 353–363, 2013.

[36] “Monthly Plug-In Sales Scorecard.” [Online]. Available: http://insideevs.com/monthly-plug-in-sales-scorecard/. [Accessed: 28-Aug-2017].

[37] E. Ramos Muñoz, G. Razeghi, L. Zhang, and F. Jabbari, “Electric vehicle charging algorithms for coordination of the grid and distribution transformer levels,” *Energy*, vol. 113, pp. 930–942, 2016.

[38] “MelRok Energy IOT.” [Online]. Available: https://melrok.com/#/pages/main.html. [Accessed: 07-Feb-2018].

[39] Kia, “Kia Soul EV.” [Online]. Available: https://www.kia.com/us/en/vehicle/soul-

ev/2016/charge. [Accessed: 02-May-2018].

[40] U.S. Department of Energy, “Find and Compare Cars.” [Online]. Available: https://www.fueleconomy.gov/feg/Find.do?action=sbs&id=36553. [Accessed: 02-May-2018].

[41] “Duralast Platinum Battery.” [Online]. Available: https://www.autozone.com/batteries-starting-and-charging/battery/duralast-platinum-battery/319460_187780_0. [Accessed: 06-Mar-2018].

[42] “How to Convert Reserve Capacity to Amp Hours.” [Online]. Available: https://sciencing.com/how-8681870-convert-reserve-capacity-amp-hours.html. [Accessed: 06-Mar-2018].

[43] C. Marnay, L. Liu, J. Yu, D. Zhang, J. Mauzy, B. Shaffer, X. Dong, W. Agate, and S. Vitiello, “White Paper on Benefit Analysis of Smart Grid Projects.”

[44] “Chargepoint.” [Online]. Available: https://na.chargepoint.com/charge_point. [Accessed: 01-May-2018].

[45] Southern California Edison (SCE), “Rate Schedule TOU-GS-2-B for Medium-Sized Businesses,” 2015.

[46] M. Younghein and E. Martinot, “Beyond 33% Renewables: Grid Integration Policy for a Low-Carbon Future,” no. 11/25/2015, 2015.

[47] C. P. U. Commission, “Actions to Limit Utility Cost and Rate Increases,” *Calif. Public Util. Comm.*, no. May, 2018.

[48] C. Loutan, J. Goodin, D. Hou, and J. Pinjuv, “CAISO’s Proposed TOU Periods to Address Grid Needs with High Numbers of Renewables,” pp. 1–18, 2016.

[49] “Today’s Renewables,” *California ISO*. [Online]. Available: http://www.caiso.com/informed/Pages/CleanGrid/TodaysRenewables.aspx. [Accessed: 19-Jul-2016].

[50] U. S. EPA, “eGRID 2010 Summary Tables,” no. February, pp. 0–12, 2014.

[51] G. Razeghi, “The Development and Evaluation of a Highly-Resolved California Electricity Market Model to Characterize the Temporal and Spatial Grid, Environmental, and Economic Impacts of Electric Vehicles,” 2013.

[52] U. S. EPA, “eGRID2014v2 Summary Tables,” 2017.

[53] B. Shaffer, B. Tarroja, and S. Samuelsen, “Dispatch of fuel cells as transmission integrated grid energy resources to support renewables and reduce emissions,” *Appl. Energy*, vol. 148, no. x, pp. 178–186, 2015.

[54] K. Forrest, B. Shaffer, B. Tarroja, and S. Samuelsen, “A Comparison of Fuel Cell and Energy Storage Technologies’ Potential to Reduce CO2 Emissions and Meet Renewable Generation Goals,” *ECS Trans.* , vol. 71, no. 1, pp. 193–203, 2016.

[55] “Energy+Environmental Economics.” [Online]. Available: https://www.ethree.com/. [Accessed: 20-Feb-2018].

[56] V. C. Güngör, D. Sahin, T. Kocak, S. Ergüt, C. Buccella, C. Cecati, and G. P. Hancke, “Smart grid technologies: Communication technologies and standards,” *IEEE Trans. Ind. Informatics*, vol. 7, no. 4, pp. 529–539, 2011.

[57] Zengquan Yuan, Haiping Xu, Huachun Han, and Yingjie Zhao, “Research of smart charging management system for Electric Vehicles based on wireless communication networks,” *2012 IEEE 6th Int. Conf. Inf. Autom. Sustain.*, pp. 242–247, 2012.

[58] T. Markel, M. Kuss, and P. Denholm, “Communication and Control of Electric Vehicles Supporting Renewables,” *IEEE Veh. Power Propuls. Syst. Conf.*, no. August, pp. 27–34, 2009.

APPENDIX

Table 25. *CO_2 Emissions using Bldg. Profiles as Cost Load*

CO_2 Emissions (pounds) (Building Cost Load)						
Vehicle Traffic	**APS**	**ECPS**	**MPS**	**MSTB**	**SCPS**	**SSPS**
Base	42.16	44.31	28.72	12.21	26.28	85.37
100	211.74	220.17	209.87	205.35	216.82	222.62
300	641.51	653.55	635.26	625.53	648.47	659.41
500	1070.72	1084.66	1062.57	1045.61	1073.86	1092.87
700	1498.50	1518.12	1488.93	1471.58	1500.37	1527.43
900	1920.32	1953.57	1911.88	1894.50	1924.34	1963.02

Table 26. *CO_2 Emissions w/Poll Rate using Bldg. Profiles as Cost Load*

CO_2 Emissions with Poll Rate (pounds) (Building Cost Load)						
Vehicle Traffic	**APS**	**ECPS**	**MPS**	**MSTB**	**SCPS**	**SSPS**
Base	42.30	44.30	28.86	12.29	26.30	85.30
100	212.24	220.35	210.51	206.33	217.19	222.72
300	642.96	654.58	637.03	627.97	650.06	660.24
500	1073.46	1086.47	1065.46	1049.45	1076.66	1094.40
700	1502.40	1520.58	1492.83	1476.78	1504.28	1529.61
900	1925.33	1956.70	1917.02	1900.45	1929.39	1965.82

Table 27. *CO_2 Emissions using SCE TOU Rate as Cost Load*

CO_2 Emissions (pounds) (SCE TOU Rate Cost Load)						
Vehicle Traffic	**APS**	**ECPS**	**MPS**	**MSTB**	**SCPS**	**SSPS**
Base	45.37	45.22	31.84	13.63	27.20	86.04
100	225.45	226.35	225.45	226.35	225.48	226.34
300	678.27	679.15	678.27	679.15	679.47	678.05
500	1128.04	1131.42	1127.83	1131.09	1128.79	1132.21
700	1582.46	1580.41	1581.95	1584.94	1582.04	1587.15
900	2030.14	2034.28	2030.14	2034.28	2030.14	2034.28

Table 28. *CO_2 Emissions w/Poll Rate using SCE TOU Rate as Cost Load*

CO_2 Emissions with Poll Rate (pounds) (SCE TOU Rate Cost Load)						
Vehicle Traffic	**APS**	**ECPS**	**MPS**	**MSTB**	**SCPS**	**SSPS**
Base	45.27	45.13	31.77	13.60	27.15	85.87
100	225.01	225.90	225.01	225.90	225.05	225.89
300	676.94	677.83	676.94	677.83	678.15	676.71
500	1125.82	1129.23	1125.61	1128.90	1126.58	1129.99
700	1579.36	1577.33	1578.76	1581.85	1578.95	1584.04
900	2026.22	2030.27	2026.22	2030.27	2026.22	2030.27

Table 29. *CO_2 Emissions using Future TOU Rate as Cost Load*

CO_2 Emissions (pounds) (Future TOU Rate Cost Load)						
Vehicle Traffic	**APS**	**ECPS**	**MPS**	**MSTB**	**SCPS**	**SSPS**
Base	40.91	41.08	28.55	12.39	24.46	77.49
100	204.23	205.33	204.23	205.33	204.24	205.32
300	611.55	614.31	611.55	614.31	613.46	616.67
500	1023.64	1020.77	1023.98	1020.70	1021.24	1021.44
700	1430.76	1433.12	1429.38	1434.68	1428.18	1429.64
900	1833.45	1844.12	1833.45	1844.12	1833.45	1844.12

Table 30. *CO_2 Emissions w/Poll Rate using Future TOU Rate as Cost Load*

CO_2 Emissions with Poll Rate (pounds) (Future TOU Rate Cost Load)						
Vehicle Traffic	**APS**	**ECPS**	**MPS**	**MSTB**	**SCPS**	**SSPS**
Base	41.16	41.32	28.72	12.46	24.61	77.95
100	205.45	206.57	205.45	206.57	205.46	206.56
300	615.28	618.03	615.28	618.03	617.19	620.41
500	1029.81	1026.95	1030.15	1026.87	1027.49	1027.67
700	1439.33	1441.77	1438.05	1443.34	1436.84	1438.21
900	1844.56	1855.20	1844.56	1855.20	1844.56	1855.20

Table 31. *Cost using Bldg. Profiles as Cost Load: SCE TOU Rate*

Cost ($) (Building Cost Load: SCE TOU Rate)						
Vehicle Traffic	**APS**	**ECPS**	**MPS**	**MSTB**	**SCPS**	**SSPS**
Base	8.09	6.83	5.47	2.21	4.29	13.31
100	39.57	36.20	38.80	39.26	37.23	36.17
300	116.01	111.26	116.53	118.25	113.84	110.94
500	192.51	186.56	193.59	197.04	190.72	186.13
700	270.06	261.82	271.20	276.06	268.27	262.24
900	347.18	337.09	348.51	354.02	345.39	336.77

Table 32. *Cost w/Poll Rate using Bldg. Profiles as Cost Load: SCE TOU Rate*

Cost with Poll Rate ($) (Building Cost Load: SCE TOU Rate)						
Vehicle Traffic	**APS**	**ECPS**	**MPS**	**MSTB**	**SCPS**	**SSPS**
Base	8.01	6.82	5.42	2.19	4.27	13.26
100	39.24	36.00	38.45	38.87	36.96	35.96
300	115.06	110.48	115.48	117.02	112.83	110.16
500	190.83	185.20	191.86	195.02	189.03	184.79
700	267.67	259.90	268.83	273.32	265.88	260.33
900	344.09	334.68	345.37	350.73	342.26	334.37

Table 33. *Cost using Bldg. Profiles as Cost Load: Future TOU Rate*

Cost ($) (Building Cost Load: Future TOU Rate)						
Vehicle Traffic	**APS**	**ECPS**	**MPS**	**MSTB**	**SCPS**	**SSPS**
Base	5.74	6.81	4.05	1.85	3.91	12.74
100	29.18	32.47	29.19	28.90	31.06	32.60
300	89.22	94.39	87.80	86.17	91.38	94.89
500	149.30	155.47	147.20	143.10	150.38	155.75
700	208.60	217.42	205.89	201.50	209.24	216.80
900	266.68	279.12	264.22	259.73	267.83	279.40

Table 34. *Cost w/Poll Rate using Bldg. Profiles as Cost Load: Future TOU Rate*

Cost with Poll Rate ($) (Building Cost Load: Future TOU Rate)						
Vehicle Traffic	**APS**	**ECPS**	**MPS**	**MSTB**	**SCPS**	**SSPS**
Base	5.82	6.82	4.11	1.87	3.93	12.77
100	29.49	32.65	29.53	29.31	31.33	32.78
300	90.16	95.12	88.83	87.42	92.35	95.62
500	150.96	156.73	148.91	145.11	152.07	157.02
700	210.90	219.20	208.25	204.25	211.58	218.58
900	269.64	281.43	267.25	263.03	270.84	281.72

Table 35. *Cost using SCE TOU Rate as Cost Load*

Cost ($) (SCE TOU Rate)						
Vehicle Traffic	**APS**	**ECPS**	**MPS**	**MSTB**	**SCPS**	**SSPS**
Base	6.33	6.32	4.44	1.90	3.78	12.00
100	31.44	31.64	31.44	31.64	31.45	31.63
300	94.51	94.65	94.51	94.65	94.69	94.55
500	157.15	157.59	157.12	157.55	157.36	157.59
700	220.29	220.43	220.44	220.97	220.53	221.16
900	283.26	283.70	283.26	283.70	283.26	283.70

Table 36. *Cost w/Poll Rate using SCE TOU Rate as Cost Load*

Cost with Poll Rate ($) (SCE TOU Rate)						
Vehicle Traffic	**APS**	**ECPS**	**MPS**	**MSTB**	**SCPS**	**SSPS**
Base	6.36	6.35	4.46	1.91	3.80	12.05
100	31.59	31.78	31.59	31.78	31.60	31.78
300	94.96	95.10	94.96	95.10	95.13	95.00
500	157.91	158.32	157.88	158.28	158.10	158.33
700	221.34	221.47	221.51	222.01	221.58	222.21
900	284.58	285.06	284.58	285.06	284.58	285.06

Table 37. *Cost using Future TOU Rate as Cost Load*

Cost ($) (Future TOU Rate)						
Vehicle Traffic	**APS**	**ECPS**	**MPS**	**MSTB**	**SCPS**	**SSPS**
Base	5.19	5.23	3.62	1.58	3.11	9.84
100	25.94	26.06	25.94	26.06	25.95	26.06
300	77.68	78.00	77.68	78.00	77.89	78.34
500	130.05	129.65	130.10	129.64	129.66	129.63
700	181.62	181.89	181.45	182.29	181.27	181.63
900	232.74	234.14	232.74	234.14	232.74	234.14

Table 38. *Cost w/Poll Rate using Future TOU Rate as Cost Load*

Cost with Poll Rate ($) (Future TOU Rate)						
Vehicle Traffic	**APS**	**ECPS**	**MPS**	**MSTB**	**SCPS**	**SSPS**
Base	5.31	5.34	3.71	1.61	3.18	10.06
100	26.52	26.65	26.52	26.65	26.52	26.65
300	79.44	79.75	79.44	79.75	79.66	80.11
500	132.98	132.58	133.02	132.57	132.62	132.58
700	185.68	185.98	185.56	186.39	185.37	185.70
900	237.99	239.40	237.99	239.40	237.99	239.40

Table 39. *CO_2 Emissions STD using Bldg. Profiles as Cost Load*

CO_2 Emissions STD (%) (Building Cost Load)						
Vehicle Traffic	**APS**	**ECPS**	**MPS**	**MSTB**	**SCPS**	**SSPS**
Base	14.50	14.52	17.21	25.78	18.15	10.47
100	6.45	6.24	6.40	6.29	6.36	6.24
300	3.73	3.58	3.71	3.59	3.61	3.73
500	2.66	2.89	2.69	2.88	2.74	2.63
700	2.27	2.26	2.48	2.45	2.50	2.28
900	2.18	2.07	2.20	2.08	2.18	2.07

Table 40. *CO_2 Emissions STD w/Poll Rate using Bldg. Profiles as Cost Load*

CO_2 Emissions STD with Poll Rate (%) (Building Cost Load)						
Vehicle Traffic	**APS**	**ECPS**	**MPS**	**MSTB**	**SCPS**	**SSPS**
Base	14.45	14.52	17.09	25.63	18.14	10.48
100	6.41	6.24	6.38	6.25	6.34	6.24
300	3.72	3.57	3.70	3.57	3.60	3.72
500	2.66	2.88	2.68	2.87	2.73	2.62
700	2.27	2.25	2.48	2.44	2.49	2.27
900	2.18	2.06	2.19	2.07	2.17	2.06

Table 41. *CO_2 Emissions STD using SCE TOU Rate as Cost Load*

CO_2 Emissions STD (%) (SCE TOU Rate Cost Load)						
Vehicle Traffic	**APS**	**ECPS**	**MPS**	**MSTB**	**SCPS**	**SSPS**
Base	14.47	14.48	17.17	26.27	18.37	10.53
100	6.34	6.32	6.34	6.32	6.34	6.31
300	3.73	3.64	3.73	3.64	3.75	3.66
500	2.74	2.97	2.74	2.94	2.64	2.54
700	2.21	2.12	2.34	2.48	2.56	2.28
900	2.11	2.20	2.11	2.20	2.11	2.20

Table 42. *CO_2 Emissions STD w/Poll Rate using SCE TOU Rate as Cost Load*

CO_2 Emissions STD with Poll Rate (%) (SCE TOU Rate Cost Load)						
Vehicle Traffic	**APS**	**ECPS**	**MPS**	**MSTB**	**SCPS**	**SSPS**
Base	14.49	14.50	17.20	26.30	18.41	10.55
100	6.35	6.33	6.35	6.33	6.35	6.32
300	3.73	3.65	3.73	3.65	3.76	3.67
500	2.75	2.97	2.75	2.94	2.64	2.54
700	2.21	2.12	2.34	2.49	2.56	2.28
900	2.11	2.20	2.11	2.20	2.11	2.20

Table 43. *CO_2 Emissions STD using Future TOU Rate as Cost Load*

CO_2 Emissions STD (%) (Future TOU Rate Cost Load)						
Vehicle Traffic	**APS**	**ECPS**	**MPS**	**MSTB**	**SCPS**	**SSPS**
Base	14.28	14.53	16.90	25.25	17.88	10.46
100	6.32	6.18	6.32	6.18	6.33	6.18
300	3.69	3.45	3.69	3.45	3.53	3.81
500	2.59	2.75	2.61	2.75	2.86	2.69
700	2.34	2.35	2.63	2.41	2.45	2.21
900	2.23	1.95	2.23	1.95	2.23	1.95

Table 44. *CO_2 Emissions STD w/Poll Rate using Future TOU Rate as Cost Load*

CO_2 Emissions STD with Poll Rate (%) (Future TOU Rate Cost Load)						
Vehicle Traffic	**APS**	**ECPS**	**MPS**	**MSTB**	**SCPS**	**SSPS**
Base	14.21	14.46	16.79	25.12	17.78	10.42
100	6.29	6.15	6.29	6.15	6.30	6.15
300	3.67	3.44	3.67	3.44	3.52	3.79
500	2.58	2.74	2.60	2.74	2.84	2.68
700	2.34	2.35	2.63	2.39	2.44	2.20
900	2.22	1.93	2.22	1.93	2.22	1.93

Table 45. *Cost STD using Bldg. Profiles as Cost Load: SCE TOU Rate*

Cost STD (%) (Building Cost Load: SCE TOU Rate)						
Vehicle Traffic	**APS**	**ECPS**	**MPS**	**MSTB**	**SCPS**	**SSPS**
Base	14.75	15.89	17.41	27.42	19.13	11.46
100	6.47	6.55	6.50	6.24	6.76	6.55
300	3.73	3.83	3.76	3.71	3.84	3.86
500	2.68	2.99	2.71	2.93	2.61	2.75
700	2.26	2.21	2.33	2.52	2.56	2.55
900	2.21	2.14	2.19	2.11	2.21	2.17

Table 46. *Cost STD w/Poll Rate using Bldg. Profiles as Cost Load: SCE TOU Rate*

Cost STD with Poll Rate (%) (Building Cost Load: SCE TOU Rate)						
Vehicle Traffic	**APS**	**ECPS**	**MPS**	**MSTB**	**SCPS**	**SSPS**
Base	14.80	15.86	17.65	27.53	19.16	11.43
100	6.54	6.53	6.55	6.32	6.78	6.54
300	3.76	3.83	3.78	3.73	3.86	3.87
500	2.69	3.00	2.72	2.96	2.63	2.75
700	2.27	2.21	2.35	2.55	2.59	2.56
900	2.22	2.16	2.22	2.13	2.23	2.18

Table 47. *Cost STD using Bldg. Profiles as Cost Load: Future TOU Rate*

Cost STD (%) (Building Cost Load: Future TOU Rate)						
Vehicle Traffic	**APS**	**ECPS**	**MPS**	**MSTB**	**SCPS**	**SSPS**
Base	15.36	14.94	17.25	24.99	18.64	10.87
100	6.89	6.43	6.52	6.25	6.63	6.42
300	3.90	3.71	3.83	3.51	3.51	4.01
500	2.64	2.89	2.72	2.87	2.91	2.85
700	2.38	2.50	2.73	2.47	2.48	2.35
900	2.24	2.01	2.29	2.03	2.24	2.03

Table 48. *Cost STD w/Poll Rate using Bldg. Profiles as Cost Load: Future TOU Rate*

Cost STD with Poll Rate (%) (Building Cost Load: Future TOU Rate)						
Vehicle Traffic	**APS**	**ECPS**	**MPS**	**MSTB**	**SCPS**	**SSPS**
Base	15.16	14.86	16.95	24.83	18.55	10.86
100	6.76	6.40	6.45	6.16	6.53	6.38
300	3.86	3.68	3.77	3.47	3.48	3.97
500	2.62	2.86	2.69	2.83	2.87	2.81
700	2.37	2.47	2.71	2.42	2.46	2.31
900	2.21	1.98	2.25	1.99	2.21	1.99

Table 49. *Cost STD using SCE TOU Rate as Cost Load*

Cost STD (%) (SCE TOU Rate)						
Vehicle Traffic	**APS**	**ECPS**	**MPS**	**MSTB**	**SCPS**	**SSPS**
Base	15.22	15.43	18.57	27.99	19.27	11.19
100	6.95	6.59	6.95	6.59	6.95	6.58
300	3.88	3.87	3.88	3.87	3.99	3.88
500	2.79	3.02	2.81	3.00	2.74	2.90
700	2.35	2.29	2.42	2.67	2.70	2.67
900	2.43	2.18	2.43	2.18	2.43	2.18

Table 50. *Cost STD w/Poll Rate using SCE TOU Rate as Cost Load*

Cost STD with Poll Rate (%) (SCE TOU Rate)						
Vehicle Traffic	**APS**	**ECPS**	**MPS**	**MSTB**	**SCPS**	**SSPS**
Base	15.14	15.35	18.44	27.83	19.13	11.12
100	6.91	6.55	6.91	6.55	6.91	6.54
300	3.85	3.84	3.85	3.84	3.97	3.85
500	2.77	3.00	2.78	2.98	2.72	2.87
700	2.33	2.27	2.40	2.65	2.69	2.65
900	2.41	2.17	2.41	2.17	2.41	2.17

Table 51. *Cost STD using Future TOU Rate as Cost Load*

Cost STD (%) (Future TOU Rate)						
Vehicle Traffic	**APS**	**ECPS**	**MPS**	**MSTB**	**SCPS**	**SSPS**
Base	14.56	14.85	17.22	25.84	18.42	10.55
100	6.47	6.27	6.47	6.27	6.48	6.26
300	3.74	3.53	3.74	3.53	3.62	3.93
500	2.57	2.80	2.60	2.81	2.88	2.73
700	2.34	2.35	2.66	2.41	2.52	2.22
900	2.32	1.94	2.32	1.94	2.32	1.94

Table 52. *Cost STD w/Poll Rate using Future TOU Rate as Cost Load*

Cost STD with Poll Rate (%) (Future TOU Rate)						
Vehicle Traffic	**APS**	**ECPS**	**MPS**	**MSTB**	**SCPS**	**SSPS**
Base	14.28	14.60	16.85	25.33	18.03	10.38
100	6.35	6.15	6.35	6.15	6.35	6.15
300	3.66	3.47	3.66	3.47	3.56	3.85
500	2.54	2.75	2.56	2.76	2.83	2.68
700	2.31	2.32	2.63	2.35	2.46	2.18
900	2.28	1.89	2.28	1.89	2.28	1.89